University of Siena

Department of Biotechnology, Chemistry and Pharmacy

PhD in Biochemistry and Molecular Biology

Ciclo XXXIV

Isolation and characterization of highly functional human monoclonal antibodies against *Neisseria gonorrhoeae* and SARS-CoV-2

PhD Candidate: **Marco Troisi**

Supervisor: **Prof. Rino Rappuoli**

Academic year 2021-2022

ABSTRACT

BACKGROUND
Monoclonal antibodies (mAbs) are becoming increasingly popular in the infectious disease field where they represent a promising and innovative class of therapeutics. In this context, the aim of this PhD thesis was to identify highly effective mAbs against *Neisseria gonorrhoeae* (Ng) and SARS-CoV-2.

METHODS
Peripheral blood mononuclear cells (PBMCs) from Bexsero vaccinees and COVID-19 convalescent patients were collected. mAbs were isolated from memory B cells (MBC) and plasma cells (PCs) and subsequently their binding profile and functionality were analysed.

RESULTS
From Bexsero vaccinees, 17 mAbs capable of neutralizing *Neisseria gonorrhoeae* by *in vitro* bactericidal assay were identified. mAb potency (IC50), established by complement-mediated killing, correlated with the binding profile. Indeed, mAbs targeting well-represented surface structures were the most potent.
From COVID-19 patients, 453 neutralizing antibodies were identified. The most powerful antibody recognized the spike protein receptor-binding domain with IC100 lower than 10 ng/mL.

CONCLUSIONS
High-throughput screening of mAbs allowed the identification of potent molecules capable of killing *Neisseria gonorrhoeae* and neutralizing SARS-CoV-2. On one hand, this work contributed to better understand the protection against gonococcal infection. Indeed, results suggest that complement-mediated killing, may be used as correlate of protection and predict vaccine efficacy. On the other, a highly potent mAb against the etiological agent of COVID-19 was identified and well-characterized *in vitro* and *in vivo*, where prophylactic and therapeutic efficacy were demonstrated by extraordinarily low amounts of the candidate medication.

This work is dedicated to my family

for their endless love,

support and encouragement.

List of abbreviations

ACE2	Angiotensin-converting enzyme 2
ADCC	Antibody-dependent cellular cytotoxicity
ADE	Antibody-dependent enhancement of disease
AMR	Antimicrobial resistance
AP	Alternative pathway
B-cells	B-lymphocyte cells
BCR	B- cell receptor
BM	Bone marrow
BRC	Baby rabbit complement
CD	Connector domain
CDC	Complement dependent cytotoxicity
CDR	Complementarity determining region
CDRs	Complementary determining regions
CEACAM	Carcinoembryonic antigen-related family of cell adhesion molecules
CH	Central helix
CLL	Chronic lymphocytic leukemia
COVID-19	Coronavirus Disease 2019
CoVs	Coronaviruses
CP	Classical pathway
CT	Cytoplasmic tail
DAF	Decay accelerating factor
DMVs	Double-membrane vesicles
E	Envelope
ECDC	European Centre for Disease Prevention and Control
EDTA	Ethylenediaminetetraacetic acid
EID	Emerging infectious disease
ELISA	Enzyme-linked immunosorbent assay
ER	Endoplasmic reticulum
Fab	Fragment antigen binding
FACS	Fluorescence activated cytometric sorting
Fc	Fragment crystallizable (antibody constant domain)
FDA	Food and Drug Administration
fH	factor H
FP	Fusion peptide
FR	Framework regions
GCA	Gonococcal agar
GMMAs	Generalized Modules for Membrane Antigens
hiBRC	Heat-inactivated baby rabbit complement
HR1	Heptad repeat 1

HR2	Heptad repeat 2
HSPG	Host cell heparin sulfate proteoglycans
HV	Hypervariable
Ig	Immunoglobulin
IMGT	ImMunoGeneTics information system
L-SBA	Luminescence Based Serum Bactericidal Assay
LOS	Lipooligosaccharide
LP	Lectin pathway
M	Membrane
mAb	Monoclonal antibody
MAC	Membrane attack complex
MBC SNs	Memory B cell supernatants
MBCs	Memory B cells
MBL	Mannose-binding lectin
MCP	Membrane cofactor protein
MERS-CoV	Middle East respiratory syndrome Coronavirus
MIC	Minimal inhibitory concentration
MSM	Men who have sex with men
N	Nucleocapsid
Ng	*Neisseria gonorrhoeae*
nsp	Nonstructural proteins
NTD	N-terminal domain
NZ	New Zealand
OMV	Outer membrane vesicle
Opa	Opacity associated proteins
OPK	Opsonophagocytic uptake and killing
ORFs	Open reading frames
pAb	Polyclonal antibody
pAbs	Polyclonal antibodies
PBMCs	Peripheral blood mononuclear cells
PC SNs	Plasma cell supernatants
PCs	Plasma cells
PorB	Porin B
RBD	Receptor Binding Domain
RV	Reverse vaccinology
S	Spike
SARS-CoV-2	Severe Acute Respiratory Syndrome Coronavirus-2
sgRNA	Subgenomic RNAs
STIs	Sexually transmitted infections
TAP	Transcriptionally active PCR
TCC	Terminal cascade complex

Tfp	Type IV pilus
TM	Transmembrane domain
TMPRSS2	Cellular cathepsin L and transmembrane protease serine 2
TP	Terminal pathway
VHH	Camelid single domain antibody
WBCs	White blood cells
WGS	Whole genome sequencing
WHO	World Health Organization

List of tables

List of Figures

Table of contents

1 Antibodies

1.1 General introduction

Antibodies are a class of proteins responsible for the defense of the host against pathogenic invaders. Highly specific, these molecules are produced by the B-lymphocyte cells (B-cells) of the host's own immune system and can interact strongly with a broad spectrum of target proteins (also known as antigens) [1]. Also, antibodies can recruit other cells within the immune system to eliminate pathogens [2]. This is one of the reasons why antibodies have become popular therapeutic agents, but they have also found application in other areas such as industrial processes, research, imaging, and diagnostics.

Considering the large differences in shape, size, and amino acid composition between various antigens, the antibody-binding surface must be highly adaptable. Antibodies are produced by B-cells which derive from pluripotent hematopoietic stem cells. In adult human subjects, as in all mammals, B-cells develop in the bone marrow (BM) from hematopoietic precursor cells, playing a vital role in adaptive immunity [3].

Early BM-dependent stages of B-cell development include the functional rearrangement process of the immunoglobulin heavy (H) chain gene segments VH, DH, and JH together with the VL-JL rearrangements of the light chain (L-chain) gene segments in order to generate a B-cell repertoire expressing antibodies [4].

The rearrangement process will be explained in the following sub-chapter. Eventually, mature B cells leave the bone marrow and circulate in the blood and lymphatic systems.

Antibodies exist in a membrane form, called B- cell receptor (BCR) on the surface of a naïve B-cell. Following an encounter with an antigen, the naïve B-cell promptly divides and differentiates into memory B cells and effector B cells (also called plasma cells (PCs)) [5]. Memory B cells (MBCs) have a longer life span than naïve B cells, and they express the same membrane-bound antibody as naïve B cells. On the other hand, PCs, which have little, or no membrane-bound antibody, produce the secreted version of the BCR as free antibodies [6].

In addition to antigen recognition, B-cells also require T-cell stimuli to differentiate into plasma cells [7]. Although each B-cell produces one unique antibody, the vast repertoire of B-cells results in an enormous diversity. Apart from the immune system's capability to create a vast diversity of antibodies, each antibody also possesses the ability to bind to a specific region, called epitope, on its respective antigen [8]. When several different B-cells produce an antibody response towards the same antigen, such antibodies are called polyclonal antibodies (pAbs). The ability of several polyclonal antibodies to bind different epitopes can produce an overall high and broad response although the contribution from each member can vary greatly [9]. Contrary to pAbs, monoclonal antibodies (mAbs) refer to identical copies of an antibody produced by the same B-cell.

A huge breakthrough in 1975 allowed B-cells with a finite lifetime to be immortalized and thus produce an infinite amount of mAbs [10]. This technology, called the hybridoma technology, has revolutionized the field of antibody generation for practical applications.

More recently, the possibility to high throughput sequence the antibody repertoire has expanded our knowledge of antibody diversity and supported monoclonal antibody discovery for therapy and vaccine development [11].

1.2 The structure of the antibody molecule

The antibody molecule has two distinct functions. Firstly, the antibody should bind to foreign antigens encountered by the host and, secondly, should mediate effector functions to neutralize invaders. The Fc region is responsible for binding to effector cells and for activating other functions of the immune system, such as antibody-dependent cellular cytotoxicity (ADCC), phagocytosis and components like the complement system [12]. In contrast, the antigen-binding region must bind to a wide array of antigens and, to accomplish this, the antibody molecule has adopted a unique appearance in the form of a Y- shaped molecule **(Figure 1.2.1).**

The basic antibody molecule (of the immunoglobulin G subclass) consists of four polypeptide chains, two identical light chains and two identical heavy chains. The molecular weight of one light chain (L) and one heavy chain (H) is approximately 22 kDa and 55 kDa respectively. Each heavy chain is connected to a light chain by one disulphide bond to form a heterodimer (H+L). The two heterodimers are joined by similar disulphide bridges to form the basic four chain $(H+L)_2$ antibody structure with an approximate molecular weight of 150 kDa. Depending on the isotype, each antibody molecule can either adopt the basic four chain $(H+L)_2$ form or multiple units $((H+L)_2)_n$ of this basic structure [13][14].

The terminal regions of the two arms of the Y-molecule are called variable regions (V regions: VL for light chain and VH for heavy) and are responsible for the variety between different antibodies. Interestingly, most of the variety within the V regions is concentrated in distinct loop regions called complementarity determining regions (CDRs) [15]. The three CDRs in each VL and VH constitute the antigen binding site of the antibody molecule, whereas the segments between the CDR regions within VL and VH show much less variation and are thus called framework regions (FR) for their role in maintaining the structure of the antibody molecule [16]. The regions of conserved sequences beyond the variable regions are called constant regions: CL in light chain and CH in heavy chain.

There are two isotypes of light chains in humans and mice, kappa (κ) and lambda (λ) and a standard antibody molecule contains only one light chain isotype, either kappa or lambda, but not both. As for the heavy chain, there are five major isotypes in humans, each corresponding to a different heavy chain constant region: μ, δ, γ, ε, and α. The length of the constant regions is approximately 330 amino acids for δ, γ, and α and 440 amino acids for μ and ε. As a result, the five different isotypes give rise to five different antibody classes: IgM (μ), IgD (δ), IgG (γ), IgE (ε), and IgA (α). Furthermore, minor amino acid sequence differences within the human α and γ heavy chains have led to further sub-isotypes: α1 and α2 for α and γ1, γ2, γ3 and γ4 for γ. Since the isotype of the heavy chain does not affect its pairing ability to the light chain, heavy chains of any class may pair with either κ or λ light chains. The light chain consists of one variable (VL) and one constant (CL) domain. The heavy chain also contains one variable (VH) domain and either three (CH1, CH2, CH3) or four (CH1, CH2, CH3, CH4) constant domains depending on the isotype. IgG, IgD and IgA have three heavy chain constant domains whereas IgM and IgE have four. Also depending on the isotype, the different domains are connected by flexible hinge regions that allow movement and adjustments between the domains. While IgA, IgD and IgG possess a highly flexible hinge between CH1 and CH2, no such hinge exists in IgE and IgM [17][18].

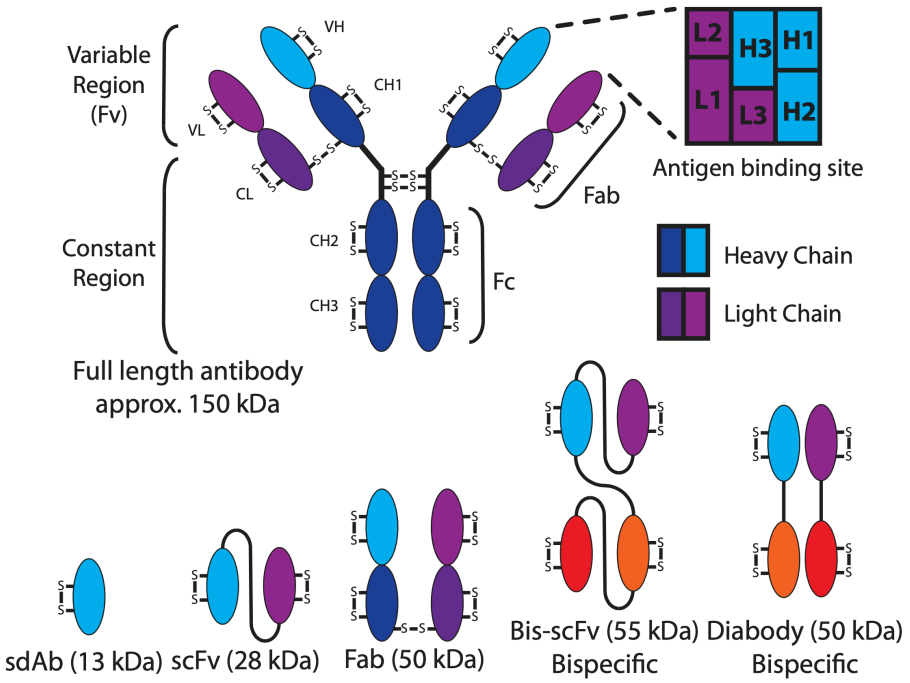

Figure 1.2.1. Structure of the antibody molecule and antibody fragment-based scaffolds. The figure was inspired by Tae Hyun Kang, 2020.

1.3 Classes of immunoglobulins

Immunoglobulin G (IgG), the most abundant isotype in serum, is composed of two γ heavy chains, two κ or λ light chains and consists of the basic $(H+L)_2$ monomeric structure. As described earlier, differences within the four γ heavy chains have originated four IgG subclasses: IgG1, IgG2, IgG3 and IgG4 [19]. IgM constitute about 5-10% of the total serum immunoglobulins and monomeric IgM is expressed as membrane bound antibody on B-cells whereas PCs secrete IgM as a pentamer [20]. The five units are arranged with their Fc regions in the center of the pentamer and the 10 antigen binding arms on the periphery of the molecule. IgM is the first immunoglobulin class produced in a primary response. Due to its pentameric structure with 10 antigen-binding sites, IgM has higher valency than the other isotypes [21]. In addition, IgM is more efficient than IgG at activating complement since two or more Fc regions in proximity are required [22]. IgA

exists primarily as a monomer in serum, but polymeric forms can exist [23], while IgE antibodies play a role in hypersensitivity reactions.

Immunoglobulin domains are folded into a structure called the immunoglobulin fold with an approximate size of 110 amino acids. This structure consists of a "sandwich" of two beta sheets, each containing antiparallel beta strands connected by loops. Antibodies have two types of immunoglobulin folds, consisting of either seven or nine beta strands (and an extra loop). The former is the structural unit of the constant regions, whereas the latter is found in the variable region. Unsurprisingly, it is the loops connecting the antiparallel beta strands of the VL and VH domains that correspond to the CDRs [13].

1.4 How antibody diversity is created *in vivo*

The human kappa and lambda light chains and heavy chains are coded by separate multigene families situated on different chromosomes (chromosome 2 and 22, respectively). In unarranged germline DNA, each of these multigene families contains several coding sequences, called gene segments, separated by noncoding regions. During B-cell maturation, these gene segments are brought together to form functional immunoglobulin genes. The kappa and lambda light chain families contain V, J and C gene segments and the rearranged VJ segments encode the variable domain (VL) of the light chains. The heavy chain family contains V, D, J and C segments and the rearranged VDJ gene segments encode the variable domain (VH) of the heavy chain. In each gene family, the C gene segments encode the constant domains [24].

During B-cell maturation, the heavy chain variable region genes rearrange first, followed by rearrangement of the light chain variable gene regions. During rearrangement in the kappa light chain, any of the functional Vk genes can combine with anyone of the Jk genes to form the VL domain. The C gene is then joined to the VJ segments, resulting in a completely rearranged antibody light chain. The lambda light chain in humans undergoes a similar rearrangement. On

the other hand, generation of a functional heavy chain requires two separate rearrangement events within the variable region. The first step involves joining any one of the DH genes with any JH gene to form a resulting DHJH unit. A VH segment then joins to form a VDJ unit that encodes the entire heavy variable region. In the final step, a C gene segments is attached to form the final immunoglobulin heavy chain construct. Joining of V-(D)-J segments is imprecise. Further junctional diversity at the VJ and VDJ is created by trimming the coding joints as well as by adding extra nucleotides at the junctions [25].

In summary, antibody diversity in humans is created in several different ways *in vivo*. Firstly, multiple V, D and J gene segments can be randomly combined, and imprecise joining of V-(D)-J gene segments lead to additional diversity. It is the diversity at the V-(D)-J interface that forms the third hypervariable region (CDR3) of the heavy and light chains. Furthermore, addition of extra nucleotides at the coding joints adds more diversity. Finally, after a mature B-cell encounters an antigen, an *in vivo* affinity maturation process called somatic hypermutation further introduces diversity and improves the affinity of the antibody.

1.5 The antibody-antigen interface

1.5.1 The epitope

Antibodies recognize specific immunogenic markers, called epitopes, on their target antigen. The corresponding interacting surface on the antibody is called the paratope and consists of different amino acids in the CDRs. Epitopes are usually classified as continuous or discontinuous, depending on whether the amino acids that form the epitope are contiguous or not. It is generally acknowledged that most protein epitopes are discontinuous and consist of two to five short stretches of residues that are distant in the protein sequence but are brought together into a single unity by the folding of the protein chain [26][27]. Discontinuous epitopes are structurally defined by the amino acids in contact with the paratope residues in a crystallographic complex. In contrast, continuous epitopes are identified by the

ability of short peptide fragments of the protein to bind to an antibody. The distinction between these two epitope classes is however not black and white. A discontinuous epitope can consist of several continuous stretches. In other cases, not all residues in a continuous epitope will interact with a paratope, with only a subset of residues present at the surface of a native protein where they are usually a part of a more complex discontinuous epitope [28].

1.5.2 The Paratope

As of today, there are several methods and approaches available to identify and number the antigen binding regions (CDR regions) [29]. The oldest scheme (Kabat numbering scheme) relied solely on alignment of antibody sequences and determining the positions with the highest sequence variability [30]. A more recent way to define CDRs relies on the international ImMunoGeneTics information system (IMGT) which uses the database of germline variable immunoglobulin sequences [32].

While CDRs are often used to identify paratopes, not all residues contained in the CDRs are found to bind the antigen. According to earlier studies, only about 20–30% of the residues within the CDRs form contacts with the antigen [30][32] with the contacting residues more commonly located at the central regions of the binding site. The non-contacting residues within the CDRs, in contrast are important for maintaining the structural conformations of the hypervariable loops [33][15].

1.6 The Epitope-Paratope Interface

The interacting interface between the antigen binding site (epitope) and the antibody binding site (paratope) consists of several non-covalent chemical interactions including hydrogen bonds, van der Waals forces, electrostatic interactions, and hydrophobic interactions. These non-covalent interactions

determine the binding strength (also called affinity) between the antibody and antigen. The driving force behind complex formation between an antigen and antibody is the change in Gibbs free energy ($\Delta G=\Delta H-T\Delta S$) [34]. The changes in the enthalpy component (ΔH) are the results of hydrogen bonds, electrostatic and van der Waals interactions whereas changes in the entropy component (ΔS) are associated with changes in conformational freedom upon binding [35].

Apart from affinity, another important concept is antibody specificity, which refers to the ability for the antibody to distinguish an antigen from another.

When discussing the affinity and specificity between the antibody and its antigen, the geometric and chemical complementary between the epitope and paratope need to be considered [36].

1.6.1 Geometric complementarity

From a protein engineering point of view, it is important to be able to understand the length and amino acid composition preferences found in antibody CDR domains as well as any differences in these parameters between different targets. Several studies have analyzed the length and composition of matured antibodies as well as the specific CDR residues involved in binding [37][38][39][40][41].

It is well-known that CDRH3 has the highest length diversity / distribution. Whereas the other CDR loops each had a one over-represented length, numerous antibodies had various lengths (7 to 18 residues long) in the CDRH3 loop. In addition, the largest spread in CDR length is also found in CDRH3. This means two things. Firstly, for instance, while CDRL3 rarely has a length below 6 residues and above 13 residues, CDRH3 can have lengths as low as 3 and as high as 25. Secondly, CDRH3 also shows a more considerable variation between different classes (e.g., peptides & proteins) of antigen binders compared to other CDR loops.

The diversity of the first and second CDR regions of the heavy and light chains are restricted by the number of V genes available. On the contrary, the CDR3

regions are the results of V-(D)-J recombination, making these loops much more diverse with regards to both sequence and length. Since H3 has an extra recombination (V-D-J) compared to L3 (V-J), H3 is the most variable loop in a B cell produced antibody and it occupies a central location in the binding site and provides many important antigens contact residues.

1.6.2 Chemical complementarity

Apart from geometric complementarity, the amino acids in the epitope-paratope interface need to provide the necessary chemical complementarity. Although the CDRs are also known as hypervariable regions, their sequences are not completely random. Several studies (in addition to / including those studies mentioned in the section above) have shown that the amino acid composition of CDR loops differs from antibody framework regions and from generic protein loops. [28][38][41][42][43].

Tyrosine is the most abundant amino acid in antigen binding sites, accounting for about 10% of the total CDR composition and 25% of the antigen contacts in functional antibodies [42][43]. In addition to tyrosine, tryptophan, which has similar properties as tyrosine is also overrepresented in CDR loops compared to generic loops. Phenylalanine can be considered as a neutral amino acid, as it is claimed to be favored by some [28][44] whereas others suggest that phenylalanine is underrepresented [45].

The reason behind aromatic side chain preference is simple: these side chains can interact with a diverse group of targets through a cumulative collection of relatively weak noncovalent interactions. Also, aromatic side chains can also interact with alkyl carbons through the C–H–π interaction, and with negative charged side chains through anion–π interactions [46]. Although each individual interaction is weak, the combined effect is considerable. Tyrosine possesses hydrophilic character in addition to these aromatic and hydrophobic traits, and it becomes clear why tyrosine can form hydrogen bonds, hydrophobic and van der Waals interactions with a wide array of antigens.

1.7 Mapping of the epitope

Epitope mapping is a term used to describe techniques employed to identify and locate the epitope on the protein surface. Mapping the interactions between an antibody and antigen has several benefits, allowing us to understand immune responses and autoimmunity as well as aiding vaccine design and unravel the mechanism of action of an antibody [47]. The experimental methods developed to map epitopes can roughly be divided into structural and functional. Structural methods interpret the protein structure residues in direct contact with the antibody but may not always reveal contribution of amino acids in binding strength. Functional methods use assays to identify and characterize residues important for binding. As each method has its own advantage and disadvantage, a combination of different methods almost always is preferred.

In this work, other than discovering new potential therapeutic monoclonal antibodies (mAbs), we focused our attention on defining their targets (antigens). Once antigens are discovered, the next step will be to unravel specific residues involved in the interaction between mAbs and antigens. Below I describe the most common techniques which allow characterization of the binding of the mAbs to their targets.

1.7.1 Structural mapping

The most accurate and reliable method for identifying epitopes and paratopes is X-ray crystallography [48]. Often regarded as the only method to define a structural epitope [49], very accurate key contacts between the epitope and paratope side chains can be extracted from the crystal complex. Amino acids within a 4 Å distance are generally considered as contacting residues [47]. This technique not only provides precise identification of both continuous and discontinuous epitopes, but also information about binding strength [50]. However, this technique is also dependent on the availability of the antigen and antibody with a certain degree of purity. Obtaining the pure antibody is usually

relatively straightforward, whereas the antigen can be more problematic or even very difficult in the case of membrane proteins [47].

1.7.2 Functional Mapping

Functional methods include techniques based on detection of antibody binding to synthetic peptides (peptide scanning), antigen fragments or recombinant antigens (e.g., antigen mutants, or antigens expressed using selection systems such as phage display) and alternation of the target protein to attribute a change in binding to a specific residue.

In peptide scanning, synthetic overlapping peptides covering the targeted antigen sequence are immobilized on a solid support and binding of an antibody is detected using immunoblot, dot blot, or an ELISA format [51][52]. This method is unlikely to be able to identify complex conformational epitopes involving tertiary and/or quaternary structures. Although it is possible to mimic discontinuous and conformational epitopes by constraining peptides via disulphide bridges [53], peptide scanning is nonetheless most ideal for mapping linear and relatively simple conformational epitopes.

1.8 Engineering Antibodies

Antibody engineering refers to modifying and/or improving the properties of antibodies or antibody fragments. Engineering includes *de novo* selection and affinity maturation in addition to other subfields including improving stability, engineering for reducing immunogenicity, modifying Fc effector function, improving pharmacokinetics, and manufacturability.

It is an important reminder that a full antibody is a 150 kDa molecule and having tunnel vision by just focusing on affinity in the variable domain is suboptimal. For example, therapeutic or *in vivo* diagnostic applications require a long serum half-life and resistance to aggregation, precipitation, and protease degradation [54].

Industrial applications demand antibodies with a long half-life and/or activity in organic solvents at high temperatures [55][56]. Furthermore, manufacturing (therapeutic) antibodies needs high levels of expression in addition to chemical and physical stability to withstand degradation (physical and chemical degradation including oxidation, aggregation, degradation, fragmentation, deamination [57]) during manufacturing, transport, storage, and delivery [58].

1.8.1 Improving Affinity

Affinity maturation or improving the affinity of an antibody / antibody fragment is probably the most popular antibody engineering subfield. An improved affinity is often correlated with enhanced efficacy, improved pharmacokinetics, and lower dosing/toxicity [90].

Numerous strategies can be implemented for *in vitro* affinity maturation [59], by introducing mutations in either a targeted or random manner. An easy way is to randomize the entire variable region using error prone PCR [60][61] in conjunction with display technologies. A very popular approach is to either mutate the CDR3 regions only [62] as they constitute the major portion of the antigen binding site. Alternatively, mutating the CDR3 in combination with peripheral residues can also be a viable option [63][64].

1.8.2 Improving Stability

The stability of mAbs can be improved by engineering the constant domains through the mutation of the CH2/CH3 or by introducing additional disulphide bridges in the respective domains [65]. Alternatively, the human variable domains can also be chosen as the subject of engineering. One approach to engineer more stable human variable domains is to introduce elements of camelid single domain antibodies (VHH) [66]. Camelid VHHs are generally well expressed, have good solubility [67] and stable at high (ca 90°C) temperatures [68]. To compensate for the lack of a VL chain, VHHs have longer CDRH3 loops to protect the VH-VL

interface, but camelization attempts of human VH domains tends to lead to reduced expression levels [66].

However, several mutations in the VH3/VL interface were identified that improved solubility, thermal refolding and melting temperature. Importantly, some of these mutations were independent of CDR3 diversity [69]. Another way to improve stability involves identification of variable germline sequences with favorable properties [56] and using alignment of the framework repertoire to identify amino acids occurring with high frequency. The consensus framework sequences can later be optimized for expression [70][71].

1.8.3 Improving pharmacokinetics and effector functions

Engineering the Fc portion of the antibody molecule aims to enhance effector functions such as ADCC, complement dependent cytotoxicity (CDC) and pharmacokinetics.

The long serum half-life of full length mAbs can be attributed to their binding to the neonatal receptor FcRn in a pH dependent manner (strongest at slightly acidic pH to marginal under neutral and basic conditions) [72]. Within the half-life mutations it is worth mentioning the mutants YTE (M252Y/S254T/T256E), LS (M428L/N434S), AAA (T307A/E380A/N434A), QL (T250Q/M428L) and V308P which retain ADCC and CDC activity as well as a slight enhancement in CDC activity [73]. Increasing half-life results in lower dosage of the mAb needed to achieve the therapeutic effect [74][75].

The Fc region has also been the target for improved effector functions. The most popular approach is via glycosylation to increase the affinity towards Fc receptors on effector cells [76][77]. For example, obinituzumab (an ADCC enhanced version of rituximab) was given the breakthrough therapy designation and approved in 2013 by the FDA [78][79].

1.8.4 Abrogation of Fc receptor binding

The majority of mAb therapeutics possess the ability to engage innate immune effectors through interactions mediated by their Fc domain. By delivering Fc-Fc gamma receptor (FcγR) and Fc-C1q interactions, mAbs can link exquisite specificity to powerful cellular and complement-mediated effector functions. Fc interactions can also facilitate enhanced target clustering to evoke potent receptor signaling [80].

In contrast to their beneficial role, in some cases antibodies have also been implicated in disease enhancement. For example, non-neutralizing Dengue-specific antibodies have been shown to mediate antibody-dependent enhancement (ADE) of disease [122].

ADE can be seen in two distinct ways: by enhanced antibody-mediated virus uptake into Fc gamma receptor IIa (FcγRIIa)-expressing phagocytic cells leading to increased viral infection and replication, or by excessive antibody Fc-mediated effector functions or immune complex formation causing enhanced inflammation and immunopathology [82]. There are examples, like the SARS-CoV-2 case and RSV infections [81], where ADE is a potential clinical risk [83][84].

Given such potential risks, in the context of mAb discovery against SARS-CoV-2, we optimized the suitability for clinical development and reduce the risk of ADE by introducing five different point mutations in Fc [85]. Specifically, the first two-point mutations (M428L and N434S) were introduced to extend the antibody half-life, while the remaining three-point mutations (L234A, L235A, and P329G) were introduced to reduce Fc-dependent functions such as binding to FcgRs [85].

1.8.5 Hexabody technology

IgG antibodies can organize into ordered hexamers on cell surfaces after binding their antigen. This process is dependent on Fc:Fc interactions, which promote C1q binding, the first step in classical pathway complement activation [86]. These

hexamers bind the first component of complement, C1, inducing complement-dependent target cell killing [87].

De Jong and colleagues from Genmab, Utrecht, identified mutations that enhance hexamer formation (hence the name “Hexabody”) and complement activation by IgG1 antibodies against a range of targets on cells from hematological and solid tumor origin [87]. IgG1 backbones with mutations E430G (in this work it will be named as Hex1) conveyed a strong ability to induce CDC of cell lines and chronic lymphocytic leukemia (CLL) patient tumor cells, while retaining regular pharmacokinetics and biopharmaceutical developability.

Along with the Hex1 mutation, the E345R/E430G/S440Y mutation (in this work named as Hex3) was used to evaluate the complement-mediated killing driving of our antibodies. Notably, the Hex3 mutant was only used in previous studies [87] as a control for the detection of hexameric species since it showed formation of hexamers in solution by HP-SEC, native MS and cryo electron tomography [87].

1.9 mAbs for bacterial infections

mAbs have been highly pursued in the anti-cancer, autoimmune, and antiviral fields with many success stories [88][89]. As of today, only a handful of antibody therapies have been licensed for infectious diseases (e.g., palivizumab for prophylaxis against respiratory syncytial virus in at risk infants) [90]. Some drug candidates for treatment of Ebola Virus Disease (EVD) [91] have been studied, monoclonal antibody (mAb) cocktails have shown great potential as EVD therapeutics. The most known mAb cocktail, used as a therapeutic, is ZMapp, manufactured by «Leaf Biopharmaceutical» since 2004 [92]. Recent conceptual and technological advances in mAb development could have an enormous impact in the field of infectious diseases, particularly in the context of Emerging Infectious Disease (EID) outbreaks and AMR pathogens.

In fact, the frequency of AMR has reached an apex. The root cause of many of these infections are pathogens like *Enterococcus species, Staphylococcus aureus, Klebsiella pneumoniae, Acinetobacter baumannii, Pseudomonas aeruginosa, Enterobacter species, and Escherichia coli,* which thrive in the nosocomial environment and are the bacterial species that have seen the largest rise in the acquisition of antibiotic resistance genes [93]. Also, AMR in *Neisseria gonorrhoeae*, which is the focus of this work, is an escalating global public health problem [94].

To fight infections caused by antibiotic-resistant bacteria, there is one potential path ahead: to use novel types of nonantibiotic antibacterial agents. mAbs targeting bacteria is a suitable alternative as they are generally considered safe, due to their low immunogenicity and lack of cross-reactivity with human tissues. Because of their high specificity for the target pathogen, mAbs cause no collateral damage to the microbiota. Despite these clear advantages, the use of mAbs as antibacterial agents is still limited, as reported in **Table 1** [95]. This limitation is partially due to the difficulty in finding optimal bacterial target antigens.

Table 1. The table reports a list of mAbs against bacteria that have entered the clinical trials.

Bacterial species	Drug	Type	Target	Phase
Bacillus anthracis	Obiltoxaximab	Humanized IgG1	Protective antigen (toxin)	IV
	Thravixa	Human IgG1	Protective antigen (toxin)	I
	Valortim	Human IgG1	Protective antigen (toxin)	I
	Raxibacumab	Human IgG1	Protective antigen (toxin)	IV
Clostridium botulinum	XOMA 3ab	Mix of 3 humanized IgG1	Botulinum neurotoxin type B (toxin)	I
	NTM-1632	Mix of 3 humanized IgG1	Botulinum neurotoxin type B (toxin)	I
Clostridium difficile	Actoxumab	Human IgG1	*C. difficile* toxin A (toxin)	III
	Bezlotoxumab	Human IgG1	*C. difficile* toxin B (toxin)	III
Escherichia coli	Edobacumab	Mouse IgM	LPS lipid A	III
	Nebacumab	Human IgM	LPS lipid A	III
	T88	Human IgM	LPS lipid A	III
STEC*	Shiga toxin MAbs, cαStx1 and -2	Mix of 2 humanized IgG1	*E. coli* Stx1 and Stx2	II
Pseudomonas aeruginosa	Aerucin	Human IgG1	*P. aeruginosa* alginate	II
	Panobacumab	Human IgM	*P. aeruginosa* LPS O11	II
	KB001	Human PEGylated Fab	*P. aeruginosa* PcrV (secretion system)	II
	MEDI3902	Bispecific human IgG1	*P. aeruginosa* PcrV and Psl	II
Staphylococcus aureus	Salvecin, AR-301, KBSA-301	Human IgG1	*S. aureus* alpha-hemolysin (toxin)	II
	ASN100	Mix of 2 human IgG1	HlgAB, HlgCB, LukED, LukSF, and LukGH (toxins)	II
	Tefibazumab	Humanized IgG1	*S. aureus* ClfA	II
	MEDI4893	Human IgG1 modified	*S. aureus* alpha-hemolysin (toxin)	II
	514G3	Human IgG3	*S. aureus protein A*	II
	Pagibaximab	Chimeric IgG1	Lipoteichoic acid	III
	Aurograb	scFv	GrfA (lipoprotein)	III
Multiple species	F598	Human IgG1	Poly-*N*-acetylglucosamine	II

*STEC: Shiga toxin-producing Escherichia coli.

2 The complement system

The consequences of recognition of a target structure by an antibody depends on which effector functions the antibody can initiate. For instance, an antibody's effector functions can be mediated by the activation of the complement system [96]. The complement system is primarily viewed as a first responder to microbial infections [97] and is comprised of plasma proteins which mostly circulate as inactive zymogens [101][102]. In addition to the protective role of Complement in innate immunity, it is increasingly apparent that the system is also responsible for the modulation of several complex tissue regeneration and coagulation processes [103][104][105][106][107][108].

2.1 Complement activation

Complement activation occurs primarily via one or all of three possible initiation pathways: the Classical pathway (CP), Lectin pathway (LP) and Alternative pathway (AP) which lead to activation of the Terminal pathway (TP). In fact, as shown in the **Figure 2.1.1**, all three activation pathways converge with the cleavage of the proteins C3 and C5 into their constituent fragments. C3a and C5a are anaphylatoxins which attract and activate white blood cells (WBCs) by binding to G-protein-coupled receptors (C3aR and C5aR) [100]. C3b from the upper cascade is an opsonin [109] which covalently binds to pathogen surfaces via a thioester domain [110] and marks them for destruction by interacting with CR1 on phagocytic cells [100]. C5b from the lower cascade is the first building block of the membrane attack complex (MAC), otherwise known as the terminal cascade complex (TCC) which forms pores pathogen membranes and induces lysis [100].

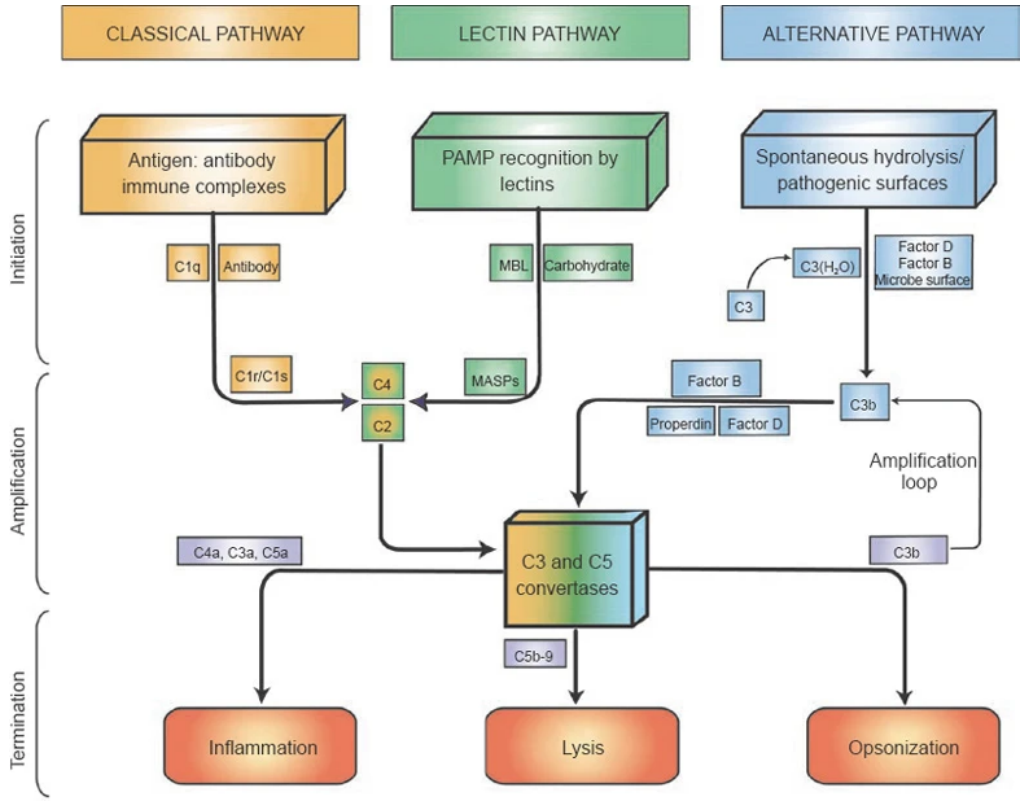

Figure 2.1.1. The complement pathways: The classical pathway is activated when C1q binds to antibody attached to antigen, activating C1r and C1s, which cleave C4 and C2. The lectin pathway is activated when mannose-binding lectin (MBL) encounters conserved pathogenic carbohydrate motifs, activating the MBL-associated serine proteases (MASPs) and again cleaving C4 and C2. C4 and C2 cleavage products form the classical and lectin pathway C3 convertase. The alternative pathway (AP) is activated when C3 undergoes spontaneous hydrolysis and forms the initial AP C3 convertase, C3(H_2O) Bb, in the presence of Factors B and D, leading to additional C3 cleavage and eventual formation of the AP C3 convertase (C3bBb) and AP C5 convertase (C3bBbC3b). The figure was taken from Dunkelberger, J., 2009.

Recognition of bacterial cells occurs via soluble pattern-recognition molecules (lectin pathway) or antibodies (classical pathway). Antibody-mediated complement activation is depicted in **Figure 2.1.2**. C1 binds to antibodies on the surface and triggers formation of a C3 convertase enzyme that converts C3 into C3b. At high C3b densities on the surface, the C3 convertase switches substrate, from C3 to C5, and is now called a C5 convertase. C5 convertases convert C5 into the chemoattractant C5a and C5b that trigger formation of the MAC (C5b-9) [111].

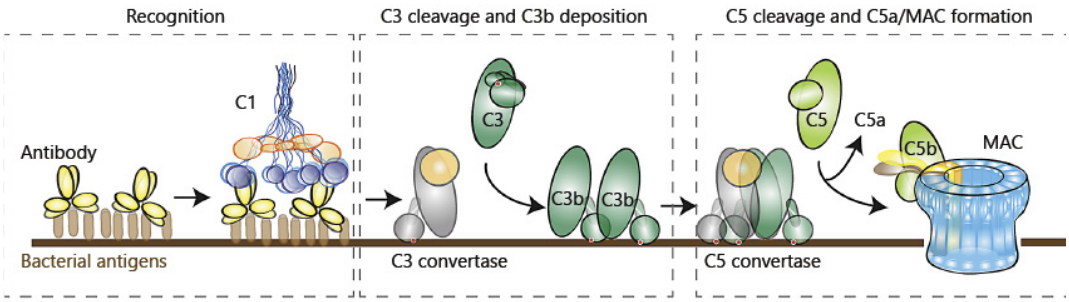

Figure 2.1.2. The complement reaction leading to the MAC formation. The figure was taken from Dunkelberger, J., 2009.

2.1.1 Classical and lectin pathways

The CP and LP can be activated by specific pattern recognition molecules on exogenous material surfaces. C1q of the CP binds to CRP as well as immune complexes containing IgG and IgM [112], complementing the adaptive immune system [110].

The equivalent pattern recognition molecule of the LP is mannose-binding lectin (MBL), which recognises sugars (including glucose, fructose, and mannose) on pathogen surfaces [98], [111]. Stable binding of C1q or MBL is achieved only when their ligands are clustered on a surface in a specific pattern.

Serine proteases are associated with C1q (C1r and C1s) and MBL (MASP1 and MASP2) in a Ca2+ dependent manner and hence the addition of chelating agents such as ethylenediaminetetraacetic acid (EDTA) to serum samples is used to prevent CP or LP activation [98]. C1q binding to immune complexes leads to the activation of C1r which in turn activates C1s [110] and similarly, upon MBL binding to its substrates, MASP1 activates MASP2.

C1s and MASP2 cleave C4 into fragments C4a and C4b which can bind locally via its thioester domain to immune complexes or cell surfaces [112]. The locally bound C4b then binds to C2 which is cleaved in-situ by C1s, MASP1 or MASP2to form a C3 convertase and a fragment of C2 [113].

2.1.2 Alternative pathways

Under normal physiological conditions, the AP is continuously active at a relatively low level, due to a process known as tick-over [114]. Tick-over is the spontaneous hydrolysis of a labile thioester bond within C3 [115] to produce small quantities of C3(H_2O).

The result of tick-over is the continuous generation of the enzymatically active protein complex C3(H_2O) Bb, a C3 convertase with a half-life of 77 seconds [116] which cleaves C3 to produce low standing concentrations of C3a and C3b. The C3b thioester is relatively short-lived, ensuring that C3b binding occurs locally [98]. The low, sentinel concentration of short-lived C3b opsonin assures AP activation on any surface with exposed hydroxyl or amine residues.

2.1.3 Terminal pathway

The dynamic equilibrium between C3 convertase and C5 convertase formation due to competition for C3b has been observed as a flux control point of complement activation, in which the upper cascade appears to reach a threshold concentration of C3b before triggering the TP [121]. C5 cleavage is the last enzymatic step in complement activation and C5b sequentially binds to complement components C6, C7, C8 and C9 to form the cytotoxic MAC capable of lysing cell membranes [122].

2.1.4 Complement regulation

Host cells are protected from complement activation by expressing a collection of membrane regulators. These include CR1, membrane cofactor protein (MCP) and decay accelerating factor (DAF) which deactivate C3 and C4 convertases. In addition, MAC inhibitory protein (CD59) prevents MAC formation by blocking the binding of C9 to C8. Expression of cell surface complement regulators is not always desired and confers protection of tumour cells against complement-induced lysis [123].

Reduced complement activation is sought during shock and certain autoimmune diseases [124]. While long-term suppression of the complete complement system may increase risk of infection and additional antimicrobial prophylaxis is used to counter this risk [125].

However, C3 depletion during sepsis strongly correlates with increased mortality (sensitivity 78.4% and specificity 99.8%) [126], exemplifying how complement activation can be both protective and harmful to the host.

3 *Neisseria gonorrhoeae*

Neisseria gonorrhoeae (Ng) was discovered in 1879 by Neisser and in 1882 it was cultivated by Leistikow and Löffler [128]. In fact, there is evidence suggesting that the pathogen has been infecting humans for thousands of years. Hippocrates described infections resembling male gonococcal urethritis and ancient Chinese writings have been recovered describing similar. Eventually, in 1879, microbiologist Albert Neisser definitively identified the causative organism, *Neisseria gonorrhoeae* [129].

Effective therapeutics were not available until the mid-20th century, when the sulfonamides were introduced [130]

3.1 *Neisseria gonorrhoeae* burden

Ng is the causative agent of gonorrhea, a sexually transmitted disease estimated to cause 86.9 million cases globally per annum [209]. Ng is listed as a high priority pathogen for research into novel treatments by the World Health Organization (WHO) [132] because of its ability to quickly develop resistance to antibiotics [133]. Recently emerged strains of Ng showed resistance to most of the currently available antibiotics including high-level resistance to ceftriaxone which represents the last remaining option for empirical first-line treatment [133]. Despite efforts over many decades, no vaccine has been successfully developed against Ng yet.

3.2 Biology of *Neisseria gonorrhoeae*

Ng is a fastidious gram-negative coccus and an obligate human pathogen. Ng belongs to the genus *Neisseria*, which includes 12 species that colonize human mucosal surfaces. Strict growth requirements in culture include a temperature of 35-37 °C and approximately 5% CO_2 [134]. Because the organism has complex nutritional needs, special media have been developed for growing it in the laboratory. Ng requires iron for growth and is usually able to extract it from the human host; therefore, iron must be supplemented in the culture medium. Media must also be supplemented with glucose, lactate, or pyruvate as these provide a carbon source for the pathogen [217]. Colonies appear on agar plates within 12-48 h, but viability decreases dramatically after 48 h.

3.3 Cell surface structures

Ng has a typical gram-negative cell envelope with an inner cytoplasmic membrane, a peptidoglycan cell wall, and an outer membrane. Type IV pili, Opa proteins, LOS and Por protein play an important role in Ng pathogenesis as well as in serum resistance [138]. Given their importance, they will be now discussed.

3.3.1 Lipooligosaccharide

Lipooligosaccharide (LOS) is an important component of the outer membrane of Ng and contributes to the virulence of gram-negative bacteria [132]. LOS consists of glycolipids which help to maintain the structure of the outer membrane. The structure of consists of a Lipid A moiety to serve as an anchor to the membrane, a core oligosaccharide, and a polymer of a repeating polysaccharide [133].

Notably, the structure of LOS expressed by Ng is variable (**Figure 3.3.1**). During infection, different sugars are attached to the core, depending on which LOS biosynthetic proteins are expressed [134]. The length and composition of the side

chains varies widely because the LOS biosynthetic enzymes are highly phase variable [135]. The family of genes that transfer sugar residues, the *lgt* genes, are highly phase variable. Single nucleotide insertions within the poly-C or poly-G repeats in the *lgt* genes are a result of slip-strand mispairing during replication [136]. This allows the genes to be turned "on" or "off" quickly, ultimately resulting in various side chains attaching to the LOS core. Additionally, several promoters are found within the cluster of genes that encode for the glycosyltransferases, contributing to further variation in the LOS expression at any time [137]. The side changes can undergo spontaneous conversion at any time when the cell begins to express different glycosyltransferases, allowing a single cell to alter its LOS production. Hybrid genes are created by recombination of the different glycosyltransferase genes, contributing to antigenic diversity [225] as well as to the ability of the bacterium to evade immune system defenses [139].

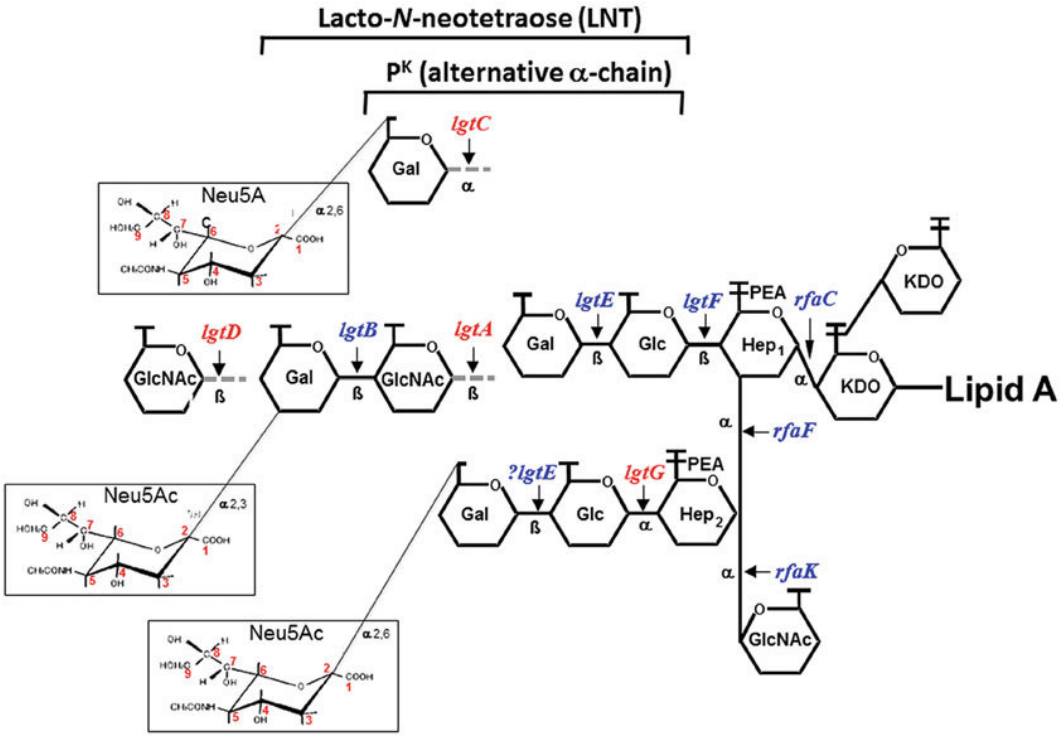

Figure 3.3.1 General structure of Ng lipooligosaccharide (LOS). Ng LOS consists of three oligosaccharide (OS) chains. The OS chains branch from two heptose residues attached to lipid A. Phase variable genes involved in LOS biosynthesis are shown in red: nonvariable genes in blue. Neu5Ac (sialic acid) is shown in the boxes. LOS branching is terminated either by sialic acid or otherwise by addition of hexose(s). The image was taken from Peter Rice, 2019.

3.3.2 Opa

Opacity associated proteins (Opa) are another set of highly variable proteins found in the outer membrane of Ng [140]. Ng typically encode 11 Opa proteins but only expresses up to 3 at a time [141]. Variability in the expression of the different Opa proteins occurs at the translational level, by frameshifts that occur among the *opa* genes due to varying numbers of repeats of the leader sequence [142]. Hypervariable (HV) regions of the *opa* genes contribute to the antigenic diversity seen among expressed Opa proteins [150]. Differential expression of Opa proteins can be found among isolates of the same strain.

Opa proteins can be divided into two groups, depending on the human cellular receptor to which they bind [231]. Most Opa proteins interact with the carcinoembryonic antigen-related family of cell adhesion molecules (CEACAM) The other class of Opa proteins binds host cell heparin sulfate proteoglycans (HSPG) [151].

Opa proteins are made up of 8 antiparallel β-strands that form a barrel in the outer membrane. This part of the protein remains relatively conserved throughout the family. Four extracellular loops link the β-strands of the barrel together, and loops 2 and 3 contain the HV regions of the protein [152]. Opa^{+} bacterial cells are almost always present in natural gonococcal infection [153].

3.3.3 Pili

Type IV pili (Tfp) protrude from the outer membrane of Ng. Tfp are relatively conserved in different gram-negative bacteria and are important for pathogenesis, motility, and transformation [154]. Several different proteins are associated with Tfp structure and biogenesis. The pilus itself is a helical structure comprised primarily of the major pilin, PilE. Five PilE subunits are arranged into three distinct layers of the pilus: a highly conserved core, a less-conserved central layer, and a hypervariable outer layer [154]. The structure of the pilus reveals a core made up of the N-terminus ends of the subunits, organized into a helix of overlapping α-helices. The amino terminal of pilE is highly conserved among

different pilins [155]. Each pilin subunit has a 4-stranded antiparallel β-sheet and a sugar loop. The 4-stranded antiparallel β-sheet and sugar loop from each subunit are held together by hydrogen bonds to form a continuous β-sheet that makes up the central layer of the pilus fiber. The outermost region of the pilus has a β-hairpin and the C-terminal tail. The outer layer is poorly conserved and is flexible to allow for a large variety of amino acids, contributing to the antigenic variation among Ng pilins [237].

The pilus extends beyond the outer membrane, passing through the membrane protein PilQ (**Figure 3.3.2**) [157] . Retraction of the pilus back through PilQ and into the cell contributes to the twitching motion seen among piliated gonococci. Expression of several proteins is involved in pilus formation and pilus- associated functions [158]. Among others, two ATPases, PilF and PilT are involved in pilus assembly and retraction, respectively [159]. PilV is associated with adhesion to host epithelial cells and PilD is involved with pilin processing and translocation to the membrane surface [160].

PilE undergoes both phase and antigenic variation. Regions of silent loci, pilS, may be spontaneously recombined at the expression locus, pilE, allowing for the expression of antigenically variable pili [161] The regions of pilS are donated to pilE in a non-reciprocal manner; thus, the original pilS sequence does not change [162]. Homologous recombination with DNA from other gonococcal cells also contributes to the variability among pilins [163].

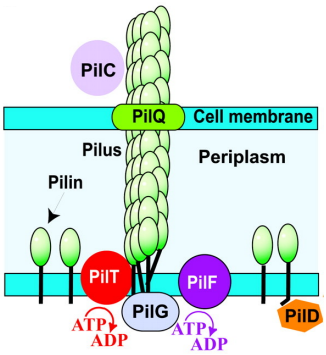

Figure 3.3.2 Type IV pilus schematization. The figure was taken from Berenike Maier,2004.

3.3.4 Porins

Porins B (PorB) are water-filled channels that traverse the outer membrane of Ng, and the most abundant protein in the outer membrane. This hydrophilic channel is a trimer of three identical subunits. Together, the subunits form a β-pleated-barrel structure [164]. The barrel functions as a channel across the hydrophobic membrane, allowing the flow of ions and other small molecules between the bacterium and the environment [165]. PorB also contributes to the pathogenicity of Ng [138].

Ng PorB can be found in one of two classes, PorB1A (PIA) or PorB1B (PIB). The alleles for both PIA and PIB are found at the same locus and each strain of Ng expresses only one of the two subclasses, though PIA/PIB hybrids are possible [166]. There are significant differences between PIA and PIB. The two classes have different orientations in the outer membrane. P1A is oriented such that a short portion of the N-terminus exposed to the environment, whereas both termini of P1B are embedded in the outer membrane and the central portion is exposed to the extracellular environment [167]. Genetic variation is found among the exposed portions of both subclasses of PorB, a characteristic that is used in subtyping strains.

Both forms of porin contribute to the pathogenicity of Ng. PorB can translocate into the eukaryotic cell membrane, inhibit phagosome maturation, assist with bacterial entry into host cells, and down-regulate cell surface receptors necessary for immune function [161].

Of the two subclasses of porin, PorB1A is more commonly found in disseminated gonococcal infections [162] PIA is associated with mediating serum resistance, which the bacterium to escape normal human immune system responses [163]. PIA is also better at facilitating host cell invasion than PIB [160]. PIB, on the other hand, is usually associated with localized infections and contributes to anti-microbial resistance.

3.4 Pathogenesis of *Neisseria gonorrhoeae*

Neisseria gonorrhoeae infections are typically self-limiting and restricted to mucosal sites, however in some cases, untreated infection of females can lead to pelvic inflammatory disease, infertility, and ectopic pregnancies [164]. Infection with Ng results in an initial neutrophilic inflammatory response at the site of infection and limited, short-lived humoral responses [165]. Indeed, experimental infection of human subjects showed that acquisition and subsequent clearance of an infection does not protect against further infections with Ng [166].

3.4.1 Interactions with complement

The ability of Ng to evade recognition and attack from the human complement system is a major feature of host adaptation by this species. [131]. So, an intact CP is essential to kill Neisseriae, evidenced by the lack of bactericidal activity *in vitro* with use of IgG- and IgM-depleted serum [174][175], and C1q depletion [176]

Several strains of *Neisseria gonorrhoeae* can regulate the CP and are complement-resistant by virtue of their ability to bind to the CP inhibitor, C4b-binding protein (C4BP) [177]. Also, there is unequivocal evidence that LPS sialylation in Ng enhances resistance against complement [178]. In fact, analogues of CMP-Neu5Ac (the substrate for gonococcal LOS sialylation), lead to substitution of gonococcal LOS with the sialic acid analogue that counteracts the complement inhibitory function of Neu5Ac and attenuates gonococcal colonization in mice [179].

Finally, Ng shields itself from complement recognition, thus subverting complement activation in both the cervical epithelium and human serum. In the cervical epithelium, *Neisseria gonorrhoeae* binds the alternative complement pathway regulator factor H through sialylated LOS and Porin. Factor H (fH) acts as an alternative complement pathway regulatory protein and host structures

bound to fH are considered as self and are not targeted for opsonization and lysis. [138]. In the serum, *Neisseria gonorrhoeae* can bind the classical complement pathway regulator C4BP to the Porin (**Figure 3.4.1**), a molecule that has a similar function to fH.

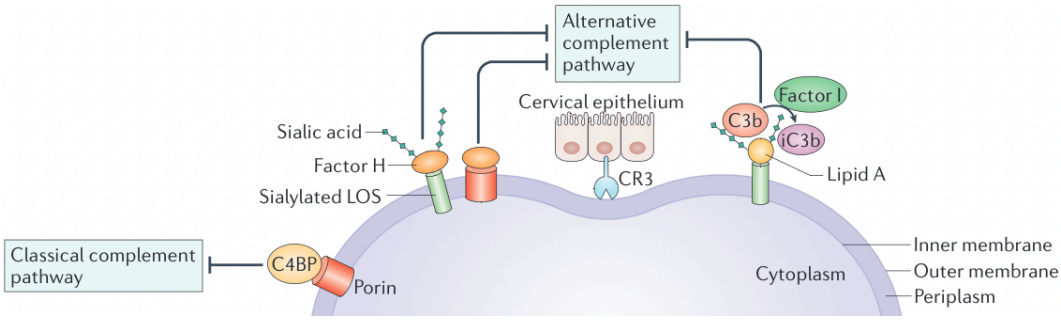

Figure 3.4.1 *Neisseria gonorrhoeae* binds complement proteins to prevent opsonization and killing by membrane attack complexes and sialylates its lipooligosaccharide (LOS) to hide from the complement system. Image taken from Sarah Jane Quillin, 2018.

Understanding such mechanisms may help the development of vaccines and therapeutics that target virulence mechanisms. The development and success of fHbp-based group B meningococcal vaccines is one such example [180].

Our knowledge of complement evasion mechanisms may also be utilized to develop new drugs against multidrug-resistant gonorrhea.

3.5 Clinical aspects of infection with *Neisseria gonorrhoeae*

Gonorrhoea is one of the most common sexually transmitted infections (STIs) [132]. Uncomplicated genital gonorrhoea manifests as purulent urethritis in male and cervicitis in females, but infection may be asymptomatic in ≤ 10% of men and ≥ 50% of women [181]. Most rectal and most pharyngeal infections are asymptomatic, but pharyngitis and proctitis may occur. Infection of the conjunctivae may also occur. Complications may include epididymitis in men and pelvic inflammatory disease with potential infertility [182]. Neonatal infection can occur in infants born to infected mothers. Ophthalmia neonatorum, if not

diagnosed and treated appropriately, may result in scarring and blindness. Disseminated infection is rare but may lead to arthritis, endocarditis, and meningitis [181].

3.5.1 Risk factors for gonorrhoea infection

Gonorrhoea is most common in the younger age group < 25 years [183] and is also associated with men who have sex with men (MSM). Partner characteristics are an important factor also with adolescents whose partner has had an STI in the previous year being three times more likely to have have an STI [265].

3.6 Antimicrobial resistance (AMR) in *Neisseria gonorrhoeae*

The emergence of resistance to nearly all major classes of antimicrobials makes gonorrhea increasingly difficult to treat. In the 1930's, the sulfonamides were introduced and used to successfully treat infections with Ng. However, by the mid 1940's, resistance to sulfonamides made the drugs useless against gonococcal infections. Sulfonamides were no longer recommended for the treatment of GC infections by 1949. Around the same time (the mid-1940's), penicillin was introduced as the drug of choice for gonorrhea infections. In 1958, strains of Ng with decreased susceptibility to both penicillin and streptomycin were reported [185]. Over the next 40 years, the minimal inhibitory concentration (MIC) of penicillin slowly increased, indicating resistance to the antibiotic. By 1987, treatment failure with penicillin was widespread and the drug was no longer recommended for the treatment of GC infections. Also, in the 1980's, resistance to tetracycline became widespread, leading the withdrawal of tetracycline as a recommended treatment option by the CDC [257]. In the 1996, fluoroquinolones were introduced as a treatment for gonorrhea; however, resistance to this class of antibiotics began to develop soon after, and by 2007 the CDC stopped recommending the use of fluoroquinolones to treat Ng infections because of the development of widespread resistance and treatment failure. The expanded

spectrum cephalosporins, cefixime and ceftriaxone are currently the only antibiotics recommended against Ng, but unfortunately resistance to these antibiotics is also increasing. Also, the percentage of gonococcal strains with decreased susceptibility to ceftriaxone in Japan increased dramatically from 2001 to 2007. In 2009, reports of treatment failure with ceftriaxone and cefabuten began to emerge in the treatment of pharyngeal gonorrhea [186].

Eventually, an increase in isolates with decreased susceptibility to azithromycin and cefixime, cefpodoxime, and ceftriaxone was also observed [188]. Susceptibility to these drugs is clearly decreasing and it is only a matter of time before they will no longer be useful for treatment of gonococcal infections.

Figure 3.6.1 adapted from Unemo and Shafer 2011 [133] summarizes the AMR in Ng.

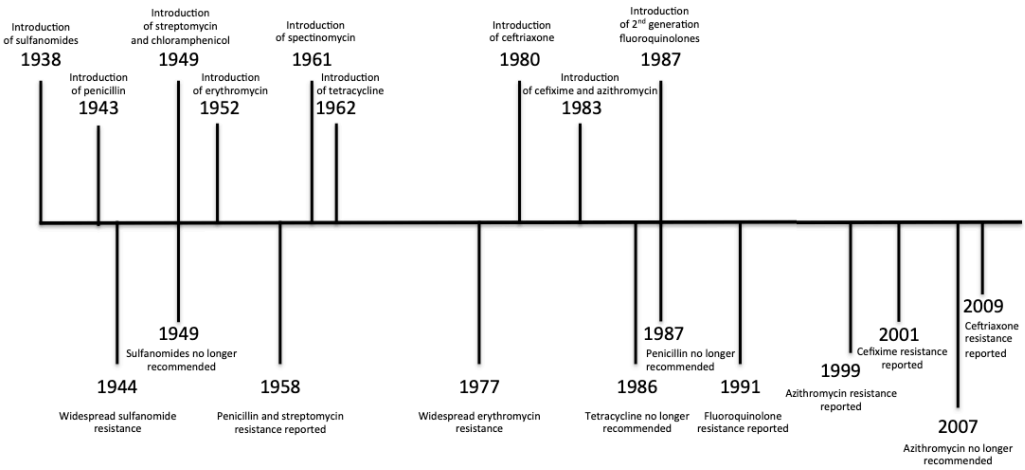

Figure 3.6.1 Timeline of antibiotics used in the treatment of *Neisseria gonorrhoeae* infections.

3.7 Future treatment options: mAbs and vaccines

Since the late 1800s, sera from humans or animals containing antibodies have been widely used for prophylaxis and therapy of viral and bacterial diseases [189]. Serum therapy of most bacterial infections was abandoned in the 1940s [190] after antibiotics became widely available. Over time, the failing efficacy of antibiotics

and the high mortality rate among high-risk patients calls for new treatment modalities for bacterial infections. However, polyclonal antibody preparations have continued to be used for some toxin-mediated infectious diseases and venomous bites [191]. Serum immunoglobulin has continued to be also used for viral diseases where there are few treatments available although mostly for prophylaxis either prior to an anticipated exposure or following an exposure to an infectious agent [184].

3.7.1 Gonococcal mAb-based therapy

In the antibacterial mAb field, products are based on toxin neutralization (*Bacillus anthracis, Clostridium difficile*) [185] [186] but, as discussed, mAbs can have different modes of action, such as virulence factor neutralization, complement-mediated bacterial lysis, and enhancement of opsonophagocytic uptake and killing (OPK) [187].

Natural infection with *Neisseria gonorrhoeae* may elicit a substantial antibody response directed against gonococcal structure, like LOS. For instance, the murine mAb 2C7 was previously identified by Sanjay Ram and colleagues [188]. 2C7 was shown to react with 95% or 100% of Ng recovered directly from cervical secretions or minimally passaged clinical isolates, respectively. 2C7 also has complement-dependent bactericidal activity against gonococci [188] [199] indicating that the gonococcal LOS is also immunogenic.

In this work, we used the chimerized mAb 2C7 carrying the modified Fc (E430G Hex1), which enhances complement activation and increases bactericidal activity, as a positive control to establish and validate an *in vitro* assay which measures the ability of mAbs to kill *Neisseria gonorrhoeae*.

3.7.2 *Neisseria meningitidis* serogroup B vaccine cross-protects against gonorrhea: proof of principle

Unfortunately, to date, vaccines against Ng tested in humans have largely failed to stimulate protection from infection [202]. Only four candidate vaccines (whole cell, partially autolyzed, pilus-based, or protein I-based) have progressed to clinical trials but none provided protection [203].

Neisseria meningitidis and *Neisseria gonorrhoeae* are closely related species that share numerous antigens. A retrospective case-control study found that reduced rates of gonorrhea occurred among sexual health clinic patients (age 15–30 years) following their vaccination with the outer membrane vesicle (OMV) vaccine, MeNZB, against *Neisseria meningitidis* serogroup B [204] with an efficacy estimated to be 31%. OMVs are a complex mixture of outer membrane components that are naturally released by gram-negative bacteria [205]. OMVs are typically enriched with bioactive proteins, toxins, and virulence factors. They play a critical role in the bacteria-bacteria and bacteria-host interactions. Along with coordinated secretion of bacterial effector proteins, OMVs can help bacteria to survive and adapt in hostile environments [194].

Notably, the study provided an important proof of principle, which led to the conclusion that it is indeed plausible to hypothesize that meningococcal OMV vaccines may also induce functional antibodies against *Neisseria gonorrhoeae*.

MeNZB is no longer available, and the serogroup B vaccine 4CMenB (Bexsero) used in this study contains the same OMV components with the addition of three recombinant proteins, named NHBA, fHbp, and NadA [207]. NHBA is a surface-exposed lipoprotein ubiquitously expressed by *Neisseria meningitidis* which binds heparin, and it was demonstrated the contribution to meningococcal adhesion to epithelial cells [196]. fHbp is a lipoprotein present on the surface of *Neisseria meningitidis* that improves the survival of the bacterium in human blood by binding human factor H (fH), a down-regulator of the complement alternative pathway [197] . Lastly, NadA is one of the surface adhesins of *Neisseria*

*meningitide*s which interacts with several cell types and plays an important role for host cell interaction [198].

3.7.3 From Reverse Vaccinology to Reverse Vaccinology 2.0

The discovery of vaccine antigens through whole genome sequencing (WGS) is captured in the term *Reverse Vaccinology* (RV), which was first introduced by Rappuoli for the development of an effective vaccine against serogroup B *Neisseria meningitidis* (Bexsero) [208]. It is worth emphasizing that the formulation of this complex vaccine could not have been achieved without the systematic, WGS-based approach. In contrast to conventional vaccine development strategies, RV offers a method to facilitate rapid vaccine design and reduces reliance on the traditional, relatively tedious, and labor-intensive approach based on Pasteur's principles of isolating, inactivating, and injecting the causative agent of an infectious disease. The genome sequence provides at once a catalog of virtually all protein antigens that the pathogen can express at any time. RV poses the question of whether any of the potential antigen candidates can provide protective immunity without knowing whether the antigen is abundant, immunogenic, or expressed *in vitro* [199].

Nowadays, the high throughput discovery of protective human antibodies, sequencing of the B cell repertoire, and the increasing structural characterization of protective antigens and epitopes has provided the molecular and mechanistic understanding which led to the "*Reverse Vaccinology 2.0"*.

The *Reverse Vaccinology 2.0* approach, depicted in **Figure 3.7.1**, was indeed used in this work for the interrogation of single-sorted B cells through direct screening of mAbs. Starting from single B-cells sorted, we were able to characterize the genetic and functional properties of the produced mAbs in order to identify protective antigens and, eventually, epitopes.

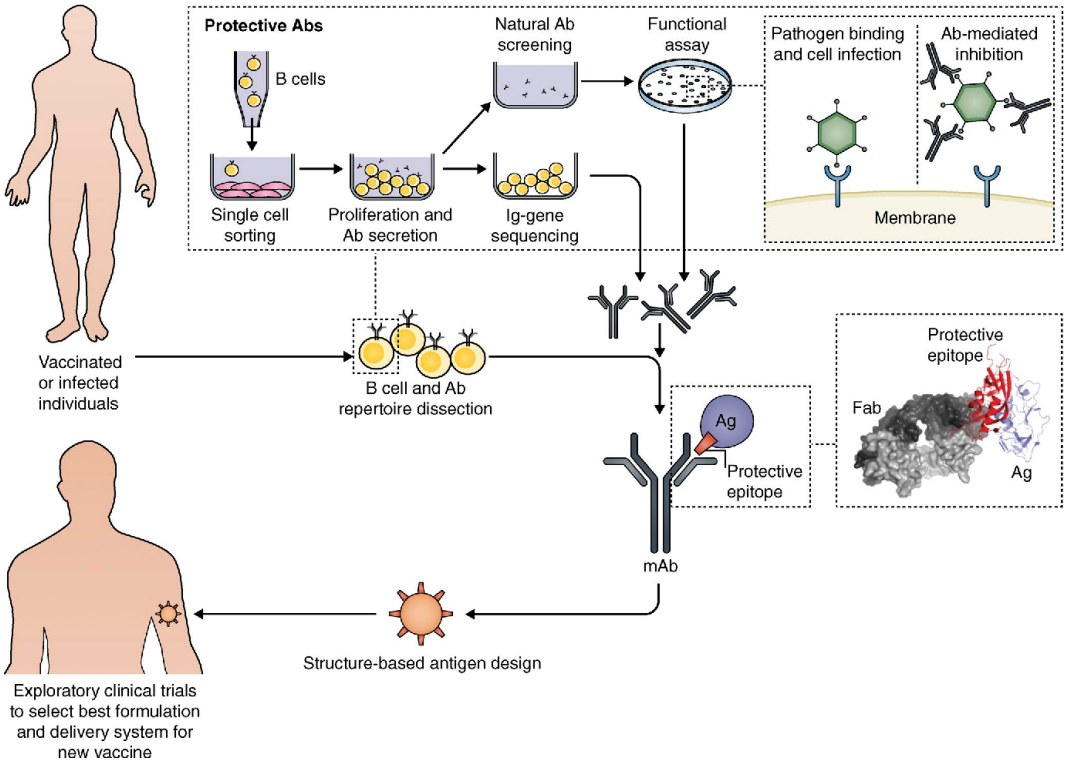

Figure 3.7.1 Representation of how human B cells enable the identification of protective mAbs from vaccinated or infected subjects. Single B cell sorting and culturing in the presence of feeder cells allow direct screening and selection of naturally produced mAbs with functionality and recovery of the corresponding Ig gene sequence. This approach allows for the interrogation of single-sorted B cells through direct screening of mAb functionality. The figure was taken from Rappuoli, 2016.

4 SARS-CoV-2

4.1 The emergence of a third novel Coronavirus

On 31st December 2019, the Chinese authorities reported to the WHO [209] the occurrence of several cases of a mysterious pneumonia. The origin of the Coronavirus Disease 2019 (COVID-19) pandemic was traced back to a cluster of pneumonia cases connected to a wet seafood market in Wuhan City, Hubei Province, China. At the beginning of March 2020, the virus began to spread in Italy [210].

Based on the data provided daily by the European Centre for Disease Prevention and Control (ECDC), since 31st December 2019 and as of week 48 2021, 266,018,810 cases of COVID-19 have been reported, including 5,265,092 deaths.

Fortunately, on 14th December 2020, the first vaccine against COVID-19, developed by Pfizer BioNTech, was approved for emergency use authorization by the Food and Drug Administration (FDA) in the United States. It was the first vaccine manufactured with the mRNA technology [211].

4.2 SARS-CoV-2 genomics and structure

Coronaviruses (CoVs) are a group of enveloped, positive-sense single-stranded RNA viruses [212]. All the highly pathogenic CoVs, including Severe Acute Respiratory Syndrome Coronavirus-2 (SARS-CoV-2), belong to the Betacoronavirus genus, group 2. The SARS-CoV-2 genome sequence shares ~80% sequence identity with SARS-CoV and ~50% with Middle East respiratory syndrome Coronavirus (MERS-CoV) [213]. It comprises 14 open reading frames (ORFs), two-thirds of which encode 16 nonstructural proteins (nsp 1–16) that

make up the replicase complex. The remaining one-third encodes nine accessory proteins (ORF) and four structural proteins: spike (S), envelope (E), membrane (M), and nucleocapsid (N), of which Spike mediates CoV entry into host cells [214].

4.2.1 Spike glycoproteins

CoV entry into host cells is mediated by spike (S) glycoprotein [216] which represents an attractive antiviral target. S protein is composed of two functional subunits, including the S1 and S2 subunits. The S1 subunit consists of N-terminal domain (NTD) and receptor binding domain (RBD) [216]. The function of S1 subunit is to bind to the receptor on host cells, while S2 subunit contains fusion peptide (FP), heptad repeat 1 (HR1), central helix (CH), connector domain (CD), heptad repeat 2 (HR2), transmembrane domain (TM), and cytoplasmic tail (CT). Also, S2 subunit mediates the fusion of the membranes of viruses and host cells. The S1/S2 protease site induces cleavage of the spike glycoprotein at the S2' cleavage site to activate the protein which then promotes fusion of the membranes of viruses and host cells through irreversible conformational changes. [299].

4.2.2 The Receptor Binding Domain (RBD)

The SARS-CoV-2 Spike RBD mediates direct contact with angiotensin-converting enzyme 2 (ACE2), and an S1/S2 polybasic cleavage site that is proteolytically cleaved by cellular cathepsin L and transmembrane protease serine 2 (TMPRSS2) [216]. TMPRSS2 facilitates viral entry at the plasma membrane surface, whereas cathepsin L activates SARS-CoV-2 Spike in endosomes and can compensate for entry into cells that lack TMPRSS2 [215], [216]. Once the genome is released into the host cytosol, ORF1a and ORF1b are translated into viral replicase proteins, which are cleaved into individual nonstructural proteins (nsps). Such nsps form the RNA-dependent RNA polymerase. Here, the replicase components rearrange the endoplasmic reticulum (ER) into double-membrane vesicles (DMVs) that facilitate viral replication of genomic and subgenomic

RNAs (sgRNA); the latter are translated into accessory and viral structural proteins that facilitate virus particle formation (**Figure 4.2.1)** [217].

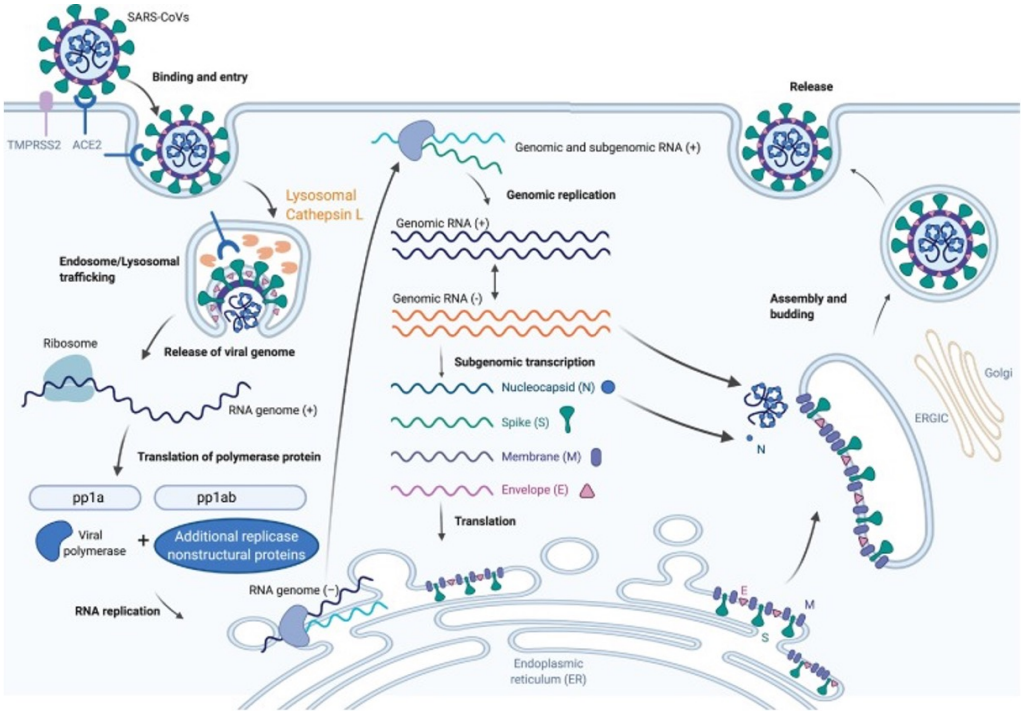

Figure 4.2.1 The Severe Acute Respiratory Syndrome Coronavirus 2 (SARS-CoV-2) lifecycle. It begins by binding of the envelope Spike protein to angiotensin-converting enzyme 2 (ACE2), The RNA genome is released into the cytosol, where it is translated into the replicase proteins. The polyproteins (pp1a and pp1b) are cleaved by a virus-encoded protease into individual replicase complex nonstructural proteins (nsps) Replication begins in virus-induced double-membrane vesicles (DMVs) derived from the endoplasmic reticulum (ER), which ultimately integrate to form elaborate webs of convoluted membranes. Here, the incoming positive-strand genome then serves as a template for full-length negative-strand RNA and subgenomic (sg)RNA. Finally, subsequent positive-sense RNA genomes are incorporated into newly synthesized virions, which are secreted from the plasma membrane. The figure was taken from Andrew G. Harrison, 2020.

A crucial study [207] showed that RBD goes through conformational transitions like a hinge, leading to the hide or exposure of the determinants of the spike protein to engage a host cell receptor. This process will form the following two states: “down” conformation and “up” conformation. In the “down” conformation, SARS-CoV-2 could not recognize the ACE2 on the host cells (**Figure 4.2.2**).

Importantly, the development of RBD-targeting vaccines and neutralizing antibodies, showed the strong ability to inhibit viral entry through disrupting the

binding between RBD to the receptor ACE2, which could provide a wider perspective to the design novel therapeutic approaches as well as vaccines against COVID-19.

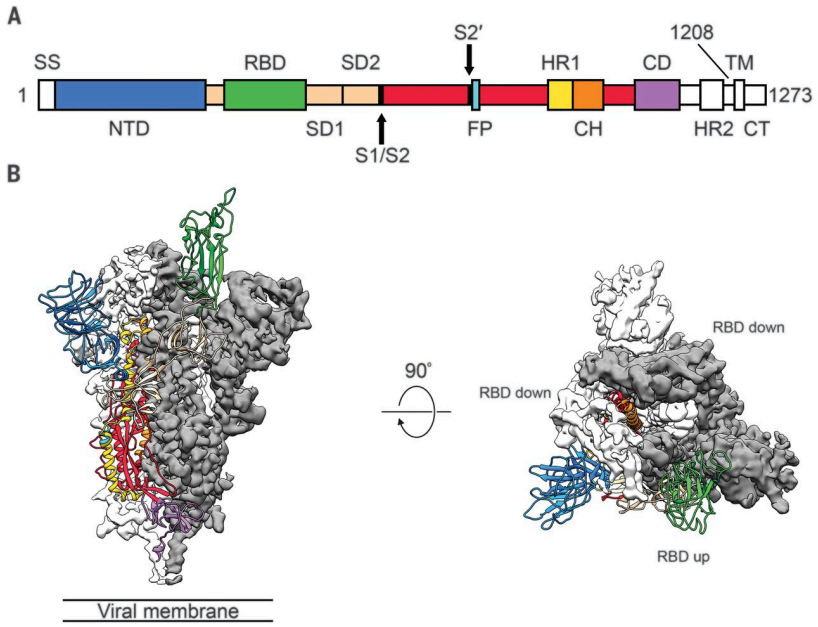

Figure 4.2.2 Cryo-EM of the SARS-CoV-2 spike protein in the prefusion conformation. (**A**) Schematic of SARS-CoV-2 **S** primary structure colored by domain. (**B**) Side and top views of the prefusion structure of the 2019-nCoV S protein with a single RBD in the up conformation. Image taken from Daniel Wrapp, 2020.

4.3 Passive immunotherapy and neutralizing antibodies

Administration of convalescent plasma to 5,000 COVID-19 hospitalized patients demonstrated to be safe as the occurrence of serious adverse events was low and likely to be beneficial when given at an early stage of COVID-19 [303]. Indeed, during the first months of this pandemic, many groups have been active in isolating and characterizing mAbs from COVID-19 convalescent patients or from humanized mice, and some of them have been progressing quickly to clinical trials for the prevention and cure of SARS-CoV-2 infection [303].

The dose of mAbs so far used in clinical trials against SARS-CoV-2 is high, ranging from 500 to 8,000 mg. High dosage has cost-associated implications

making this therapeutic intervention extremely costly and therefore available almost exclusively in high-income countries.

In this work, we identified and characterized extremely potent antibodies which can be used at low dosage to make them affordable and conveniently delivered by intramuscular injection. In addition, we mitigated the risk of ADE by engineering their Fc region [126]. The workflow is depicted in the **Figure 4.3.1**.

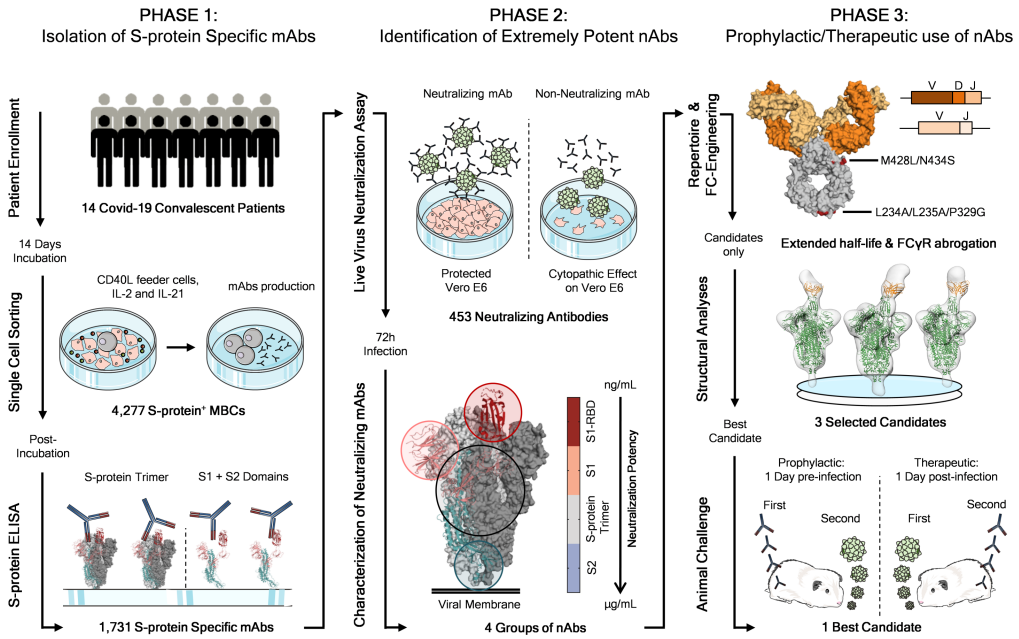

Figure 4.3.1 Worflow used for the identification of SARS-CoV-2 neutralizing antibodies (nAbs). Phase 1 consisted in the enrolment of COVID-19 patients from which PBMCs were isolated. Memory B cells were single cell sorted, and after 2 weeks of incubation, antibodies were screened for their binding specificity against the S protein trimer and S1/S2 domains. Once S protein-specific mAbs were identified, phase 2 started. All specific mAbs were tested *in vitro* to evaluate their neutralization activity against the authentic SARS-CoV-2 virus. nAbs were selected for further functional characterization. Phase 3 starts with the characterization of the heavy and light chain sequences of selected mAbs and the engineering of the Fc portion of three most promising candidates. Finally, the most potent antibody was tested for its prophylactic and therapeutic effect. The figure was taken from Emanuele Andreano, 2021.

5 Aim of the thesis

In the context of antimicrobial resistance (AMR) and emerging infectious diseases, we put our efforts into the discovery of highly effective monoclonal antibodies (mAbs) capable of either neutralizing or attenuate bacterial and viral infections.

Specifically, this work aimed to identify functional mAbs against *Neisseria gonorrhoeae* (Ng) and SARS-CoV-2.

Using the *Reverse Vaccinology 2.0* approach we:

- Isolated mAbs against *Neisseria gonorrhoeae* (Ng) from people vaccinated with 4CMenB Bexsero (®), a meningococcal serogroup B vaccine, to unveil the antigens and mechanism(s) responsible for the mediated cross-protection.

- Isolated mAbs from SARS-CoV-2 convalescent donors to rapidly identify extremely potent mAbs capable of neutralizing the SARS-CoV-2 infection.

The final goal of this work is to accelerate the identification of novel antigens/epitopes in order to implement novel therapeutic and prophylactic interventions based on the use of mAbs.

6 Materials and Methods

6.1 Single cell sorting of Bexsero vaccinees

Peripheral blood mononuclear cells (PBMCs) were isolated from heparin-treated whole blood by density gradient centrifugation (Ficoll-Paque PREMIUM, Sigma-Aldrich). After separation, PBMCs were stained with Live/Dead Fixable Aqua (Invitrogen, Thermo Fisher Scientific, US) in 100 µL final volume diluted 1:500 at room temperature (RT). After 20 min incubation cells were washed with PBS and unspecific bindings were saturated with 50 µL of 20% normal rabbit serum (Thermo Fisher Scientific, US) in PBS. Following 20 min incubation at 4°C cells were washed with PBS and the staining mixes were used for plasma cells (PCs) and memory B cells (MBCs) isolation. PCs, from Visit 2, were stained with CD19 v450 (BD cat# 560354), CD20 PercP Cy5.5 (BD cat# 560907), CD27 PE (BD cat# 340425), CD38 BB515 (BD cat# 564498) and IgD Alexa700 (BD cat# 348230). MBCs, from Visit 3, were stained with CD19 V421 (BD cat# 562440), IgM PerCP-Cy5.5 (BD cat# 561285), CD27 PE (BD cat# 340425), IgD-A700 (BD cat# 561302), CD3 PE-Cy7 (BioLegend cat# 300420), CD14 PE-Cy7 (BioLegend cat# 301814), CD56 PECy7 (BioLegend cat# 318318) and New Zealand OMVs labeled with Alexa-488 for 30 min at 4°C. Stained PCs and MBCs were single cell-sorted with BD FACS Aria III (BD Biosciences) into 96-well plates containing DEPC water, RNAseOut, BSA or 384-well plates containing 3T3-CD40L feeder cells, respectively. PCs were stored at -80°C until RT-PCR was performed while MBCs were incubated with IL-2 and IL-21 for 14 days at 37°C in 5% CO_2.

6.2 Single cell Reverse Transcription –Polymerase Chain Reaction (RT-PCR) and Ig gene amplification

From the original 384-well sorting plate, 5 µL of cell lysate was used to perform RT-PCR. Total RNA from single cells was reverse transcribed in 25 µL of reaction volume composed of 1 µL of Ig gene-specific primer mix (10 µM) (Table S1), 1 µL of dNTP-Mix (10 mM), 2 µL 0.1 M DTT, 40 U/µL RNase OUT, $MgCl_2$ (25 mM), 5x FS buffer and Superscript IV reverse transcriptase (Invitrogen). Final volume was reached by adding nuclease-free water (DEPC). Reverse transcription (RT) reaction was performed at 42°C/10 min, 25°C/10 min, 50°C/ 60 min and 94°C/5 min. Heavy (VH) and light (VL) chain amplicons were obtained via two rounds of PCR. All PCR reactions were performed in nuclease-free water in a total volume of 25 µL. Briefly, 4 µL of cDNA were used for the first round of PCR (PCR I). PCR I master mix contained 10 µM of VH and 10 µM VL primer-mix (Table S1), 10 mM dNTP mix, 0.125 µL of Kapa Long Range Polymerase (Sigma), 1.5 µL $MgCl_2$ and 5 µL of 5x Kapa Long Range Buffer. PCR I reaction was performed at 95°C/3 min, 5 cycles at 95°C/30 sec, 57°C/30 sec, 72°C/ 30 sec and 30 cycles at 95°C/30 sec, 60°C/30 sec, 72°C/30 sec and a final extension at 72°C/2 min. All nested PCR reactions (PCR II) were performed using 3.5 µL of unpurified PCR I product and PCR II primer-mix (Table S1), using the same cycling conditions as PCR I. PCR II products were then purified by Millipore MultiScreen PCR 96 plate according to the manufacturer's instructions. Samples were eluted in 30 µL nuclease-free water into 96-well plates and quantified by Qubit Fluorometric Quantitation assay (Invitrogen).

6.2.1 Cloning of variable region genes and recombinant antibody expression in the transcriptionally active PCR fragment format (TAP)

Vector digestions were carried out with the respective restriction enzymes AgeI, SalI and XhoI as previously described by Tiller and colleagues [211]. Briefly, 75 ng of IgH, Igl and Igk purified PCR II products were ligated by using the Gibson Assembly strategy (NEBuilder HiFi DNA Assembly Master Mix, New England

Biolabs) into 25 ng of IgG1, Igl or Igk expression vectors. The reaction was performed in 5 µL total volume. The ligation product was 10-fold diluted in nuclease-free water and used as the template for transcriptionally active PCR (TAP) reaction which allowed the direct use of linear DNA fragments for *in vitro* expression. The entire process consists of one PCR amplification step using TAP primers (Table S1) that add functional promoter (human CMV) and terminator sequences (SV40) onto the PCR II products. TAP reaction was performed in a total volume of 25 µL using 5 µL of Q5 polymerase (NEB), 5 µL of GC Enhancer (NEB), 5 µL of 5X buffer, 10 mM dNTPs, 0.125 µL of forward/reverse primers and 3 µL of ligation product. TAP reaction was performed by using the following cycling conditions: 98°C/2 min, 35 cycles composed of 98°C/10 sec, 61°C/20 sec, 72°C/1 min and 72°C/5 min as the final extension step. TAP products were purified under the same PCR II conditions, quantified by Qubit Fluorometric Quantitation assay (Invitrogen) and used for transient transfection in the Expi293F cell line according to the manufacturer's instructions.

6.2.2 Flask expression and purification of human monoclonal antibodies

Expi293F cells (Thermo Fisher Scientific) were transiently transfected with plasmids expressing the antibody heavy and light chains in a 1:2 ratio. The transfection process lasts for six days at 37°C with 8% CO_2 in shaking conditions according to the manufacturer's protocol (Thermo Fisher Scientific, US). ExpiFectamine 293 transfection enhancers 1 and 2 were added 16 to 18 h post-transfection to boost cell viability and protein expression. Cell cultures were harvested six days after transfection. Supernatants collected were then pooled and clarified by centrifugation (4,500 xg, 15 min, 4°C) followed by filtration through a 0.22 mm filter. Chromatography was conducted at room temperature using the AKTA Go purification system from GE Healthcare Life Sciences. Affinity chromatography was used to purify expressed monoclonal antibodies using an immobilized protein G column able to bind to the Fc region. Specifically, filtered culture supernatants were purified with a 1 mL HiTrap Protein G HP column (GE Healthcare Life Sciences) previously equilibrated in Buffer A (0.02 M NaH_2PO_4 pH 7). The flow rate for all steps of the HiTrap Protein G HP column was 1

mL/min. Culture supernatants were applied to 1 mL HiTrap Protein G HP column. The column was equilibrated in Buffer A for at least 6 column volumes (CV) which was collected as the column wash. Each monoclonal antibody was eluted from the column by applying a step elution of 6 CV of Buffer B (0.1 M glycine-HCl, pH 2.7) and by collecting 1 mL elution fractions. Eluted fractions were analyzed by non-reducing SDS-PAGE and fractions showing the presence of IgG were pooled together. Final pools were dialyzed in PBS buffer pH 7.4 using Slide-A-Lyzer G2 Dialysis Cassette 3,5K (Thermo Fisher Scientific) overnight at 4°C. The dialysis buffer used was at least 200 times the volume of the sample. Antibody concentration was determined by measuring the absorbance at 520 nm using Pierce BCA Protein Assay Kit (Thermo Fisher Scientific). All the purified antibodies were aliquoted and stored at -80°C.

6.3 Bacterial strains and culture conditions

Fresh cultures of different Ng strains (**Table 2**) were prepared from frozen stocks by streaking onto gonococcal agar (GCA) consisting of agar base supplemented with 1% v/v IsoVitaleX (BD Biosciences, Franklin Lakes, NJ, USA). On the following day, bacteria were grown in gonococcal (GC) liquid medium at 37°C, 5% CO_2 starting from OD_{600} 0.1 until mid-log phase cultures, i.e., OD_{600} 0.5.

Table 2. *Neisseria gonorrhoeae* strains used in this study.

Ng strains	Isolation site	Porin	Source
FA1090	Lab strain	PorB1B	ATCC
BG27	Clinical isolate	PorB1B	University of Bristol, UK
F62	Lab strain	PorB1B	ATCC
WHO F	WHO strain*	PorB1A	Örebro University Hospital, Sweden
WHO N	WHO strain*	PorB1A	Örebro University Hospital, Sweden

*The WHO reference strains are intended for internal and external quality assurance and quality control in laboratory investigations.

6.4 Whole-bacterial cell enzyme-linked immunosorbent assay (ELISA)

After growth, bacteria were first centrifuged at 4,500 xg for 5 min and then resuspended in PBS with the same volume. Bacteria were seeded into 384-well plates and incubated at 37°C, 5% CO_2 for 30 min. After incubation, plates containing bacteria were automatically washed twice by using a washer dispenser (BioTek EL406, Agilent Technologies, US) with PBS, Tween20 0.05%, 150 µL/well. Bacteria were fixed with 0:5% formaldehyde at RT for 30 min. Wells were washed and the saturation step followed using PBS, BSA 1% in 75 µL to avoid unspecific binding and plates were incubated at 37°C for 1 h. After incubation, wells were washed, and primary antibodies contained into the TAP-supernatants were added in a 1:5 ratio in PBS, BSA 1%, Tween20 0.05% in 25 µL /well final volume and incubated for 1 h at 37°C without CO_2. Wells were washed and 25 µL /well of alkaline phosphatase-conjugated goat anti-human IgG (Sigma-Aldrich, US) and IgA (Southern Biotech) were used as secondary antibodies. A final wash followed and then pNPP (p-nitrophenyl phosphate) (Sigma-Aldrich) was used as a substrate to detect the binding of the mAbs. Absorbance was measured by using the Varioskan Lux Reader (Thermo Fisher Scientific, US) at 405 nm. Samples were considered as positive if OD at 405 nm (OD_{405}) was three times the blank.

6.5 Screening for binding by Luminex

In order to perform the screening, two different panels were implemented (**Table 3**) based on reagent availability. Panel 1 only, included recombinant proteins NHBA, fHbp and NadA present in the Bexsero formulation along with the gonococcal PorB and the meningococcal PorA. While both Panel 1 and 2 included Outer Membrane Vesicle (OMV) from a New Zealand (NZ) meningococcal group B strain. Also, different gonococcal OMVs and Generalized Modules for

Membrane Antigens (GMMAs) were present in both Panels in order to assess cross-reactivity of mAbs. GMMAs are OMVs derived from gram-negative bacteria engineered to provide an over-vesiculating phenotype [212]. GMMAs used in our experiments were Δlpx, which is a knockout mutant encoding UDP-GlcNAc acyltransferase required for the first step of lipid A biosynthesis [213]. Antigens were obtained in PBS and coupled to different Luminex beads (MagPlex). 5 µl of transfection supernatants were incubated with 5 µl of the antigen mixture diluted 1:7 in PBS, Tween20 0.05%, 1% BSA for 1 hour with shaking at 1,200 xg. Beads were washed 3 times with PBS, Tween20 0.05% and incubated for 45 min with R-Phycoerythrin-AffiniPure F(ab')2 Fragment Goat Anti-Human IgG, Fcγ Fragment Specific (109-116-098; Jackson Immunoresearch, US). After 3 washes, beads were resuspended in PBS, Tween20 0.05% and signals were acquired by BioPlex 3D suspension array system (#BioPlex3D; BIO-RAD).

Table 3 Antigens used for binding screening by Luminex.

Luminex Panel 1			Luminex Panel 2		
Porins	OMVs	GMMAs	Proteins	OMVs	GMMAs
PorB_1a	FA1090	MS11_Δlpx	NadA	FA1090	MS11_Δlpx
PorB_1b	BG27	SK92_Δlpx	NHBA	BG27	SK92_Δlpx
PorA_MenB	WHO F	F62_Δlpx	fHbp	WHO F	F62_Δlpx
	WHO N	FA1090_Δlpx		WHO N	
	NZ	BG27		NZ	

*Luminex Panel 1 was used for Sbj 1 and Sbj 2 screening (Visit 2 and 3).
**Luminex Panel 2 was used for Sbj 3 and Sbj 4 screening (Visit 2 and 3).

6.6 Luminescence-Based Serum Bactericidal Assay (L-SBA)

To study the activity of the mAbs which were positive for binding to at least one Ng strain, we designed an assay based on the detection of ATP as a proxy of viable bacteria.

Baby rabbit complement (BRC) (Cedarlane, Burlington, Canada) was used as a source of complement in L-SBA assays. BRC was diluted to 10% v/v for FA1090 strain, while 20% v/v was used for BG27 strain. BRC was heat-inactivated (hiBRC) at 56°C for 30 min before use as a complement inactivated control.

Ng was grown to mid-log phase and resuspended in Dulbecco's modification of PBS (PBSB) as detailed above. Reactions were performed by incubating bacteria with TAP supernatants in PBSB, 2% FBS and 0.1% glucose and in the presence of 10% v/v of BRC in round bottom 96-well plates. hiBRC control adjusted to a final volume of 50 µL in PBSB, 2% FBS and 0.1% glucose was used. The reactions were incubated for 2 h at 37°C, 5% CO_2. After the incubation, plates were centrifuged for 8 min at 4,500 ×g. The supernatant was discarded to remove ATP derived from dead bacteria and the pellets were re-suspended in 30 µL of 1% PBS. This suspension was transferred to a 96-well white flat bottom plate (Greiner Bio-One, Kremsmünster, Austria) and an equal volume of BacTiter-Glo reagent (Promega, US) was added to each well. The reaction was incubated for 5 min at RT on an orbital shaker before the luminescence signal was read using a Varioskan™ LUX multimode microplate reader (Thermo Fisher Scientific, Waltham, MA, USA).

6.7 SDS-PAGE and Immunoblotting for anti-LOS mAbs

Ng LOS was prepared as follows. FA0190 was grown in 50 mL, as descrived, and centrifuged at 4,500 xg, 5 min. Bacterial pellet was then lysed with 1% Triton-X-100, 150 mM NaCl, 2 mM EDTA, 20 mM Tris-HCl pH 7.5 and Proteinase K treatment was used to eliminate protein antigens. Protease K–digested bacterial lysates were separated on 12% Bis-Tris gels (Invitrogen) with MES running buffer (Invitrogen) and LOS was visualized by silver stain (Bio-Rad). LOS was transferred to polyvinylidene difluoride membranes (Millipore, Billerica, MA) by electroblotting. Membranes were then blocked with PBS, 1% milk for 1 h at 37°C

and probed with purified mAbs at 10 µg/mL, overnight at 4°C. mAb-reactive LOS bands were visualized with anti-human (IgG conjugated to alkaline phosphatase.

6.8 Binding characterization by cytofluorimetry

After bacterial growth, bacteria were first centrifuged at 4,500 xg, 5 min and then resuspended and diluted in PBS, 1% BSA to reach OD_{600} 0.2. 50 µL of bacterial suspension were seeded onto 96-well round bottom TC-treated microplates (Corning, US). Bacterial suspensions were centrifuged (4,500 xg, 5 min) and resuspended in a mixture with PBS, 1% BSA and primary antibodies at 10 µg/mL in 50 µL. An incubation step of 1 h followed, at 37°C, 5% CO_2. Bacterial suspensions were centrifuged (4,500 xg, 5 min) and resuspended in a mixture of PBS, 1% BSA and a goat anti-Human IgG secondary antibody, labeled with Alexa Fluor 488 (Thermo Fisher Scientific, US) in 50 µL. Bacterial suspensions were centrifuged (4,500 xg, 5 min) and fixed with 0.5% formaldehyde at RT for 30 min. After fixation, bacterial suspensions were centrifuged (4,500 xg, 5 min) and re-suspended in PBS in a final volume of 50 µL. The samples were read using BD FACS Canto II flow cytometer. At least 10,000 counts were acquired for each sample. The analysis was carried out using FlowJo (version 10).

6.9 Binding characterization by confocal imaging

Bacteria were grown, as described above, and re-suspended in PBS to achieve a final OD_{600} 0.2. 50 µL of diluted bacterial suspensions were seeded onto a 96-well glass-bottom plate (Perkin Elmer, US) and incubated for 30 min at 37°C, 5% CO_2 to allow adhesion of bacteria. After incubation, bacteria were fixed with 0.5% formaldehyde. After two washing steps, 50 µL of saturation buffer (PBS, 1% BSA) were added and the plate was incubated for 1 h at 37°C. After saturation, a mixture containing PBS, 1% BSA and primary antibodies (10 µg/mL) in 50 µL

was added. Samples were incubated for 1 h at 37°C. A washing step with 100 µL of PBS followed the incubation, and a goat anti-Human IgG secondary antibody, labeled with Alexa Fluor 488, was added (Thermo Fisher Scientific, US). The plates were incubated for 30 min at 37°C. After two washing steps with 100 µL of PBS, 4′,6-diamidino-2-phenylindole (DAPI) was added at a final concentration of 0.1 µg/mL to the pellet and incubated for 30 min at 4°C. Images were taken with Zeiss LSM700 microscopy system using a 100x objective and confocal settings.

7 Results part I: discovery of mAbs against *Neisseria gonorrhoeae*

7.1 Enrolment of Bexsero-vaccinated subjects

Subjects involved in this study have received two doses of Bexsero vaccine. Blood withdrawal occurred three times (Visits 1-3) (**Figure 13**). This first phase consisted in the enrolment of subjects (N=9) from which PBMCs, serum and plasma were isolated. During Visit 1 only plasma and serum were collected. Visit 2 occurred 7 days after the second dose, with the aim of isolating plasma cells (PCs) from the PBMCs, along with serum and plasma. Visit 3 occurred 28 days after the second dose in order to isolate memory B cells (MBCs) from PBMCs, along with serum and plasma. Notably, results presented in this work refer to a smaller cohort (N=4). **Figure 7.1.1** shows the immunization schedule that was used for this study.

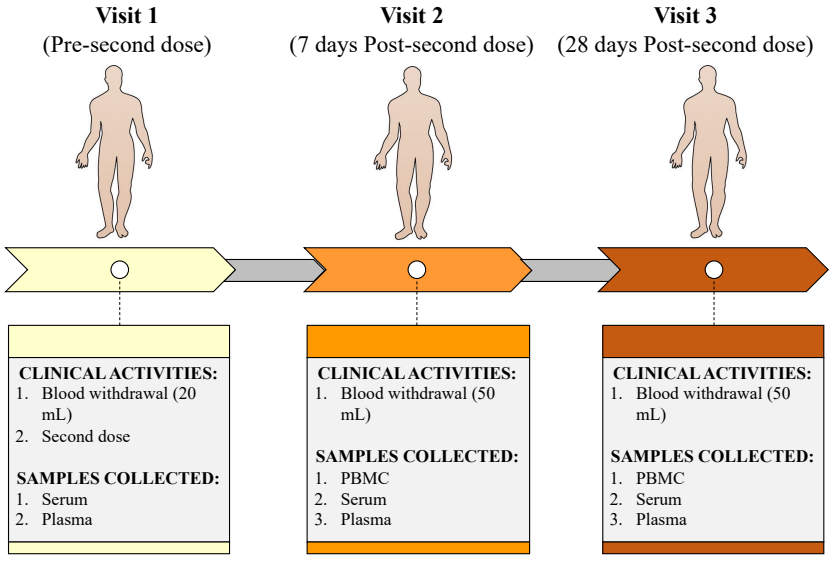

Figure 7.1.1. Immunization schedule for sample collection from Bexsero vaccinees.

7.2 Isolation of plasma cells and memory B cells

7.2.1 Plasma cells (PCs) from Visit 2

PCs were retrieved 7 days post second dose as the increase in PC numbers in peripheral blood is observed between day 7 and day 14, when long-lived plasma cells are produced in the germinal centers (GCs) [214]. As PCs do not proliferate [215], they were directly sorted into a lysis buffer (DEPC water, RNAseOut, BSA) and stored at -80°C until RT-PCRs. PCs were gated as $CD19^{+}$ $CD20^{-}$ $CD27^{+}$ $CD38^{+}$ IgD^{-} B cells (**Figure 7.2.1).** A total of 4,992 PCs were successfully collected (**Table 4**).

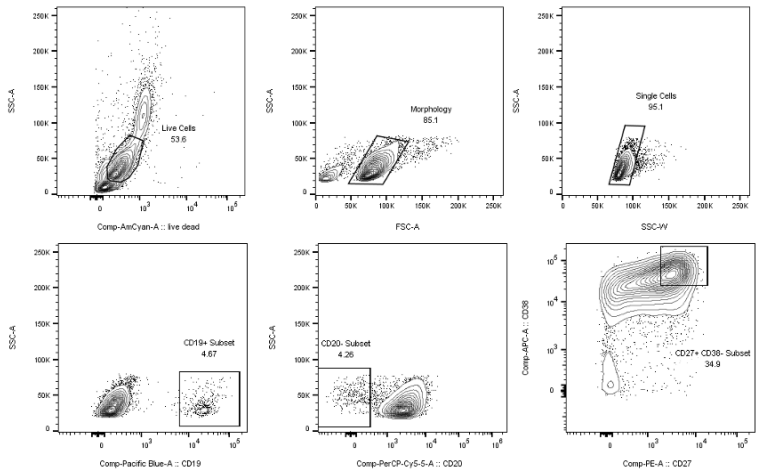

Figure 7.2.1. Gating strategy used for single cell sorting of PCs Live cells were gated on single cells, followed by gating on $CD19^{+}$ $CD20^{-}$ $CD27^{+}$ $CD38^{+}$ IgD^{-} cells to exclude T cells and monocytes and to gate on $CD19^{+}$ B-cells. PCs were sorted by FACS Aria III cytometer.

Table 4. Summary of PCs sorting. The Table reports the number of single cells sorted for each subject analyzed in this study.

Subject	Viable cells	Single PCs Sorted	N° of plates
Sbj 1	19.8×10^6	1920	20
Sbj 2	34.2×10^6	1920	20
Sbj 3	40.6×10^6	672	7
Sbj 4	34.4×10^6	480	5
Total		4992	52

7.2.2 Memory B cells (MBCs) from Visit 3

To isolate MBCs specific for OMVs New Zealand (NZ), contained in the Bexsero formulation, PBMCs from Bexsero vaccinees were collected and stained with fluorescently labeled OMVs NZ^+. PBMCs were isolated 28 days after Bexsero second dose, when the primary antibody response has resolved, and antigen-specific cells are at their proliferation peak [214]. The gating strategy depicted in **Figure 7.2.2** was used to single-cell sort, into 384-well plates, IgG^+ and IgA^+ MBCs binding to OMVs NZ. The sorting strategy aimed to specifically identify class-switched MBCs ($CD19^+$ $CD27^+$ IgD^- IgM^-) in order to select only MBCs that underwent the maturation processes. A total of 4,609 OMVs NZ^+ MBCs were successfully retrieved with frequencies ranging from 0.81% to 2.73% (**Table 5**). After the sorting, MBCs were incubated over a layer of 3T3-CD40L feeder cells in the presence of IL-2 and IL-21 stimuli for 2 weeks to allow natural production of immunoglobulins [216].

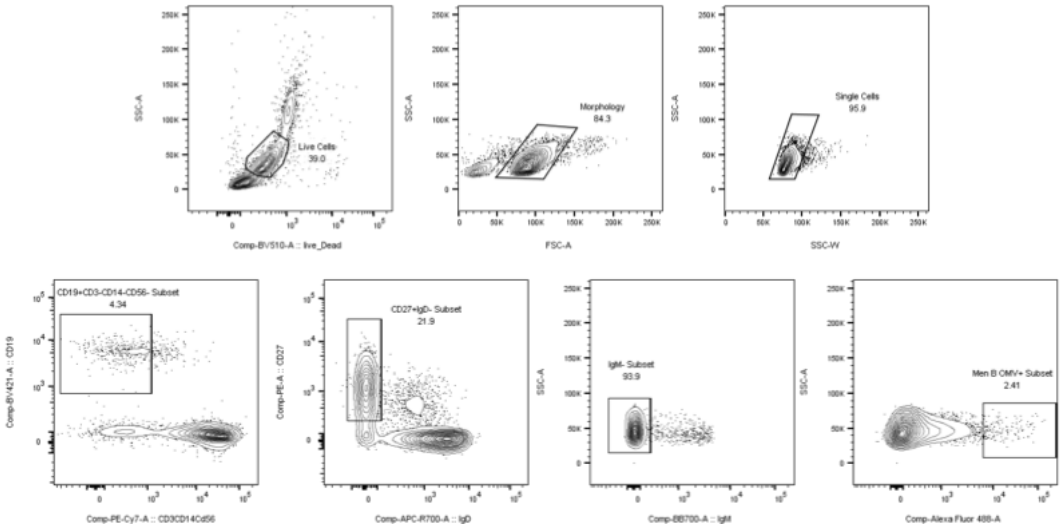

Figure 7.2.2. Gating strategy used for single cell sorting of MBCs. Cells were selected for live/dead, morphology, and singlets. Cells were then gated for $CD19^+$ IgD^- IgM^- and OMV NZ^+.

Table 5 Summary of MBCs sorting. The Table reports the frequency of antigen-specific cells and the number of single MBCs sorted for each subject analyzed in this study.

Subject	Viable cells	Antigen specific MBCs (%)	Single MBCs Sorted
Sbj 1	40.6 x 10^6	2.39	2004
Sbj 2	34.2 x 10^6	0.81	756
Sbj 3	49 x 10^6	2.41	1232
Sbj 4	36.4 x 10^6	2.73	616
Total			4608

7.3 Identification of mAbs binding to Ng (whole-bacterium binders)

To simplify the screening of sorted PCs and MBCs, a whole bacterial cell enzyme-linked immunosorbent assay (ELISA) was established and optimized. The assay was performed in 384-well plates and was used to detect plasma cell supernatants (PC SNs) from Visit 2, and MBC supernatants (MBC SNs) from Visit 3, able to bind to different Ng strains (**Table 2**). The screening of Sbj 1 and Sbj 2 was performed against BG27, WHO F and WHO N strains, which were used to establish and validate the assay. Notably, the Ng strains used for Sbj 3 and Sbj 4 were different, except for BG27. Indeed, FA1090 and F62 replaced WHO F and WHO N as they resulted susceptible to the baby rabbit complement in L-SBA assay (not shown).

7.3.1 Whole bacterial cell ELISA Sbj 1 and Sbj 2, Visit 2

PC mAbs were expressed as full-length immunoglobulins, carrying the Hex3 mutation, as discussed previously, using the transcriptionally active PCR (TAP) method with more than 90% expression efficiency. 96 PC SNs from Sbj 1 and Sbj 2 (N=192) were expressed. PC SNs were tested for the ability to bind to BG27, WHO F and WHO N strains. A panel of 16 and 25 PC SNs was identified for Sbj 1 for Sbj 2, respectively (**Figure 7.3.1** (**A**)). The majority was able to cross-bind the three strains. The overall frequency of PC SNs positive for Ng ranged between 16% and 26%. The binding distribution of positive SNs was consistent, with the

majority able to cross-bind all the three strains tested (approaching 50%) and were named as “tri-specific” mAbs (**Figure 7.3.1** (**B**)).

Figure 7.3.1. Sbj1 and 2_Visit_2 whole-bacterial cell ELISA analysis and distribution. (**A**) Heat map of positive PC SNs screened for binding against BG27, WHO F and WHO N strains. (**B**) PC SNs distribution is shown on the donut charts. Threshold of positivity was set as two times the value of the blank**.**

7.3.2 Whole-bacterial cell ELISA Sbj 1 and Sbj 2, Visit 3

After 14 days of incubation to allow natural production of immunoglobulins, MBC SNs were screened against BG27, WHO F and WHO N strains (**Table 2**). A total of 2,004 MBC SNs from Sbj 1 and 756 MBC SNs from Sbj 2 were screened. 227 and 96 positive SNs from Sbj 1 and 2 were identified, respectively. The overall percentage of positive MBC SNs was very consistent, ranging around 12%. Compared to Visit 2, the binding distribution of the SNs was quite different. In particular, the majority of SNs was able to bind specifically the BG27 strain

only (almost 70%), while only 17% and 16% SNs from sbj1 and 2, respectively, was able to cross-bind all the Ng strains (**Figure 7.3.2**).

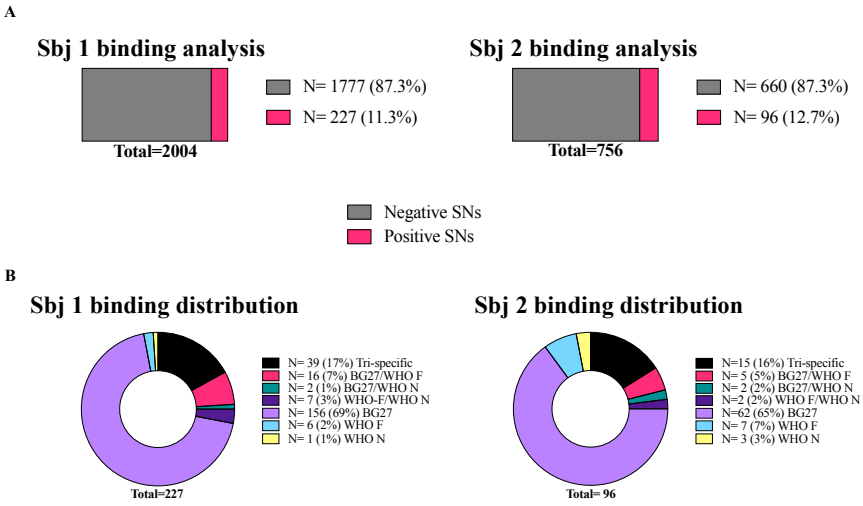

Figure 7.3.2. Sbj1_Sbj2_Visit_3 whole-bacterial cell ELISA analysis and distribution. MBC SNs were screened for binding against BG27, WHO F and WHO N strains. (**A**) Positive MBC SNs are shown in red. (**B**) MBC SNs binding distribution. Threshold of positivity was set as two times the value of the blank.

7.3.3 Whole-bacterial cell ELISA Sbj 3 and Sbj 4, Visit 2

As for Sbj 1 and Sbj 2, a whole bacterial cell enzyme-linked immunosorbent assay (ELISA) was performed on FA1090 strain. 192 PC SNs from Sbj 3 and Sbj 4 (N=384) were expressed as full-length immunoglobulins, with Hex3 mutation, as explained previously, and then tested for binding. A panel of 61 and 44 PC SNs was identified for Sbj 3 for Sbj 4, respectively. The overall frequency of positive PC SNs was 32% for Sbj 3 and 23% for Sbj 4 (**Figure 7.4.3**).

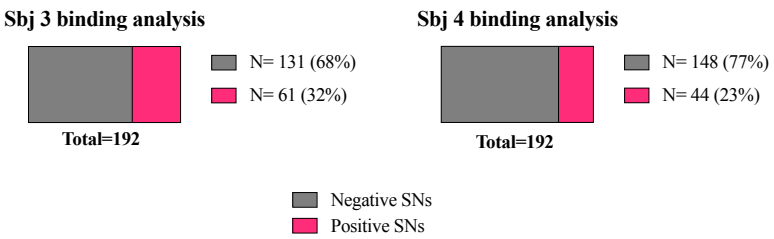

Figure 7.3.3. Sbj3_Sbj4_Visit_2 whole-bacterial cell ELISA analysis and distribution. PC SNs were screened for binding against FA1090. Positive PC SNs are shown in red. Threshold of positivity was set as two times the value of the blank**.**

7.3.4 Whole-bacterial cell ELISA Sbj 3 and Sbj 4, Visit 3

Naturally produced immunoglobulins were screened against FA1090, BG27 and F62 strains. A total of 1,232 and 616 MBC SNs from Sbj 3 and 4 were screened, respectively. A panel of 151 and 79 positive SNs from Sbj 3 and 4 was identified (**Figure 7.4.4** (**A**)). The overall percentage of positive MBC SNs was 12%, consistent with Sbj 1 and 2 Visit 3, although the panel of Ng strains was different. This scenario is partially justified by the presence of BG27 in both panels, which confirmed to be the most recognized strain during the screenings. As for the distribution of tri-specific mAbs (i.e., able to bind all of the three strains), this was very similar for Sbj 3 and 4, approaching 34% and 30%, respectively (**Figure 7.4.4** (**B**)).

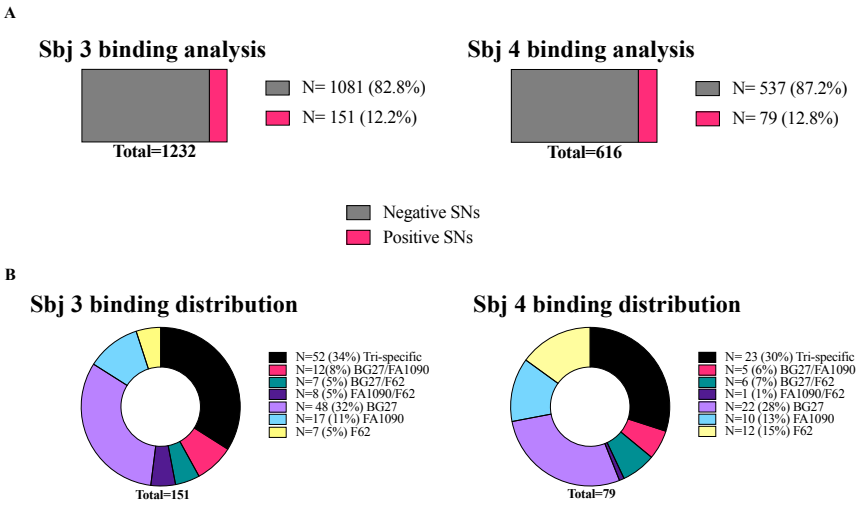

Figure 7.3.4. Sbj3_Sbj4_Visit_3 whole-bacterial cell ELISA analysis and distribution. MBC SNs were screened for binding against FA1090, BG27, and F62 strains. (**A**) Positive MBC SNs are shown in red. (**B**) MBC SNs binding distribution. Threshold of positivity was set as two times the value of the blank**.**

7.4 Identification of mAbs capable of binding to OMVs/GMMAs

Subsequently, PC and MBC SNs were tested for binding to GMMAs, OMVs and to Bexsero recombinant proteins in a multiplex Luminex assay. To increase the throughput of our approach, SNs were tested at a single-point dilution (1:5). SNs identified were classified as cross OMVs/GMMAs, protein-specific binders, or OMV NZ binders, based on the ability to react with the different antigens and the panel of antigens used. The panel of antigens changed based on the availability of reagents. Specifically, Panel 1 was used for Sbj 1 and 2, while Panel 2 was used for Sbj 3 and 4 (**Table 3**).

7.4.1 Luminex Sbj 1 and Sbj 2 (Visit 2)

From Sbj 1, 20 out of 96 (21%) positive PC SNs were identified, while from Sbj 2, positive SNs were 15 out of 96 (16%) (**Figure 7.4.1 (A**)). The majority of SNs from Sbj 1 was able to bind OMV NZ only (**Figure 7.4.1 (B**)), with poor PorA_MenB response, which is known to be immunodominant [217]. Whereas the 25% (N=5) was able to cross-react with most of the antigens, with the exclusion of GMMA_SK92_Δlpx. With respect of Sbj 1, Sbj 2 showed a stronger response to PorA_Men B as well as Ng_PorB. In particular, the majority of SNs positive for meningococcal and gonococcal Porins were able to cross-react to both strains, leading to the conclusion that they could recognize shared epitopes. Another difference lies in the distribution of cross-reactive mAbs against OMVs/GMMAs between the two subjects, which was higher for Sbj 1. The complete binding distribution is depicted in **Figure 7.4.1** (**B**).

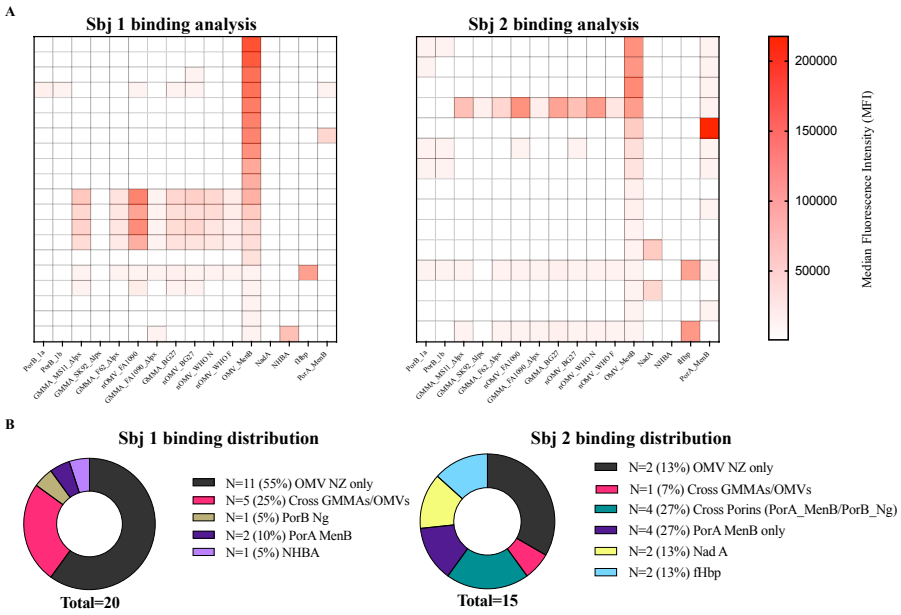

Figure 7.4.1. Sbj1_Sbj2_Visit_2 bacterial OMVs/GMMAs analysis and distribution. (**A**) Heat map of PC SNs screened for binding to OMVs and GMMAs from different gonococcal strains along with Porins and Bexsero recombinant proteins. (**B**) PC SNs distribution is shown on the donut charts. Threshold of positivity was set as three times the background fluorescence**.** Negative SNs are not shown.

7.4.2 Luminex Sbj 1 and Sbj 2 (Visit 3)

In the same way, naturally released MBC SNs were tested by Luminex. Panel 1 (**Table 3**) was used, except for PorB_MenB and Bexsero recombinant proteins, as they were not available. The classification criteria were the same used for Visit 2, with the aim to identify either cross-reactive or protein-specific binders. From Sbj 1, 191 SNs were positive out of 2,004 (9,5%), while 56 out of 756 (7,4%) were positive for Sbj 2 (**Figure 7.4.2** (**A**)). Unsurprisingly, the majority of SNs was able to bind OMV NZ only (**Figure 7.4.2** (**B**)) which accounted roughly for the 60% for both subjects. Cross-reactive SNs represented the 10% and 19% of Sbj 1 SNs and Sbj 2 SNs, respectively. The remaining SNs were mostly positive against Porins (PorB1B and PorB1A) and few Ng strains or only one, defined as bi-specific or strain specific. In particular, 5% of SNs (N=12) from Sbj 1 were positive for at least one allelic form of Porin (mostly PorB1B), while 9% of SNs (N=9) were positive for one allelic form of Porin only, either PorB1A or PorB1B.

The complete binding distribution for both subjects is depicted in **Figure 7.4.2** (**B**).

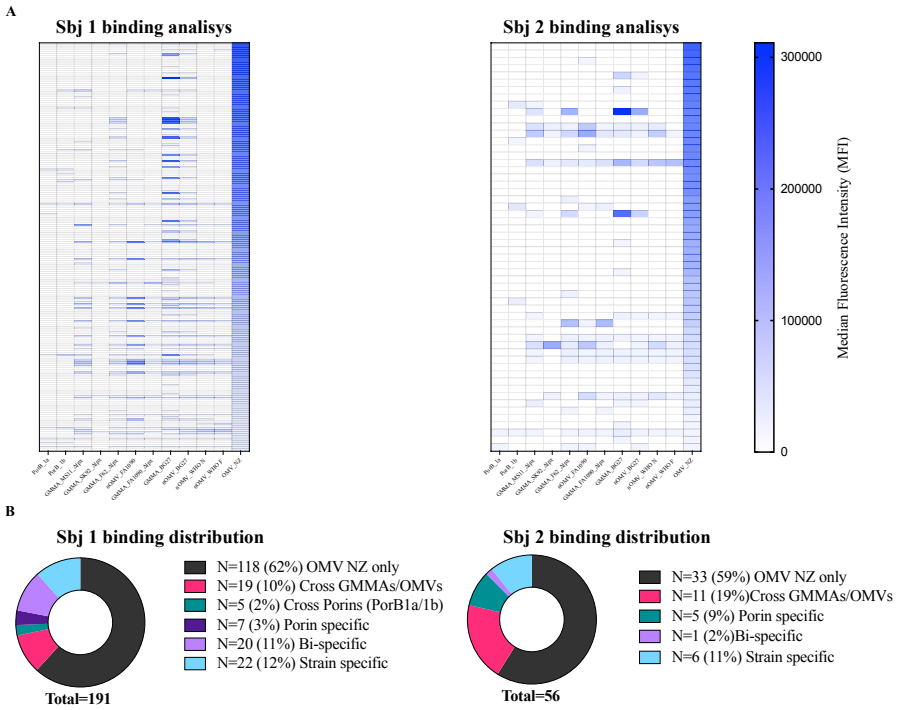

Figure 7.4.2. Sbj1_Sbj2_Visit_3 bacterial OMVs/GMMAs analysis and distribution. (**A**) Heat map of MBC SNs screened for binding to OMVs and GMMAs from different gonococcal strains along with Porins and Bexsero recombinant proteins. (**B**) MBC SNs distribution is shown on the donut charts. Threshold of positivity was set as three times the background fluorescence. Negative SNs are not shown.

7.4.3 Luminex Sbj 3 and Sbj 4 (Visit 2)

As shown in **Table 3**, panel 2 used for Sbj 3 and 4 was slightly different. In particular, Porins and Bexsero recombinant proteins were not present. This change was due to limited availability of the reagents.

From Sbj 3, 20 out of 96 (21%) positive PC SNs were identified, while from Sbj 4, positive SNs were 18 out of 96 (19%) (**Figure 7.4.5 (A)**). The majority of positive SNs from Sbj 3 was able to bind OMV NZ only (45%). The 40% was able to cross-react with most of the antigens. For Sbj 4, the trend was slightly different with the majority of SNs recognizing the OMV NZ only (61%), while only 22% (N=4) cross-reacted with most of the antigens. Interestingly, one cross-

reactive SN from Sbj 4 was negative for OMV NZ. The complete binding distribution for both subjects is depicted in **Figure 7.4.5** (**B**).

Figure 7.4.3. Sbj3_Sbj4_Visit_2 bacterial OMVs/GMMAs analysis and distribution. PC SNs were screened for binding to OMVs and GMMAs from different gonococcal strains. Threshold of positivity was set as three times the background fluorescence**.** Negative SNs are not shown.

7.4.4 Luminex Sbj 3 and Sbj 4 (Visit 3)

Likewise, MBC SNs from Visit 3, which were previously found to be positive in ELISA, were tested by Luminex and Panel 2 was used for the screening (**Table 3**). From Sbj 3, 170 out of 1,232 (13,7%) SNs were identified, but 51% of 170 SNs (N=88) was positive for OMV NZ only. On the other hand, 23% of the SNs (N=39) was capable of binding most of the antigens present on panel 2. The remaining 26% was able to bind only WHO F, WHO N and BG27 OMVs (**Figure 7.4.6** (**B**)). Regarding Sbj 4, 57 out of 616 SNs were identified (9%) and, unsurprisingly, the majority of SNs was able to bind OMV NZ only (63%). The cross GMMAs/OMVs accounted for 14% (N=8) and the remaining 23% (N=13) was able to bind only WHO F, WHO N and BG27 OMVs (**Figure 7.4.6** (**B**)).

Consistently with ELISA screenings, the BG27 strain was the most recognized strain.

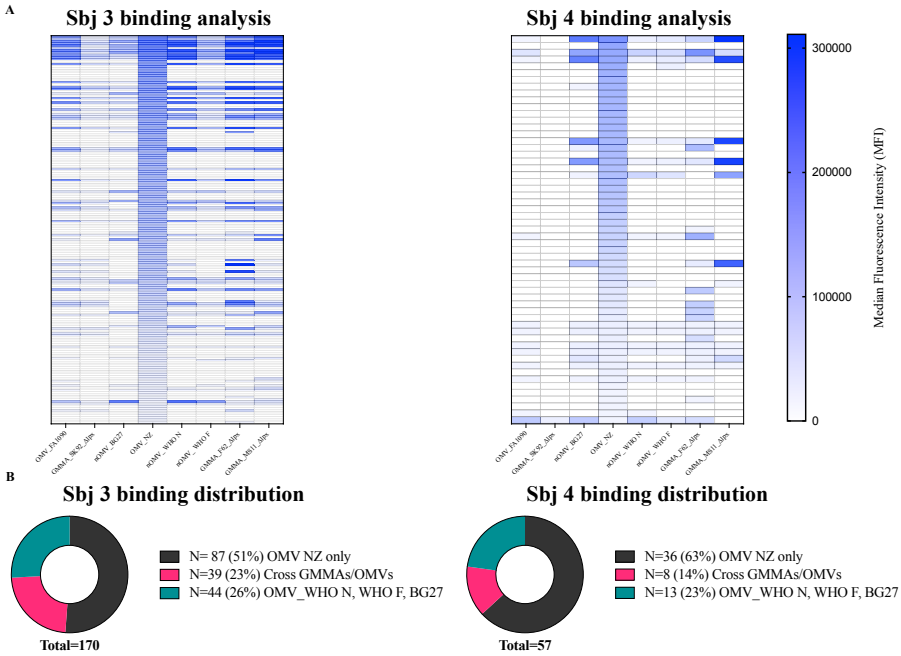

Figure 7.4.4. Sbj3_Sbj4_Visit_3 bacterial OMVs/GMMAs analysis and distribution. (**A**) Heat map of MBS SNs screened for binding to OMVs and GMMAs from different Ng strains. (**B**) MBC SNs distribution is shown on the donut charts. Threshold of positivity was set as three times the background fluorescence. Negative SNs are not shown.

7.5 Summary of binding assays

Both ELISA and Luminex contributed to identify mAbs capable of cross-reacting with different Ng strains. The ELISA assay, which was based on whole-bacterial cell binding, allowed the identification of antibodies able to bind either structures present on the bacterial surface and/or OMVs. Indeed, all of the mAbs identified by Luminex were positive in ELISA as well, except for OMV NZ only, possibly because they could recognize proteins absent on gonococcal OMVs. On the other hand, the Luminex assay allowed us to identify mAbs able to cross-react with more gonococcal OMVs and GMMAs, thus focusing our attention on the most

cross-reactive ones. **Table 6** summarizes the binding results obtained by ELISA and Luminex.

Table 6. Summary table of identified PC and MBC SNs by ELISA and Luminex.

	Plasma cells (Visit 2)		**Memory B cells** (Visit 3)	
Subject	ELISA	Luminex	ELISA	Luminex
1*	16	20	227	191
2*	25	15	96	56
3**	61	20	151	170
4**	44	18	79	57
Total	146	73	553	474

*ELISA was performed on BG27, WHO F and WHO N; Luminex was performed with Panel 1 (Table2).
** ELISA was performed on BG27, FA1090 and F62; Luminex was performed with Panel 2 (Table2).

7.6 L-SBA design for *in vitro* activity evaluation

In order to start a large screening, smaller test (or pilot) screenings are used to assess the quality of an assay to predict if it would be useful in a high-throughput setting. The Z-factor is an attempt to quantify the suitability of an assay for use in a full-scale, high-throughput screening which is defined by four parameters: the mean (μ), the standard deviation (σ) of both the positive (p) and negative (n) controls.

$$\text{Z-factor} = 1 - \frac{3(\sigma_p + \sigma_n)}{|\mu_p - \mu_n|}$$

We used this approach to optimize and validate our assay. The choice of experimental conditions and measurements that we adopted allowed us to calculate a Z-factor of 1, which means a huge dynamic range with tiny standard deviations, as nicely described by Zhang and colleagues [218].

To establish the assay, we started by cloning the variable regions VH and VL of the anti-gonococcal mAb 2C7 into appropriate heavy and light chain expressing

vectors [85]. To simulate a screening process, we performed a transcriptionally active PCR (TAP) to obtain DNA encoding light and heavy chains (carrying E430G mutation (Hex1)) of the mAb 2C7, as previously described. The PCR products were used to transfect the EXPI293F cell line. The obtained TAP SNs were used to perform high-throughput bactericidal assays using luminescence as a readout of bacterial viability. This assay measures luminescence generated in an ATP-dependent reaction catalyzed by luciferase and was therefore named luminescence-based serum bactericidal assay (L-SBA).

L-SBA was carried out by adapting a previously reported method which was successfully applied to analyze the bactericidal activity of mouse sera generated by immunization against different pathogens [219].

In order to assess if we were able to observe bactericidal activity, a simulation of screening was performed using different 2C7 TAP SNs (N=48) along with mock transfections TAP SNs (N=48). All of the SNs (N=96) were tested at a single point dilution of 1:5. The relative luminescence units (RLUs) of 2C7 TAP SNs were calculated and used as killing control, while sample wells with mock transfections were used as the negative reference. Specifically, the RLUs mean of mock transfections were used to set the negative reference. As shown in **Figure 7.5.1**, we were able to observe killing in all of the samples treated with 2C7, with almost no difference in RLUs, which may reflect a similar expression level of 2C7 in all of the samples. Whereas, mock transfections alone were not toxic, leading to the conclusion that there was no non-specific killing.

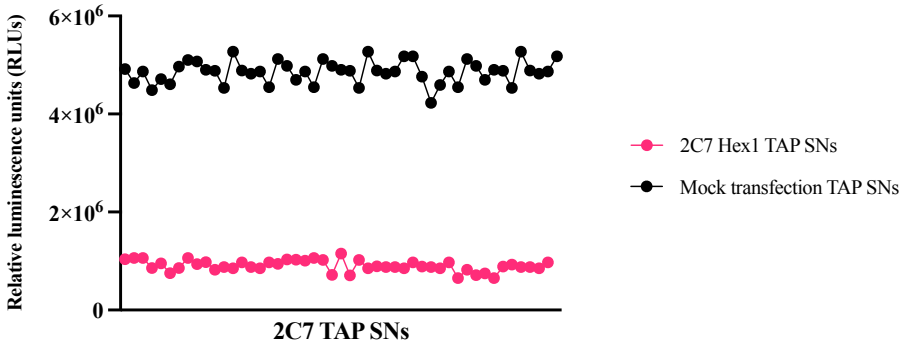

Figure 7.6.1. Simulation of screening with 2C7 TAP SNs. Different expressions of 2C7 Hex1 as TAP were used as control of killing, while mock transfections were used to set a negative control in a luminescence-based assay which measures ATP as a proxy of bacterial viability.

7.6.1 Test of plasma from Visit 3 by L-SBA

Once the assay was validated, we firstly tested the complement-mediated bacteriolysis caused by human plasma against FA1090 and BG27 to evaluate the humoral response from Visit 3 (**Figure 7.5.2**). Experiments were conducted to test the behavior of plasma under the assay conditions already established with 2C7. Plasma from Sbj 1 and 2 were found to be slightly active against FA1090 at 1:20-1:40 dilution but no impact was measured with BG27 strain, which appeared resistant to the presence of plasma. Assay conditions developed for TAP SNs screening were found not to be optimal for plasma screening, with the detection of a prozone effect when diluted at 1:5 - 1:10 for Sbj 1 and 2 with FA1090 (**Figure 7.5.2**). A prozone effect is defined for a curve readout vs. dilution (luminescence vs. plasma dilution) as a condition in which for the first points tested the readout value (RLUs) is higher than readout value obtained with points highly diluted.

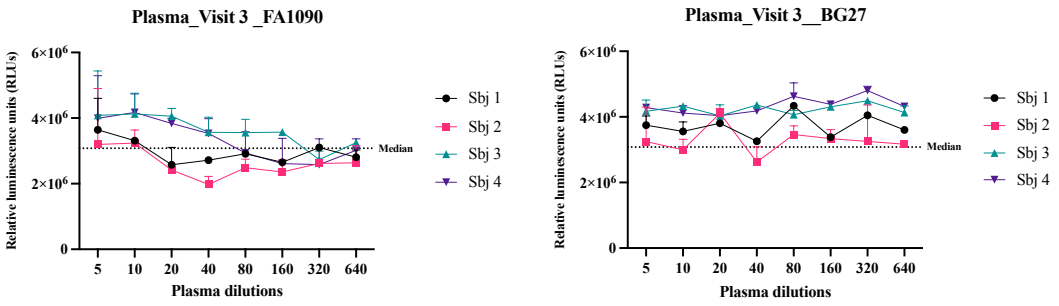

Figure 7.6.2. Test of plasma Visit 3 from Bexsero vaccinees. Bactericidal activity of individual plasma samples from subjects vaccinated with Bexsero. Bactericidal activity was assessed in the L-SBA against FA1090 and BG27 strains. For both strains, post-vaccination plasma (28 days after second dose) was tested. Plasma from the same Sbj1 and Sbj 2 showed a low bactericidal activity (1:20-1:40) against FA1090, while prozone effect was found at 1:5-1:10 dilution points. No bactericidal effect was found for BG27. The RLU median (reference control) is shown by the horizontal dotted lines. The L-SBA step titers from individual plasma (n=4) are indicated on the x-axis. Two replicates were performed for each dilution and are shown combined to display mean ± standard deviation.

7.6.2 First screening of MBCs and PC TAP SNs

In high-throughput screenings, experiments often compare many single measurements of unknown samples to positive and negative control samples. So, it can be difficult to understand the activity of an antibody (or other compounds), especially in primary screening without replicates. In this case, we could not directly calculate the variability of each SN. Thus, we assumed that each SN has the same variability as a negative reference and then we calculated the variability based on this threshold for all of the SNs investigated. We calculated the median of RLUs for each plate as a reference control. When a 10% RLU reduction compared to the median was measured, the corresponding SN was considered as a "hit". As shown in **Figure 7.5.3**, F62 displayed either very low or no serum-mediated killing after exposure to TAP SNs. In contrast, sensitivity was detected for FA1090 and BG27 strains, although to different extents (between 0%–90% killing).

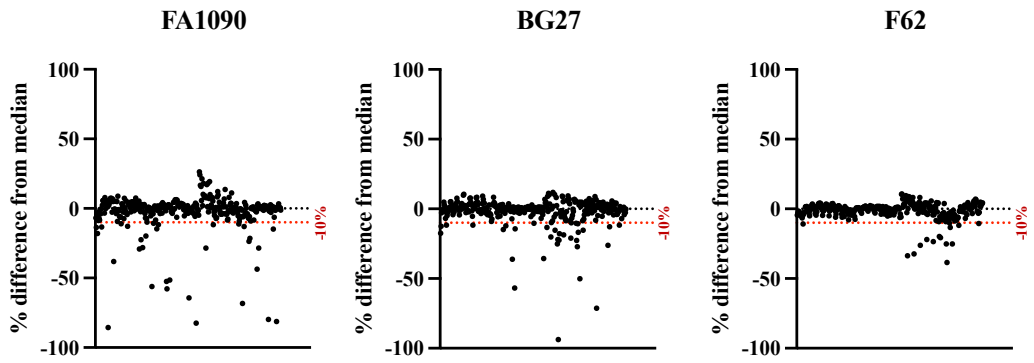

Figure 7.6.3. First screening of TAP SNs against three different Ng strains. The black dashed line represents the median value of the negative reference. The red dashed line shows the 10% reduction compared to the median value of each experiment. Dots below the red dashed line (or same level) are considered as "hit".

During this phase, a total of 699 TAP SNs (Sbj1-4), firstly selected for binding, were screened for functionality by L-SBA. The overall distribution of positive TAP SNs is illustrated in **Figure 7.5.4**.

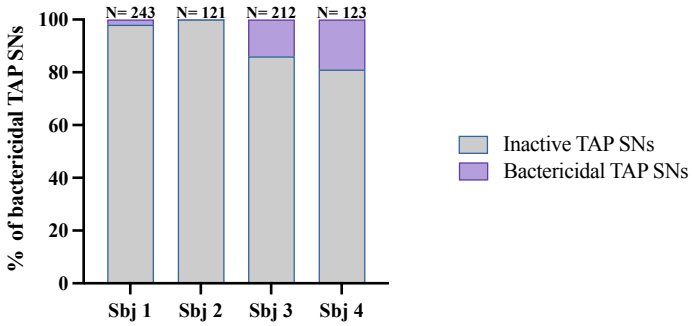

Figure 7.6.4. Distribution of bactericidal TAP SNs from first screening. TAP SNs activity based on the first screening on Ng strains (N=3) is shown. TAP SNs were tested at one single point dilution (1:5). The vast majority of TAP SNs was inactive (N= 639 - 91,5%), while only the 8,5% (N=60) of SNs have shown a possible activity. N=5 TAP SNs were identified from Sbj 1; Sbj 2 had no TAP SN active; Sbj 3 and 4 displayed the higher number of possible bactericidal TAP SNs, N= 31 (31/212 - 14%) and N=24 (24/ 123 - 19%), respectively.

7.6.3 Second screening: TAP SNs were classified into three groups

To avoid false "hits" given by non-specific killing, selected TAP SNs from the first screening (N=60) were further tested in 3 serial dilutions (1:5, 1:25, 1:125). 10% v/v of hiBRC control, adjusted to a final volume of 50 µL, was used for each sample and dilution tested. The bactericidal titre was measured when killing of bacteria, compared to the respective hiBRC control reaction, was detected. Confirmation of "hits" was obtained from three replicates compared to their respective hiBRC control, to exclude mAb-independent killing. Based on the behaviour, we classified TAP SNs in three groups (**Figure 7.5.5**). The first one was named "non-functional mAb" when the trend between BRC and hiBRC was similar, i.e., we could not appreciate any difference in RLUs in samples treated with BRC compared to hiBRC control. The second group was called "putative functional mAb" when a difference in RLUs in samples treated with BRC was obtained, although in the first dilution point only (1:5). Finally, we named as "functional mAb" each TAP SN that resulted in a clearly divergent trend between BRC and hiBRC in all of the three dilution points.

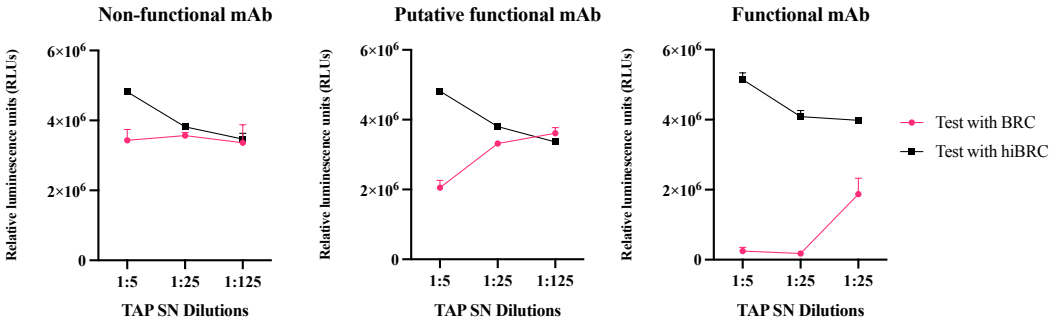

Figure 7.6.5. Classification of TAP SNs in three groups. Three different TAP SN behaviours are shown. mAbs have been classified as non-functional, putative functional and functional mAb. hiBRC controls are included as negative controls. Groups are determined based on the difference between BRC and hiBRC samples. In this example, the non-functional mAb did not exhibit bactericidal effect in any dilution point. The putative functional mAb exhibited bactericidal effect at 1:5 only. The functional mAb showed bactericidal effect in all dilution points. For each TAP SN, three replicates were performed, and results are shown as mean ± standard deviation.

Starting from N=60 TAP SNs selected from the first screening, N= 33 (55%) were classified as non-functional mAbs, 12 (20%) putative functional mAbs, and 15 (25%) functional mAbs. The distribution for each Sbj is depicted in **Figure 7.5.6**.

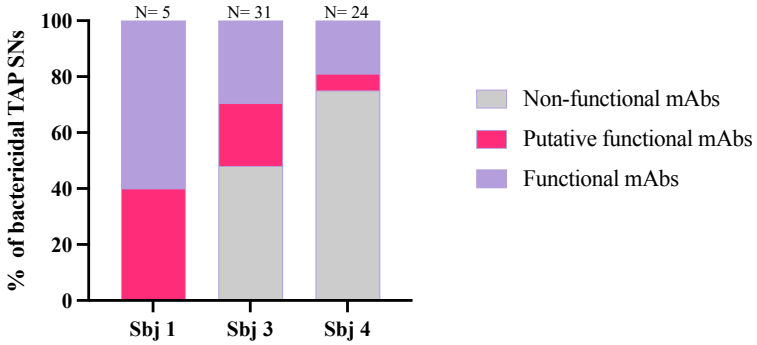

Figure 7.6.6. Bactericidal TAP SNs based on the second screening. TAP SNs were tested at three-point dilutions (1:5, 1:25, 1:125). hiBRC controls are included as negative controls (not shown). N=5 TAP SNs were tested from Sbj 1, being N=2 putative functional mAbs and N= 3 functional mAbs; N=31 TAP SNs were tested from Sbj 3, of which N=15 were non-functional mAbs, N=7 putative functional mAbs and N=9 functional mAbs. Lastly, N=24 TAP SNs were tested from Sbj4, being N=18 non-functional mAbs, N=3 putative functional mAbs and N=3 functional mAbs. Sbj 2 is not indicated as all of the mAbs were non-functional.

Subsequently, putative functional and functional mAbs (N=27) were cloned, as already described, as Hex3 for sequence recovery (variable heavy and light regions) and medium-scale expression for potency evaluation. We were able to retrieve 17 out of 27 (63%) mAb sequences.

7.6.4 Potency evaluation of selected mAbs

The potency (bactericidal activity) of an antibody is typically quantified by the inhibitory concentration (IC) values (e.g. IC50). L-SBA was exploited to characterize the bactericidal potency (IC50) of the most promising purified mAbs (N=17). All of the antibodies were tested starting from 40 µg/mL to 20 ng/mL (2-step serial dilutions (N=12)). **Figure 7.5.7** illustrates an example of a bactericidal curve obtained with our best candidate mAb identified so far, Sbj 4_mAb 04, along with 2C7, used as a control.

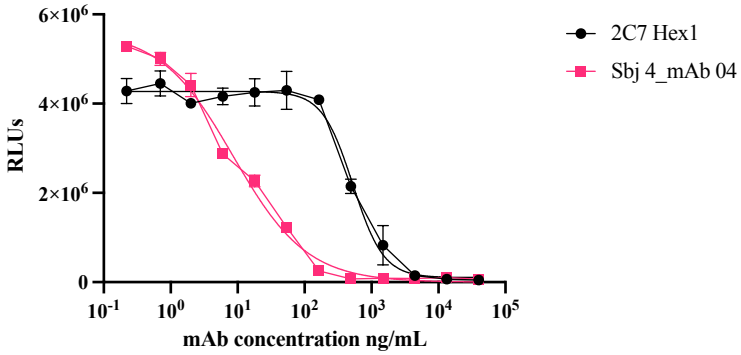

Figure 7.6.7. 2C7 Hex1 and Sbj 4_mAb 04 bactericidal curves. Each selected mAb (N=17) was tested against Ng. Bactericidal curves were obtained starting from 40 µg/mL to 20 ng/mL (2-step serial dilutions). FA1090 was used in this experiment. In this example Sbj 4_mAb 04 was tested along with 2C7 Hex1, used as a control.

Based on results, we identified mAbs with very variable IC50 values, ranging from 30 ng/mL to 10,000 ng/mL. N=5 (29%) mAbs showed IC50 greater than 1,500 ng/mL (low potency), N=4 (24%) had an IC50 between 150 and 1,500 ng/mL (moderate potency), while N= 8 (47%) were characterized by IC50 lower than 150 ng/mL (high potency) (**Figure 7.5.8**).

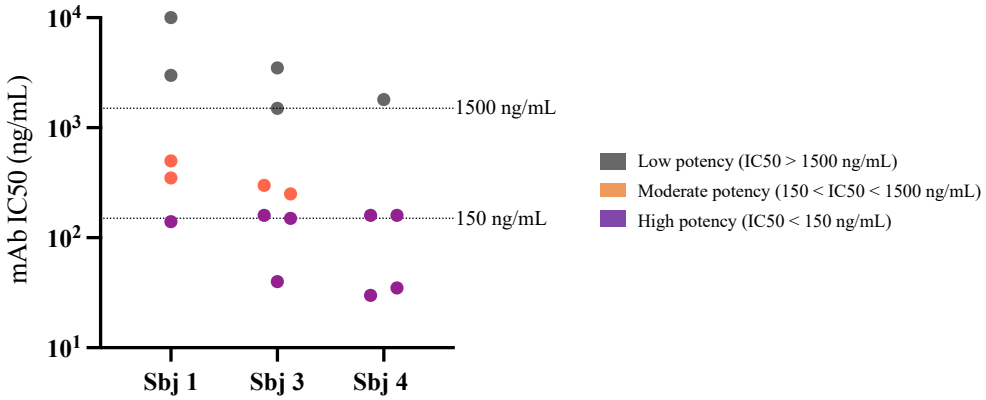

Figure 7.6.8. Selected mAbs can be classified in three groups based on IC50. Potency (IC50) of 17 selected mAbs against FA1090 and BG27 is shown. Dashed lines show different ranges of potency (150 and 1500 ng/mL). Selected mAbs with low potency (IC50 > 1,500ng/mL) are shown in gray, mAbs with moderate potency (150 < IC50 < 1,500ng/mL) are shown in red, mAbs with high potency (IC50 <150 ng/mL) are shown in purple.

mAbs retrieved and functionally characterized (N=17) are listed in Table 7, sorted by subject.

Table 7. Summary table of selected mAbs. The table shows the binding and functional profiles of mAbs.

ID		Binding profile		Functional profile	
Subject	mAb	Whole-bacterial cell ELISA	Luminex	FA1090 IC50	BG27 IC50
1	mAb 01	Tri-specific	NHBA	10 µg/mL	NA
1	mAb 02	Tri-specific	PorB1a/PorB1b	0.14 µg/mL	NA
1	mAb 03	Tri-specific	PorB1b	3 µg/mL	NA
1	mAb 04	Tri-specific	PorB1a/PorB1b	0.5 µg/mL	NA
1	mAb 05	Tri-specific	OMV NZ	0.35 µg/mL	NA
3	mAb 01	BG27 specific	OMV NZ	0.16 µg/mL	NA
3	mAb 02	BG27 specific	Negative	NA	3.5 µg/mL
3	mAb 03	BG27 specific	Negative	0.3 µg/mL	NA
3	mAb 04	BG27 specific	OMV-NZ	2.5 µg/mL	NA
3	mAb 05	Tri-specific	Negative	1.5 µg/mL	NA
3	mAb 06	Tri-specific	OMV NZ	0.15 µg/mL	NA
3	mAb 07	Tri-specific	Cross OMVs/GMMAs	NA	0.04 µg/mL
4	mAb 01	Tri-specific	Cross OMVs/GMMAs	0.035 µg/mL	NA
4	mAb 02	BG27 specific	Negative	NA	0.16 µg/mL
4	mAb 03	Tri-specific	Negative	1.8 µg/mL	7 µg/mL
4	mAb 04	Tri-specific	Cross OMVs/GMMAs OMV-NZ Neg	0.03 µg/mL	0.16 µg/mL
4	mAb 05	Tri-specific	Cross OMVs/GMMAs	0.16 µg/mL	3 µg/mL

NA=Not active

7.7 Genetic characterization of selected mAbs

The genes encoding the heavy chains (HCs) and light chains (LCs) of the 17 selected mAbs were sequenced, and their IGHV genes (Vgene and Jgene) were retrieved and analysed (LCs not shown) (**Table 8**). 10/17 mAbs used one of the most predominant HC V genes IGHV4-34, while 4/17 mAbs used the HCV genes IGHV2-5. Intrestingly, one of our best candidates used the least representative HCV genes IGHV1-2. As for V gene and J gene combination, in the majority of cases (7/10), the gene IGHV4-34 combined with IGHJ4-1. The HC V genes somatic hypermutation level and complementary determining region 3 (H-CDR3) length were also evaluated. Our selected mAbs displayed a variable level of somatic mutations when compared to their respective germlines with sequence identities ranging from 1% to 10%. The H-CDR3 length spanned from 33 to 84 amino acids (aa) with an outlayer of 114 aa and the H-CDR3 mismatches ranging from 1% to 9%.

Table 8. Heavy chain analyses of selected mAbs.

VGene	JGene	CDR3 Length	(%) CDR3 Mismatches	#VH Substitutions	(%) Vgene MuFreq
IGHV1-2*02	IGHJ3-1*02	39	0,01	4	0,01
IGHV2-5*09	IGHJ4-1*02	45	0,05	36	0,12
IGHV2-5*09	IGHJ4-1*02	45	0,06	25	0,08
IGHV2-5*09	IGHJ4-1*02	45	0,06	37	0,13
IGHV2-5*10	IGHJ5-1*02	45	0,05	30	0,1
IGHV3-9*01	IGHJ6-1*04	114	0,05	9	0,03
IGHV4-34*01	IGHJ4-1*02	33	0,05	42	0,14
IGHV4-34*01	IGHJ4-1*02	60	0,04	17	0,05
IGHV4-34*01	IGHJ6-1*02	60	0,01	6	0,02
IGHV4-34*01	IGHJ4-1*02	66	0,02	9	0,03
IGHV4-34*01	IGHJ4-1*02	75	0,08	30	0,1
IGHV4-34*01	IGHJ4-1*02	66	0,05	12	0,04
IGHV4-34*01	IGHJ6-1*03	81	0,09	12	0,04
IGHV4-34*01	IGHJ5-1*02	60	0,08	11	0,04
IGHV4-34*04	IGHJ4-1*02	72	0,02	6	0,02
IGHV4-34*04	IGHJ4-1*02	78	0,04	18	0,06
IGHV4-39*01	IGHJ3-1*01	84	0,09	30	0,1

7.8 Identification of anti-LOS mAbs by immunoblot

Immunoblot was used to rapidly identify mAbs against the lipooligosaccharide (LOS). As discussed, Ng LOS is an important component of the gonococcal outer membrane. Antibodies directed against LOS engage complement to kill Ng directly and promote opsonophagocytosis. The 2C7 epitope is conserved and expressed by 94% of Ng strains, including FA1090. **Figure 7.7.1** illustrates FA1090 LOS bound by 2C7, used as a positive control. Selected functional mAbs (**Table 7**) were tested for binding against the LOS, and only the antibody Sbj3_mAb 05 was confirmed to be positive for binding to FA1090 LOS.

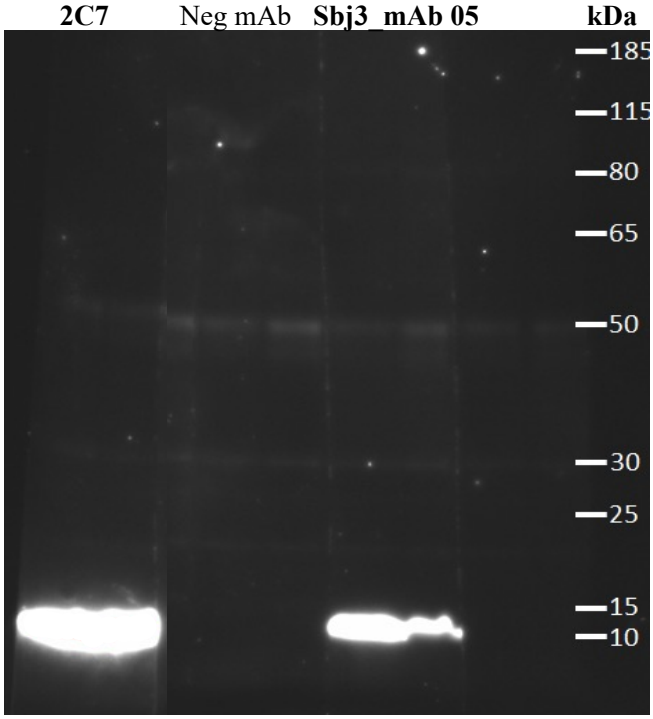

Figure 7.8.1. Identification of Sbj3_mAb 05 against FA1090 LOS. LOS of FA1090 strain was obtained in 1% Triton-X-100, 150 mM NaCl, 2 mM EDTA, 20 mM Tris-HCl pH 7,5, protease inhibitors, subjected to 12% SDS-PAGE, and electrotransferred to polyvinylidene difluoride membrane. Panel shows the 2C7 control binding to purified LOS expressed by FA1090 strain, along with two mAbs. Sbj3_mAb05 displayed the same band of 2C7.

7.9 Binding characterization by cytofluorimetry

Selected mAbs (N=17) were further characterized for binding to Ng by cytofluorimetry to investigate the antibacterial antibody binding that target surfaces of bacteria This can be done by measuring the bacterial-surface-binding antibodies and use it as a quantitative correlate of immune protection. Also, this technique has the advantage to visualize bacterial subpopulations. **Figure 7.8.1** illustrates three groups of mAbs with different binding pattern to FA1090, as compared to 2C7. 2C7 recognizes the Ng LOS which is well-exposed on the surface of the outer membrane and based on its binding we could establish the cut-off in order to classify our mAbs in three groups.

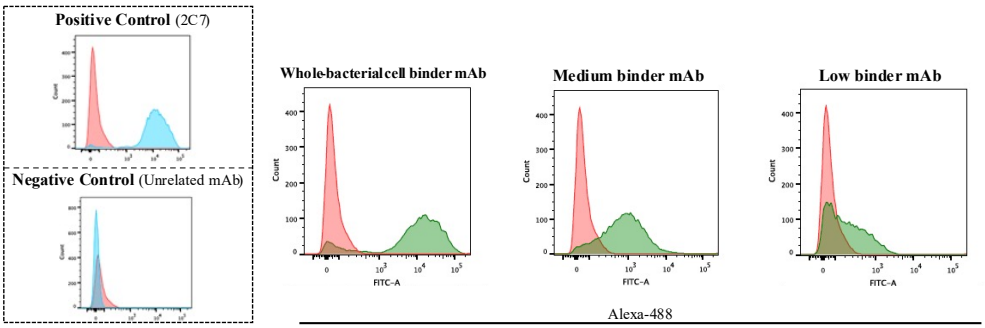

Figure 7.9.1. The binding profile of selected mAbs can be divided in three groups based on cut-off. FACS histogram of Alexa-488 labeled bacteria with mAbs. The cut-off between stained and unstained cells was set at 10^2 Alexa 488 channel**.** Red and blue histograms represent the negative control (unrelated mAb) and positive control (2C7), respectively. Green colored histograms show tested antibodies, which represent the 3 different scenarios identified, related to Alexa-488 signals. The 10^2<cut-off<10^3 was used to classify low binder mAbs. The 10^3<cut-off<10^4 was used to classify medium binder mAbs. Lastly, the cut-off >10^4 was used to classify whole-bacterial cell binder mAbs. Histograms of positive and negative populations are denoted on each graph.

We observed a correlation between mAb potency (IC50) and binding pattern. In particular, mAbs targeting well-represented surface structures (e.g., Porins), which fall in the whole-bacterial cell binder group, were most likely the ones with higher potency (**Table S2**). Interestingly, for some mAbs we observed a strain-dependent binding pattern, as shown in **Figure 7.8.2,** but no obvious correlation with functionality was noticed. Also, these different binding phenotypes were

further confirmed by confocal microscopy (**Figure 7.9.2 and 7.9.3**). These results could indicate that the antigen may be characterized by a strain-dependent surface exposure and/or expression.

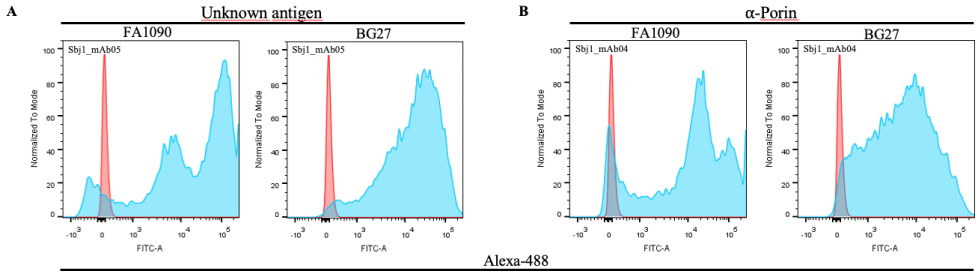

Figure 7.9.2. Histograms of two mAbs binding to FA1090 and BG27. FACS histogram of Alexa-488 labeled cells with mAbs. The cut-off between stained and unstained cells was set at 10^2 Alexa 488 channel. Red histograms represent the negative control (unrelated mAb) and blue histograms show the tested mAbs. Different bacterial subpopulations were visualized by the same mAbs tested with FA1090 and BG27.

7.10 Binding characterization by confocal microscopy

To further investigate the different binding profile (or phenotype) of selected mAbs (N=17), we tested them by confocal microscopy. The aim was to evaluate qualitatively the binding profile of the mAbs binding to the bacterial surface and possibly to further investigate correlations between the functional impact and the different antibody binding phenotypes. To meet this aim, mAbs were tested and then classified based on results obtained. 2C7 was used to define the assay conditions and establish the different binding phenotypes. **Figure 7.9.1** illustrates 2C7 binding to FA1090 and BG27 with the same binding phenotype, unsurprisingly covering the whole bacterial surfaces, being the LOS one of the most abundant antigens among Gram-negative bacteria. On the other hand, mAbs with different binding phenotypes were identified. For instance, Sbj1_mAb05 and Sbj1_mAb04 showed a strain-dependent binding, displaying a preferential mAb localization on the Ng cell surfaces, that we named side binders (**Figure 7.9.2 and 7.9.3) (Figure S1).** Lastly, Sbj1_mAb05 showed a peculiar binding phenotype, named as dot binder (**Figure 7.9.4**). Notably, we could confirm the correlation

between the antibody binding phenotypes and its potency, already suggested by flow cytometry analysis. For instance, mAbs with binding phenotypes that resembled 2C7 (**Figure 7.8.1**) showed higher potency (lower IC50) in L-SBA. Whereas dot binder mAbs (**Figure 7.8.4**) showed lower potency (higher IC50).

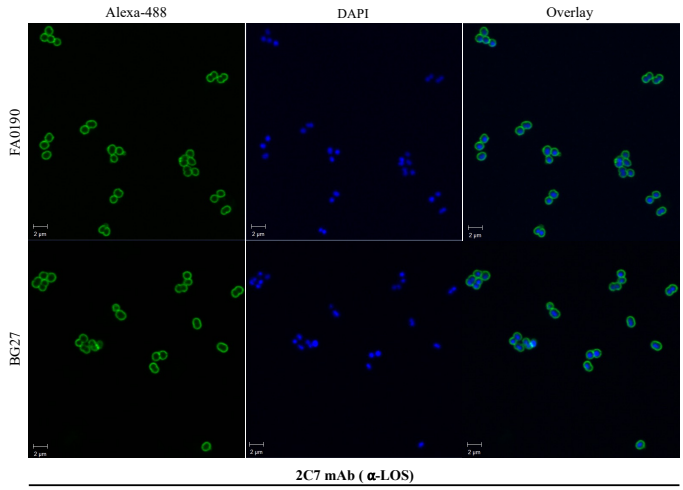

Figure 7.10.1. Confocal images of 2C7 binding to FA1090 and BG27. Overview of the 2C7 mAb binding to FA1090 and BG27. Confocal fluorescent images were acquired with 100X magnification. 488-fluorophore-conjugated 2C7 is shown in green. Bacterial strains were stained with DAPI (nucleic acid stain).

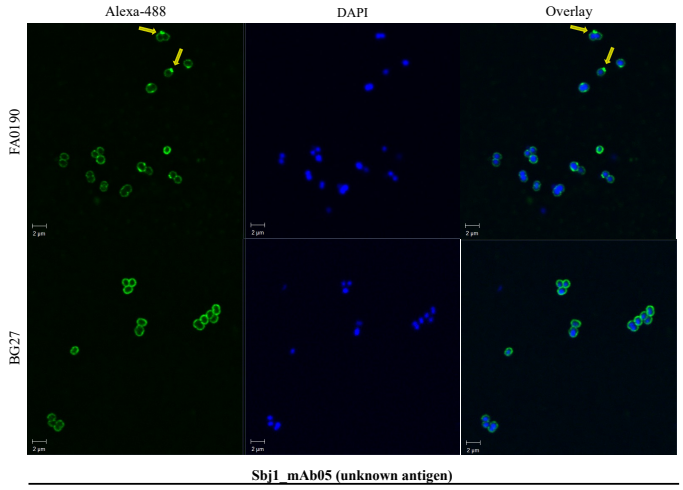

Figure 7.10.2. Confocal image of Sbj1_mAb05 binding to FA1090 and BG27. Confocal fluorescent images acquired with 100X magnification. 488-fluorophore-conjugated Sbj1_mAb05 is shown in green. Bacterial strains were stained with DAPI (nucleic acid stain). A strain-specific

binding pattern is indicated by yellow arrows, suggesting a different antigen distribution between FA1090 and BG27.

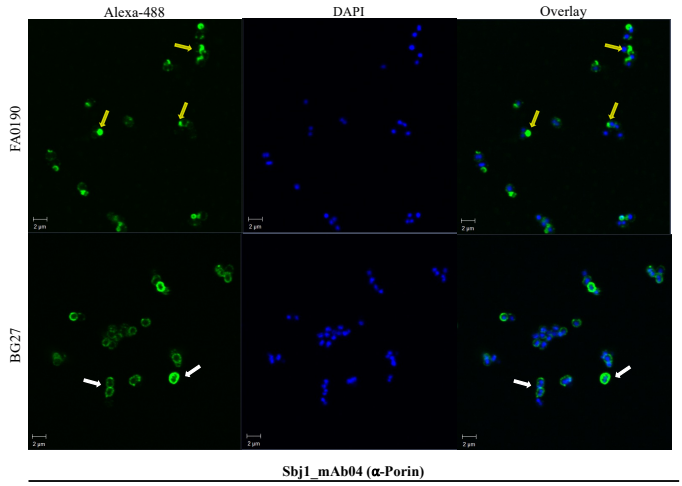

Figure 7.10.3 Confocal images of Sbj1_mAb04 binding to FA1090 and BG27. Confocal fluorescent images acquired with 100X magnification. 488-fluorophore-conjugated Sbj1_mAb04 is shown in green. Bacterial strains were stained with DAPI (nucleic acid stain). A strain-specific binding pattern is indicated by yellow arrows (top) and white arrows (bot), suggesting a different antigen distribution between FA1090 and BG27.

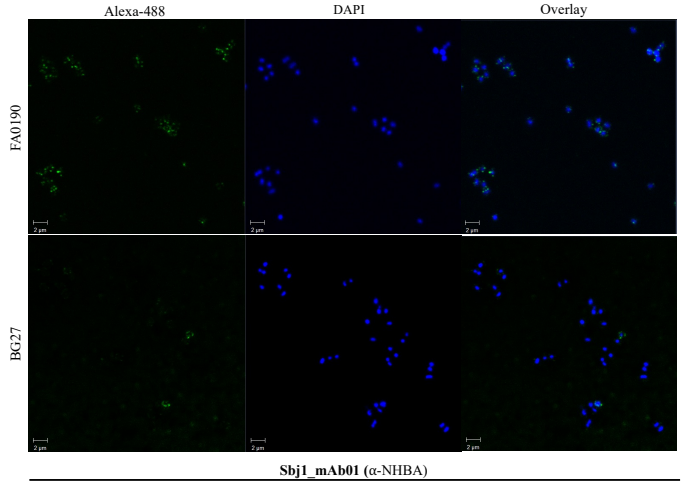

Figure 7.10.4. Confocal images of Sbj1_mAb01 binding to FA1090 and BG27. Confocal fluorescent images acquired with 100X magnification. 488-fluorophore-conjugated Sbj1_mAb01 is shown in green. Sbj1_mAb01 showed preferential distribution on the Ng cell surface.

8 Results part II: discovery of mAbs against SARS-CoV-2

8.1 Summary

By single-cell sorting spike protein-specific memory B cells from 14 COVID-19 survivors, SARS-CoV-2 neutralizing antibodies were identified. The most potent neutralizing antibodies recognized the spike protein receptor-binding domain. Only very few antibodies could neutralize the authentic virus with a potency of 1-10 ng/mL. The most potent monoclonal antibody, engineered to reduce the risk of antibody-dependent enhancement and prolong half-life. Then, prophylactic, and therapeutic efficacy in the hamster model was observed.

I was involved in this project with the aim of implementing a robust pipeline for antibody expression. This allowed a large screening of mAbs against SARS-CoV-2, thereby identifying the best candidates capable of neutralizing the new virus. The work has been published

8.1.1 S protein+ MBCs identification

A total of 4,277 S protein-binding MBCs were successfully retrieved with frequencies ranging from 0.17% to 1.41% (not shown). Following the sorting procedure, S protein+ MBCs were incubated over a layer of 3T3-CD40L feeder cells in the presence of IL-2 and IL-21 stimuli for 2 weeks to allow natural production of immunoglobulins. Subsequently, MBC supernatants containing IgG or IgA were tested for their ability to bind either the SARS-CoV-2 S protein trimer in its prefusion conformation (**Figure 8.1.1 A**) or the S protein S1 + S2 subunits (not shown) by enzyme linked immunosorbent assay (ELISA). A panel of 1,731 mAbs specific for the SARS-CoV-2 S protein were identified showing a broad range of signal intensities.

8.1.2 Neutralizing mAbs identification

All specific mAbs were tested in vitro to evaluate their neutralization activity against the authentic SARS-CoV-2 virus, and 453 nAbs were identified. Only 1.4% of them neutralized the authentic virus with a potency of 1–10 ng/mL (**Figure 8.1.1 B and C**).

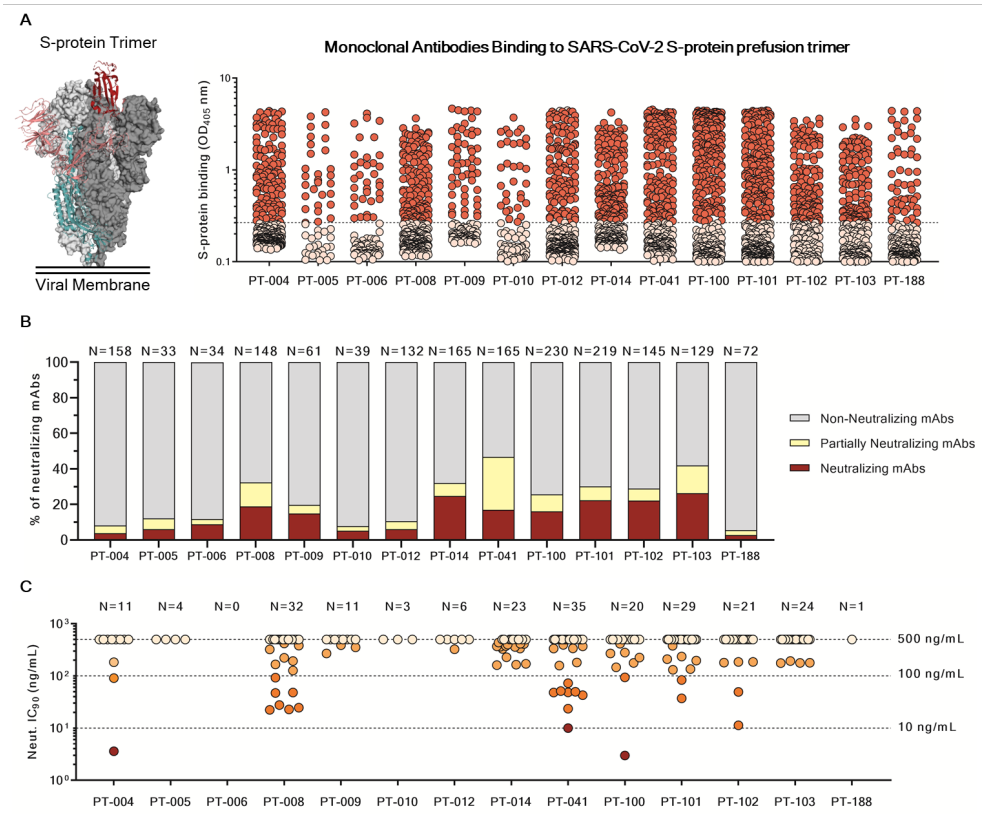

Figure 8.1.1. (A) The graph shows supernatants tested for binding to the SARS-CoV-2 S-protein stabilized in its prefusion conformation. Threshold of positivity has been set as two times the value of the blank (dotted line). Red dots represent mAbs that bind to the S protein, while pink dots represent mAbs that do not bind. **(B)** The bar graph shows the percentage of non-neutralizing (gray), partially neutralizing (pale yellow), and neutralizing antibodies (dark red) identified per each donor. The total number (n) of antibodies tested per individual is shown on top of each bar. **(C)** The graph shows the neutralization potency of each nAb tested once expressed as recombinant full-length IgG1. Dashed lines show different ranges of neutralization potency (500, 100, and 10 ng/mL).

The most potent monoclonal antibody J08 was engineered (J08-MUT) to reduce the risk of antibody-dependent enhancement and prolong half-life, neutralized the authentic wild-type virus and emerging variants containing D614G, E484K, and N501Y substitutions.

8.1.3 Prophylactic and therapeutic evaluation

Prophylactic and therapeutic efficacy were evaluated for our best candidate J08 and J08_MUT in in the hamster model which was observed at 0.25 and 4 mg/kg respectively in absence of Fc functions (**Figure 8.1.2**).

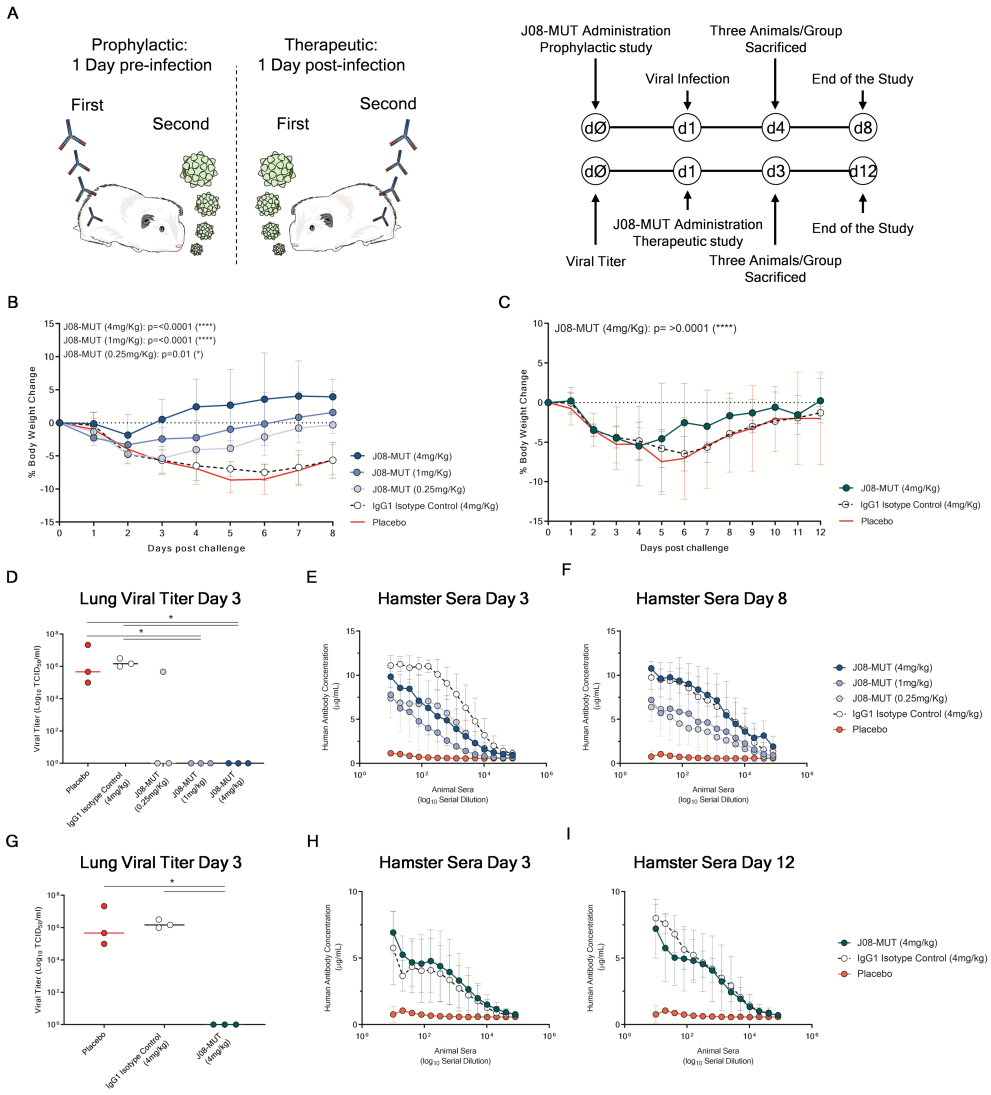

Figure 8.1.2(A) Schematic representation and timelines of prophylactic and therapeutic studies performed in golden Syrian hamster. (B and C) The figure shows the prophylactic impact of J08-MUT at three different concentrations (4, 1, and 0.25 mg/kg) **(B)** on body weight loss change **(C)**. The figure shows the therapeutic impact of J08-MUT at 4 mg/kg on body weight loss change. Mean ± SD are denoted in the graphs. (D–F) The figures show the lung viral titer at day 3 **(D)** and the detection of human antibodies in hamster sera at day 3 **(E)** and day 8 **(F)** in the prophylactic study. Mean ± SD of technical triplicates are shown. (G–I) The figures show the lung viral titer at day 3 **(G)** and the detection of human antibodies in hamster sera at day 3 **(H)** and day 12 **(I)** in the therapeutic study.

9 Discussion

The global spread of multidrug-resistant gonorrhea has spurred efforts to develop a safe and effective vaccine against the disease. A retrospective case-control study found that reduced rates of gonorrhea occurred among sexual health clinic patients following their vaccination with an outer membrane vesicle (OMV) meningococcal vaccine.

In this work we report the isolation of functional mAbs against Ng from subjects immunized with a meningococcal vaccine (Bexsero) in order to unravel the molecular mechanism(s) based on *Neisseria meningitidis* and *Neisseria gonorrohoeae* cross-protection.

Firstly, mAbs were successfully isolated and expressed as TAP supernatants. Of note, the work that was done on the discovery of mAbs against SARS-CoV 2 [85], allowed us to have a robust pipeline that was adoperated in the discovery of mAbs against Ng, as well.

After expression, mAb were characterized for binding to assess cross-reactivity to Ng. Two approaches were used to detect antibodies capable of binding structures present on surface and OMVs. It is likely that the majority of cross-reactive mAbs were directed against determinants present on both bacterial surface and OMVs, as evidenced by their cross-reactivity with both whole bacterial cells and purified OMVs and GMMAs. Unsurprisingly, mAbs reacting against PorA and recombinant proteins (fHbp, NadA and NHBA) present in the Bexsero formulation were identified. Although the antigenically variable protein PorA (absent in Ng) is immunodominant, only few antibodies were identified as reactive. Some of these mAbs were cross-reactive for Ng PorB, leading to the conclusion that they could recognize shared epitopes. However, since OMVs are complex structures, it is possible to hypothesize that functional mAbs could be raised against several other OMV components. On the other hand, vaccine

recombinant proteins FHbp and NadA are less likely to contribute to cross-protection against Ng infections. Indeed, the gonococcal fHbp has previously been shown to not be surface expressed and is unable to bind factor H, while NadA is absent. Only NHBA is surface expressed in Ng and preliminary data of mAbs raised against it support the hypothesis that NHBA could be a determinant in the cross-protection [220].

Once binding screening and characterization were performed, mAbs were screened for functionality by a complement-mediated killing assay which was optimized in this work, named L-SBA. Upon binding to bacteria, mAbs can activate the complement system leading to the lysis of Gram-negative bacteria through insertion of the membrane attack complex L-SBA facilitated the testing of mAbs on FA1090, BG27 and F62 gonococcal strains. While conventional assays measure colony forming units (CFU), which is time-consuming, this luminescent assay quantifies ATP which can be used as proxy of bacterial viability. Results suggest that, although correlates of protection against gonococcal infection have not been defined, the complement-mediated killing, which is well-established against meningococcal infections, may also predict correlate of protection efficacy against Ng.

By screening more than five thousand mAbs, expressed as TAP supernatants, 17 of them were selected as functional, with a wide range of potency (IC50), from 30 ng/mL to 10,000 ng/mL. Some mAbs were confirmed to be against Ng PorB, most likely sharing the epitopes with the meningococcal PorA. However, for the majority of mAbs, the antigens remain to be defined. Results suggests that for some mAbs (9/17) the involved antigens are present on bacterial surface only, as they were negative for binding against gonococcal OMVs. While for other mAbs (6/17) the determinants were present on both bacterial surface and OMVs. One functional mAb was identified to be against the LOS. Even though LOS is considered as a potential vaccine candidate because it is densely represented on the bacterial surface and is readily accessible as a target of adaptive immunity, it remains to be understood whether LOS evokes protective immune responses. Lastly, one functional mAb against NHBA was identified. NHBA is highly

conserved, with ≥ 97.5% amino acid identity in the *Neisseria gonorrhoeae* strains investigated to date, with variable expression between strains. The finding of NHBA promoting complement activation and mediating bacterial killing suggests that NHBA could be used as potential antigen, or in combination with others, in a rationally designed vaccine.

Then, the HC and LC gene analysis of functional mAbs was performed. IGHV4-34 was the most common germline identified, with the majority of them combining with IGHJ4-1. Intrestingly, one of the most promising mAb belongs to the germline IGHV1-2, the least represented, combined with IGHJ3-1.

As next step, functional mAbs were further investigated by flow cytometry and confocal microscopy with the aim to correlate the antibacterial antibody responses, that target surface components of Ng, with the binding profile. We observed correlation between mAb potency (IC50) and binding pattern. In particular, mAbs targeting well-represented surface structures, like Porins or LOS, were most likely to be more functional (lower IC50). Such findings suggest that measuring the bacterial-surface-binding antibodies (quantitatively and qualitatively) can be used as a correlate of immune protection, i.e. the more an antibody covers the bacterial surface, the more complement deposition can be triggered, and the more killing is observed. However, this should not be considered as a rule since no obvious differences between binding phenotypes and functional impact were found for other mAbs.

In conclusion, further studies are in progress to discover the antigen(s) involved in the cross-protection mediated by the meningococcal vaccine. Some antigens which may be involved were identified in this work. However, the correlation between mAb binding and the presence of a specific protein on the cell surface or OMV does not necessarily mean that the antibody is directed against that specific protein. An equally likely possibility is that the exposure of the actual target antigen is affected by the presence or absence of other interacting proteins. In either case, additional studies for antigen identification and characterization must be done.

10 Supplementary information

Table S 1 List of primers used in this study, related to mAb expression (sub-chapter 5.3).

RT primers

Name	Primer Probe	Sequence
IgG CH RT	R	GGAAGGTGTGCACGCCGCTGGTC
IgA CH RT	R	CCTGGGGGAAGAAGCCCTGGACC
IgM CH RT	R	GGGAATTCTCACAGGAGACGA
CK RT	R	CCTCTAACACTCTCCCCTGTTGAAG
CL RT	R	CATTCTGYAGGGGCMACTGTCTTCTC

PCR1 primers

Name	Primer Probe	Sequence
PCR1_VH1_VH7	F	CACTCCCAGGTGCAGCTGGTGCAG
PCR1_VH2	F	TGGGTCTTRTCCCAGGTCACCTTG
PCR1_VH_3	F	AAGGTGTCCAGTGTSAGGTGCAG
PCR1_VH4_6	F	GTCCTGTCCCAGGTGCAGCTGCAG
PCR1_VH5	F	GAGTCTGTTCCGAGGTGCAGCTGG
PCR1_IgG_CH	R	GTGCCAGGGGGAAGACCGATG
PCR1_IgA_CH	R	GCMGAGGCTCAGCGGGAAGAC
PCR1_IgM_CH	R	GAGACGAGGGGGAAAAGGGTTG
PCR1_VK1	F	CAGGTGCCAGATGTGHCATCCAG
PCR1_VK2	F	CTGGATCCAGTGSGGATATTGTGATG
PCR1_VK3	F	CCCAGATACCACCGGAGAAATTGTG
PCR1_VK4	F	CTCTGGTGCCTACGGGGACATCGTG
PCR1_VK5	F	CTGATACCAGGGCAGAAACGACAC
PCR1_CK	R	GAACACTCTCCCCTGTTGAAGCTCTTTG
PCR1_VL1	F	GGTCCTGGGCCCAGTCTGTGCTG
PCR1_VL2	F	GGTCCTGGGCCCAGTCTGCCCTG
PCR1_VL3	F	TCTGTGRCCTCCTATGAGCTGAC
PCR1_VL4_VL5_VL9	F	CTCTCGCAGCCTGTGCTGACTCA
PCR1_VL6	F	GTTCTTGGGCCAATTTTATGCTG
PCR1_VL7	F	GGTCCAATTCTCAGGCTGTGGTG
PCR1_VL8	F	GAGTGGATTCTCAGACTGTGGTG
PCR1_VL10	F	GTCAGTGGTCCAGGCAGGGCTGAC
PCR1_CL	R	GTGCTCCCTTCATGCGTGACC

PCR2 primers

Name	Primer Probe	Sequence
PCR2_VH1_5_7	F	GT ATC ATC CTT TTT CTA GTA GCA ACT GCA ACC GGT GTACATTCC CAG GTG CAG CTG GTG CAG TCT G
PCR2_VH2	F	GT ATC ATC CTT TTT CTA GTA GCA ACT GCA ACC GGT GTACATTCC CAG GTC ACC TTG AAG GAG TCT GGT C
PCR2_VH3	F	GT ATC ATC CTT TTT CTA GTA GCA ACT GCA ACC GGT GTACATTCC GAG GTG CAG CTG GTG GAG TCT GGG GGA G
PCR2_VH4_6_a	F	GT ATC ATC CTT TTT CTA GTA GCA ACT GCA ACC GGT GTACATTCC CAG GTG CAG CTG CAG GAG TCG GG
PCR2_VH4_6_b	F	GT ATC ATC CTT TTT CTA GTA GCA ACT GCA ACC GGT GTACATTCC CAG GTG CAG CTG CAG CAG TGG GG
PCR2_IgG_CH	R	CTT GGA GGA GGG TGC CAG GGG GAA GAC CGA TGG GCC CTT GGT GGA RGC
PCR2_IgA_CH	R	CTT GGA GGA GGG TGC CAG GGG GAA GAC CGA CTT GGG GCT GGT CGG GGA
PCR2_IgM_CH	R	CTT GGA GGA GGG TGC CAG GGG GAA GAC CGA TGG GGC GGA TGC ACT CCC
PCR2_VK1	F	GT ATC ATC CTT TTT CTA GTA GCA ACT GCA ACC GGT GTACATTCC GCC ATC CAG ATG ACC CAG TCT CCA TC
PCR2_VK2_a	F	GT ATC ATC CTT TTT CTA GTA GCA ACT GCA ACC GGT GTACATTCC GAT ATT GTG ATG ACC CAG ACT CCA CTC TC
PCR2_VK2_b	F	GT ATC ATC CTT TTT CTA GTA GCA ACT GCA ACC GGT GTACATTCC GAT ATT GTG ATG ACT CAG TCT CCA CTC TC
PCR2_VK3_a	F	GT ATC ATC CTT TTT CTA GTA GCA ACT GCA ACC GGT GTACATTCC GAA ATT GTG TTG ACA CAG TCT CCA G
PCR2_VK3_b	F	GT ATC ATC CTT TTT CTA GTA GCA ACT GCA ACC GGT GTACATTCC GAA ATT GTG ATG ACG CAG TCT CCA G
PCR2_VK4	F	GT ATC ATC CTT TTT CTA GTA GCA ACT GCA ACC GGT GTACATTCC GAC ATC GTG ATG ACC CAG TCT CCA G
PCR2_VK5	F	GT ATC ATC CTT TTT CTA GTA GCA ACT GCA ACC GGT GTACATTCC GAA ACG ACA CTC ACG CAG TCT CCA G
PCR2_CK	R	GA TTT CAA CTG CTC ATC AGA TGG CGG GAA GAT GAA GAC AGA TGG TGC AGC CAC AGT TC
PCR2_VL1	F	GT ATC ATC CTT TTT CTA GTA GCA ACT GCA ACC GGT TCCTGGGCC CAG TCT GTG CTG ACT CAG CCG CCC TCA G
PCR2_VL2	F	GT ATC ATC CTT TTT CTA GTA GCA ACT GCA ACC GGT TCCTGGGCC CAG TCT GCC CTG ACT CAG CCT GCC TCC G
PCR2_VL3_a	F	GT ATC ATC CTT TTT CTA GTA GCA ACT GCA ACC GGT TCCTGGGCC TCC TAT GAG CTG ACA CAG CCA C
PCR2_VL3_b	F	GT ATC ATC CTT TTT CTA GTA GCA ACT GCA ACC GGT TCCTGGGCC TCC TAT GAG CTG ACT CAG GAC C
PCR2_VL4	F	GT ATC ATC CTT TTT CTA GTA GCA ACT GCA ACC GGT TCCTGGGCC CAG CCT GTG CTG ACT CAA TCG TCC TCT G
PCR2_VL5-9	F	GT ATC ATC CTT TTT CTA GTA GCA ACT GCA ACC GGT TCCTGGGCC CAG CCT GTG CTG ACT CAG CCR ACT TC
PCR2_VL6	F	GT ATC ATC CTT TTT CTA GTA GCA ACT GCA ACC GGT TCCTGGGCC AAT TTT ATG CTG ACT CAG CCC CAC TC
PCR2_VL7	F	GT ATC ATC CTT TTT CTA GTA GCA ACT GCA ACC GGT TCCTGGGCC CAG GCT GTG GTG ACT CAG GAG CCC TC
PCR2_VL8	F	GT ATC ATC CTT TTT CTA GTA GCA ACT GCA ACC GGT TCCTGGGCC CAG ACT GTG GTG ACC CAG GAG CCA TC
PCR2_VL10	F	GT ATC ATC CTT TTT CTA GTA GCA ACT GCA ACC GGT TCCTGGGCC CAG GCA GGG CTG ACT CAG CCA CCC TCG G
PCR2_CL	R	G TGT GGC CTT GTT GGC TTG AAG CTC CTC ACT CGA GGG YGG GAA CAG AGT G

TAP-PCR primers

Name	Primer Probe	Sequence
TAP_PCR_F	F	TTAGGCACCCCAGGCTTTAC
TAP_PCR_R	R	AGATGGTTCTTTCCGCCTCA

Figure S 1. Correlation between flow-cytometry and confocal microscopy, related to Figure 7.7.1 and Figure 7.8.1 to 7.8.4. The figure illustrates how results obtained by flow cytometry correlates with confocal fluorescent images. The the cut-off $>10^4$ used to classify whole-bacterial cell binder mAbs, correlates with the 2C7-like phenotype. The 10^3<cut-off<10^4 used to classify medium binder mAbs, correlates with the side binder phenotype. Lastly, was used to classify low binder mAbs. Lastly, the 10^2<cut-off<10^3 used to classify low binder mAbs correlates with the dot binder phenotype.

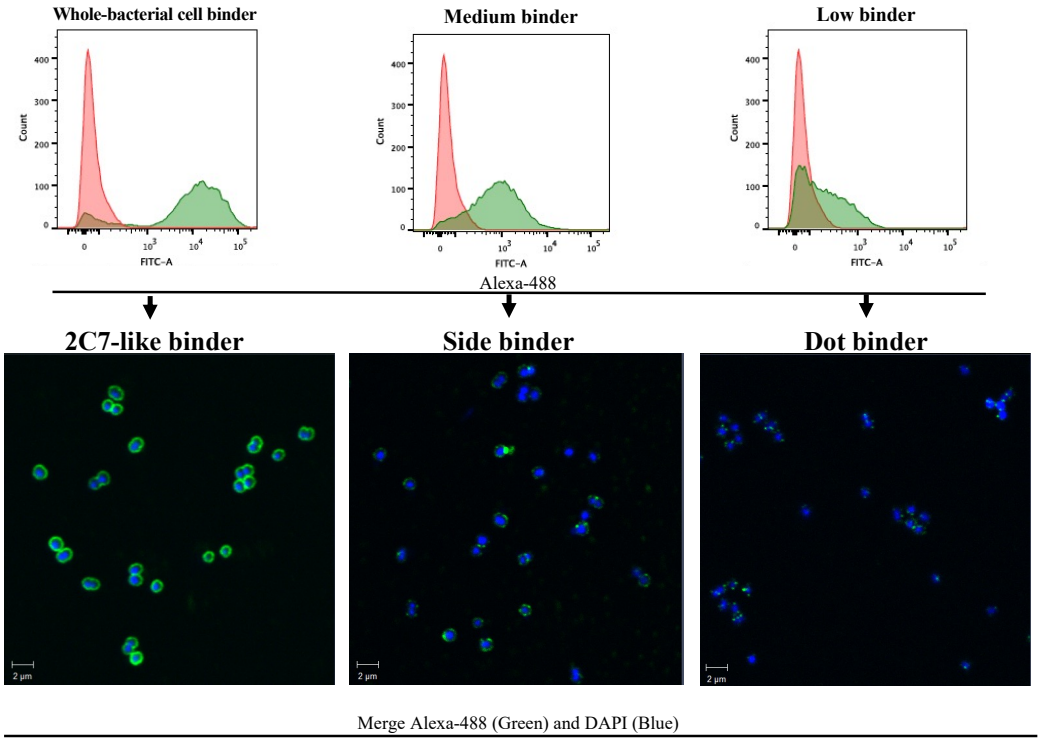

Table S 2 Binding characterization summary, related to Figure 7.7.1 and Figure 7.8.1 to 7.8.4. The table shows the correlation between binding phenotypes and potency (IC50) of selected mAbs.

ID		Flow-cytometry	Confocal microsopy	Potency on FA1090 (IC50)	Potency on BG27 (IC50)
Sbj 1	mAb 01	Low binder	Dot binder	10 µg/mL	NA
Sbj 1	mAb 02	Whole-bacterial cell binder	2C7-like binder	0.14 µg/mL	NA
Sbj 1	mAb 03	Medium binder	Strain-specific binder	3 µg/mL	NA
Sbj 1	mAb 04	Medium binder	Strain-specific binder	0.5 µg/mL	NA
Sbj 1	mAb 05	Whole-bacterial cell binder	Strain-specific binder	0.35 µg/mL	NA
Sbj 3	mAb 06	Whole-bacterial cell binder	2C7-like binder	0.16 µg/mL	NA
Sbj 3	mAb 07	Low binder	Dot binder	NA	3.5 µg/mL
Sbj 3	mAb 08	Whole-bacterial cell binder	2C7-like binder	0.3 µg/mL	NA
Sbj 3	mAb 09	Low binder	Dot binder	2.5 µg/mL	NA
Sbj 3	mAb 10	Whole-bacterial cell binder	2C7-like binder	1.5 µg/mL	NA
Sbj 3	mAb 11	Medium binder	Side-binder	0.15 µg/mL	NA
Sbj 3	mAb 12	Whole-bacterial cell binder	2C7-like binder	NA	0.04 µg/mL
Sbj 4	mAb 13	Whole-bacterial cell binder	2C7-like binder	0.035 µg/mL	NA
Sbj 4	mAb 14	Low binder	Dot binder	NA	0.16 µg/mL
Sbj 4	mAb 15	Low binder	Dot binder	1.8 µg/mL	7 µg/mL
Sbj 4	mAb 16	Whole-bacterial cell binder	2C7-like binder	0.03 µg/mL	0.16 µg/mL
Sbj 4	mAb 17	Whole-bacterial cell binder	2C7-like binder	0.16 µg/mL	3 µg/mL

NA= Not Active

Transparency statement & conflict of interest

This work results from a collaboration with GSK Vaccines Siena (IT) and Azienda Ospedaliera Universitaria Senese, Siena (IT). This work has received funding under the European Research Council (ERC) advanced grant agreement number 787552 (vAMRes).

Marco Troisi is a PhD student at the Siena University and participates in a post graduate studentship program at Fondazione Toscana Life Sciences.

Human samples ethical statement

Azienda Ospedaliera Universitaria Senese, Siena (IT) provided samples from Bexsero vaccinees donors, who gave their written consent. The study was approved by the local Ethics Committee (AOU Senese, Parere nr. 13946_2018) and conducted according to good clinical practice in accordance with the declaration of Helsinki (European Council 2001, US Code of Federal Regulations, ICH 1997).

List of pubblications

1. **Troisi M**, Andreano E, Sala C, Kabanova A, Rappuoli R. *Vaccines as remedy for antimicrobial resistance and emerging infections.* Curr Opin Immunol. 2020 Aug; 65:102-106. doi: 10.1016/j.coi.2020.09.003.

2. Vacca F, Cardamone D, **Troisi M**, Sala C and Rappuoli R (2020) Antimicrobial Resistance: *A Tale of Nasty Enemies and Powerful Weapons.* Front. Young Minds. 8:554493. doi: 10.3389/frym.2020.554493.

3. Andreano E, Nicastri E, Paciello I, Pileri P, Manganaro N, Piccini G, Manenti A, Pantano E, Kabanova A, **Troisi M**, Vacca F, Cardamone D, De Santi C, Torres JL, Ozorowski G, Benincasa L, Jang H, Di Genova C, Depau L, Brunetti J, Agrati C, Capobianchi MR, Castilletti C, Emiliozzi A, Fabbiani M, Montagnani F, Bracci L, Sautto G, Ross TM, Montomoli E, Temperton N, Ward AB, Sala C, Ippolito G, Rappuoli R. *Extremely potent human monoclonal antibodies from COVID-19 convalescent patients*. Cell. 2021 Apr 1;184(7):1821-1835.e16. doi: 10.1016/j.cell.2021.02.035.

4. Pecetta S, Pizza M, Sala C, Andreano E, Pileri P, **Troisi M**, Pantano E, Manganaro N, Rappuoli R. *Antibodies, epicenter of SARS-CoV-2 immunology*. Cell Death Differ. 2021 Feb;28(2):821-824. doi: 10.1038/s41418-020-00711-w.

11 References

[1] A. Manuscript, “Overview of the immune response,” *Journal of Allergy and Clinical Immunology*, vol. 125, no. 2, p. S345, 2010, doi: 10.1016/j.jaci.2010.01.002.

[2] N. J. N. N. P. S. Daniel E Shumer, “乳鼠心肌提取 HHS Public Access,” *Physiology & behavior*, vol. 176, no. 12, pp. 139–148, 2017, doi: 10.4049/jimmunol.1602000.Innate.

[3] K. Pieper, B. Grimbacher, and H. Eibel, “B-cell biology and development,” *Journal of Allergy and Clinical Immunology*, vol. 131, no. 4, pp. 959–971, 2013, doi: 10.1016/j.jaci.2013.01.046.

[4] D. González *et al.*, “Immunoglobulin gene rearrangements and the pathogenesis of multiple myeloma,” *Blood*, vol. 110, no. 9, pp. 3112–3121, Nov. 2007, doi: 10.1182/blood-2007-02-069625.

[5] P. C. Maity, M. Datta, A. Nicolò, and H. Jumaa, “Isotype Specific Assembly of B Cell Antigen Receptors and Synergism With Chemokine Receptor CXCR4,” *Frontiers in immunology*, vol. 9, no. December, p. 2988, 2018, doi: 10.3389/fimmu.2018.02988.

[6] M. Akkaya, K. Kwak, and S. K. Pierce, “B cell memory: building two walls of protection against pathogens,” *Nature Reviews Immunology*, vol. 20, no. 4, pp. 229–238, 2020, doi: 10.1038/s41577-019-0244-2.

[7] D. Y. Tsai, K. H. Hung, C. W. Chang, and K. I. Lin, “Regulatory mechanisms of B cell responses and the implication in B cell-related diseases,” *Journal of Biomedical Science*, vol. 26, no. 1, pp. 1–13, 2019, doi: 10.1186/s12929-019-0558-1.

[8] M. C. Jespersen, S. Mahajan, B. Peters, M. Nielsen, and P. Marcatili, “Antibody specific B-cell epitope predictions: Leveraging information from antibody-antigen protein complexes,” *Frontiers in Immunology*, vol. 10, no. FEB, pp. 1–10, 2019, doi: 10.3389/fimmu.2019.00298.

[9] J. Han *et al.*, “Polyclonal epitope mapping reveals temporal dynamics and diversity of human antibody responses to H5N1 vaccination,” *Cell Reports*, vol. 34, no. 4, p. 108682, 2021, doi: 10.1016/j.celrep.2020.108682.

[10] H. A. Parray *et al.*, “Hybridoma technology a versatile method for isolation of monoclonal antibodies, its applicability across species, limitations, advancement and future perspectives,” *International immunopharmacology*, vol. 85, p. 106639, Aug. 2020, doi: 10.1016/j.intimp.2020.106639.

[11] C. Parola, D. Neumeier, and S. T. Reddy, “Integrating high-throughput screening and sequencing for monoclonal antibody discovery and engineering,” *Immunology*, vol. 153, no. 1, pp. 31–41, Jan. 2018, doi: https://doi.org/10.1111/imm.12838.

[12] E. A. Van Erp, W. Luytjes, G. Ferwerda, and P. B. Van Kasteren, “Fc-mediated antibody effector functions during respiratory syncytial virus infection and disease,” *Frontiers in Immunology*, vol. 10, no. MAR, 2019, doi: 10.3389/fimmu.2019.00548.

[13] H. W. Schroeder and L. Cavacini, “Structure and function of immunoglobulins,” *Journal of Allergy and Clinical Immunology*, vol. 125, no. 2 SUPPL. 2, pp. S41–S52, 2010, doi: 10.1016/j.jaci.2009.09.046.

[14] H. Liu and K. May, “Disulfide bond structures of IgG molecules: Structural variations, chemical modifications and possible impacts to stability and biological function,” *mAbs*, vol. 4, no. 1, pp. 17–23, 2012, doi: 10.4161/mabs.4.1.18347.

[15] M. Dondelinger *et al.*, “Understanding the significance and implications of antibody numbering and antigen-binding surface/residue definition,” *Frontiers in Immunology*, vol. 9, no. OCT, pp. 1–15, 2018, doi: 10.3389/fimmu.2018.02278.

[16] J. L. Xu and M. M. Davis, “Diversity in the CDR3 Region of V,” *Immunity*, vol. 13, pp. 37–45, 2000.

[17] M. L. Chiu, D. R. Goulet, A. Teplyakov, and G. L. Gilliland, “Antibody Structure and Function: The Basis for Engineering Therapeutics,” *Antibodies*, vol. 8, no. 4, p. 55, 2019, doi: 10.3390/antib8040055.

[18] I. Sela-Culang, V. Kunik, and Y. Ofran, “The structural basis of antibody-antigen recognition,” *Frontiers in Immunology*, vol. 4, no. OCT, pp. 1–13, 2013, doi: 10.3389/fimmu.2013.00302.

[19] G. Vidarsson, G. Dekkers, and T. Rispens, “IgG subclasses and allotypes: From structure to effector functions,” *Frontiers in Immunology*, vol. 5, no. OCT, pp. 1–17, 2014, doi: 10.3389/fimmu.2014.00520.

[20] A. Gonzalez-Quintela *et al.*, “Serum levels of immunoglobulins (IgG, IgA, IgM) in a general adult population and their relationship with alcohol consumption, smoking and common metabolic abnormalities,” *Clinical and Experimental Immunology*, vol. 151, no. 1, pp. 42–50, 2008, doi: 10.1111/j.1365-2249.2007.03545.x.

[21] B. A. Keyt, R. Baliga, A. M. Sinclair, S. F. Carroll, and M. S. Peterson, “Structure, Function, and Therapeutic Use of IgM Antibodies,” *Antibodies*, vol. 9, no. 4, p. 53, 2020, doi: 10.3390/antib9040053.

[22] M. Basta, “Activation and Inhibition of Complement by Immunoglobulins,” *The Complement System*, pp. 517–529, 2006, doi: 10.1007/1-4020-8056-5_24.

[23] P. de Sousa-Pereira and J. M. Woof, “IgA: Structure, Function, and Developability,” *Antibodies (Basel, Switzerland)*, vol. 8, no. 4, p. 57, Dec. 2019, doi: 10.3390/antib8040057.

[24] A. M. Collins and C. T. Watson, “Immunoglobulin light chain gene rearrangements, receptor editing and the development of a self-tolerant antibody repertoire,” *Frontiers in Immunology*, vol. 9, no. OCT, pp. 1–12, 2018, doi: 10.3389/fimmu.2018.02249.

[25] D. B. Roth, “V(D)J Recombination: Mechanism, Errors, and Fidelity,” *Microbiology spectrum*, vol. 2, no. 6, pp. 10.1128/microbiolspec.MDNA3-0041–2014, Dec. 2014, doi: 10.1128/microbiolspec.MDNA3-0041-2014.

[26] L. Potocnakova, M. Bhide, and L. B. Pulzova, “An Introduction to B-Cell Epitope Mapping and In Silico Epitope Prediction,” *Journal of immunology research*, vol. 2016, p. 6760830, 2016, doi: 10.1155/2016/6760830.

[27] J. V. Kringelum, C. Lundegaard, O. Lund, and M. Nielsen, “Reliable B Cell Epitope Predictions: Impacts of Method Development and Improved Benchmarking,” *PLOS Computational Biology*, vol. 8, no. 12, p. e1002829, Dec. 2012.

[28] T. Ramaraj, T. Angel, E. A. Dratz, A. J. Jesaitis, and B. Mumey, “Antigen-antibody interface properties: composition, residue interactions, and features of 53 non-redundant structures,” *Biochimica et biophysica acta*, vol. 1824, no. 3, pp. 520–532, Mar. 2012, doi: 10.1016/j.bbapap.2011.12.007.

[29] W. M. Abbott, M. M. Damschroder, and D. C. Lowe, “Current approaches to fine mapping of antigen-antibody interactions,” *Immunology*, vol. 142, no. 4, pp. 526–535, Aug. 2014, doi: 10.1111/imm.12284.

[30] V. Kunik, B. Peters, and Y. Ofran, “Structural consensus among antibodies defines the antigen binding site,” *PLoS computational biology*, vol. 8, no. 2, pp. e1002388–e1002388, 2012, doi: 10.1371/journal.pcbi.1002388.

[31] M.-P. Lefranc, “IMGT, the international ImMunoGeneTics database,” *Nucleic acids research*, vol. 31, no. 1, pp. 307–310, Jan. 2003, doi: 10.1093/nar/gkg085.

[32] E. A. Padlan, “X-Ray Crystallography of Antibodies,” in *Antigen Binding Molecules: Antibodies and T-cell Receptors*, vol. 49, F. M. Richards, D. E. Eisenberg, and P. S. B. T.-A. in P. C. Kim, Eds. Academic Press, 1996, pp. 57–133. doi: https://doi.org/10.1016/S0065-3233(08)60488-X.

[33] B. D. Weitzner, R. L. Dunbrack Jr, and J. J. Gray, “The origin of CDR H3 structural diversity,” *Structure (London, England : 1993)*, vol. 23, no. 2, pp. 302–311, Feb. 2015, doi: 10.1016/j.str.2014.11.010.

[34] R. A. Alberty, “Standard Gibbs free energy, enthalpy, and entropy changes as a function of pH and pMg for several reactions involving adenosine phosphates.,” *Journal of Biological Chemistry*, vol. 244, no. 12, pp. 3290–3302, 1969, doi: 10.1016/s0021-9258(18)93127-3.

[35] X. Du *et al.*, “Insights into Protein-Ligand Interactions: Mechanisms, Models, and Methods,” *International journal of molecular sciences*, vol. 17, no. 2, p. 144, Jan. 2016, doi: 10.3390/ijms17020144.

[36] L. Di Rienzo, E. Milanetti, G. Ruocco, and R. Lepore, “Quantitative Description of Surface Complementarity of Antibody-Antigen Interfaces ,” *Frontiers in Molecular Biosciences* , vol. 8. p. 933, 2021.

[37] T. Te Wu and E. A. Kabat, “AN ANALYSIS OF THE SEQUENCES OF THE VARIABLE REGIONS OF BENCE JONES PROTEINS AND MYELOMA LIGHT CHAINS AND THEIR IMPLICATIONS FOR ANTIBODY COMPLEMENTARITY ,” *Journal of Experimental Medicine*, vol. 132, no. 2, pp. 211–250, Aug. 1970, doi: 10.1084/jem.132.2.211.

[38] J. C. Almagro, “Identification of differences in the specificity-determining residues of antibodies that recognize antigens of different size: implications

for the rational design of antibody repertoires," *Journal of Molecular Recognition*, vol. 17, no. 2, pp. 132–143, Mar. 2004, doi: https://doi.org/10.1002/jmr.659.

[39] E. Vargas-Madrazo, F. Lara-Ochoa, and J. Carlos Almagro, "Canonical Structure Repertoire of the Antigen-binding Site of Immunoglobulins Suggests Strong Geometrical Restrictions Associated to the Mechanism of Immune Recognition," *Journal of Molecular Biology*, vol. 254, no. 3, pp. 497–504, 1995, doi: https://doi.org/10.1006/jmbi.1995.0633.

[40] B. North, A. Lehmann, and R. L. Dunbrack, "A New Clustering of Antibody CDR Loop Conformations," *Journal of Molecular Biology*, vol. 406, no. 2, pp. 228–256, 2011, doi: https://doi.org/10.1016/j.jmb.2010.10.030.

[41] V. Kunik and Y. Ofran, "The indistinguishability of epitopes from protein surface is explained by the distinct binding preferences of each of the six antigen-binding loops," *Protein Engineering, Design and Selection*, vol. 26, no. 10, pp. 599–609, Oct. 2013, doi: 10.1093/protein/gzt027.

[42] I. S. Mian, A. R. Bradwell, and A. J. Olson, "Structure, function and properties of antibody binding sites," *Journal of Molecular Biology*, vol. 217, no. 1, pp. 133–151, 1991, doi: https://doi.org/10.1016/0022-2836(91)90617-F.

[43] S. Koide and S. S. Sidhu, "The Importance of Being Tyrosine: Lessons in Molecular Recognition from Minimalist Synthetic Binding Proteins," *ACS Chemical Biology*, vol. 4, no. 5, pp. 325–334, May 2009, doi: 10.1021/cb800314v.

[44] J. V. Kringelum, M. Nielsen, S. B. Padkjær, and O. Lund, "Structural analysis of B-cell epitopes in antibody:protein complexes," *Molecular Immunology*, vol. 53, no. 1, pp. 24–34, 2013, doi: https://doi.org/10.1016/j.molimm.2012.06.001.

[45] G. Raghunathan, J. Smart, J. Williams, and J. C. Almagro, “Antigen-binding site anatomy and somatic mutations in antibodies that recognize different types of antigens,” *Journal of Molecular Recognition*, vol. 25, no. 3, pp. 103–113, Mar. 2012, doi: https://doi.org/10.1002/jmr.2158.

[46] H.-P. Peng, K. H. Lee, J.-W. Jian, and A.-S. Yang, “Origins of specificity and affinity in antibody–protein interactions,” *Proceedings of the National Academy of Sciences*, vol. 111, no. 26, p. E2656 LP-E2665, Jul. 2014, doi: 10.1073/pnas.1401131111.

[47] W. M. Abbott, M. M. Damschroder, and D. C. Lowe, “Current approaches to fine mapping of antigen–antibody interactions,” *Immunology*, vol. 142, no. 4, p. 526, 2014, doi: 10.1111/IMM.12284.

[48] E. J. Sundberg and R. A. Mariuzza, “Molecular recognition in antibody-antigen complexes,” *Advances in protein chemistry*, vol. 61, pp. 119–160, 2002, doi: 10.1016/S0065-3233(02)61004-6.

[49] L.-F. Wang and M. Yu, “Epitope identification and discovery using phage display libraries: applications in vaccine development and diagnostics,” *Current drug targets*, vol. 5, no. 1, pp. 1–15, Mar. 2004, doi: 10.2174/1389450043490668.

[50] J. R. R. Whittle *et al.*, “Broadly neutralizing human antibody that recognizes the receptor-binding pocket of influenza virus hemagglutinin,” *Proceedings of the National Academy of Sciences of the United States of America*, vol. 108, no. 34, pp. 14216–14221, Aug. 2011, doi: 10.1073/PNAS.1111497108.

[51] H. M. Geysen, R. H. Meloen, and S. J. Barteling, “Use of peptide synthesis to probe viral antigens for epitopes to a resolution of a single amino acid,” *Proceedings of the National Academy of Sciences of the United States of America*, vol. 81, no. 13, pp. 3998–4002, 1984, doi: 10.1073/PNAS.81.13.3998.

[52] H. M. DeLisser, “Epitope mapping,” *Methods in molecular biology (Clifton, N.J.)*, vol. 96, pp. 11–20, 1999, doi: 10.1385/1-59259-258-9:11.

[53] P. Timmerman, W. C. Puijk, and R. H. Meloen, “Functional reconstruction and synthetic mimicry of a conformational epitope using CLIPS technology,” *Journal of molecular recognition : JMR*, vol. 20, no. 5, pp. 283–299, Sep. 2007, doi: 10.1002/JMR.846.

[54] P. J. Hudson, “Recombinant antibody fragments,” *Current opinion in biotechnology*, vol. 9, no. 4, pp. 395–402, 1998, doi: 10.1016/S0958-1669(98)80014-1.

[55] B. Harris and B. Harris, “Exploiting antibody-based technologies to manage environmental pollution,” *Trends in Biotechnology*, vol. 17, no. 7, pp. 290–296, Jul. 1999, doi: 10.1016/S0167-7799(99)01308-6.

[56] S. Ewert, T. Huber, A. Honegger, and A. Plückthun, “Biophysical properties of human antibody variable domains,” *Journal of molecular biology*, vol. 325, no. 3, pp. 531–553, 2003, doi: 10.1016/S0022-2836(02)01237-8.

[57] Z. Elgundi, M. Reslan, E. Cruz, V. Sifniotis, and V. Kayser, “The state-of-play and future of antibody therapeutics,” *Advanced drug delivery reviews*, vol. 122, pp. 2–19, Dec. 2017, doi: 10.1016/J.ADDR.2016.11.004.

[58] X. Yang *et al.*, “Developability studies before initiation of process development: improving manufacturability of monoclonal antibodies,” *mAbs*, vol. 5, no. 5, pp. 787–794, Sep. 2013, doi: 10.4161/MABS.25269.

[59] H. R. Hoogenboom, “Selecting and screening recombinant antibody libraries,” *Nature biotechnology*, vol. 23, no. 9, pp. 1105–1116, Sep. 2005, doi: 10.1038/NBT1126.

[60] C. Zahnd, S. Spinelli, B. Luginbühl, P. Amstutz, C. Cambillau, and A. Plückthun, “Directed in vitro evolution and crystallographic analysis of a peptide-binding single chain antibody fragment (scFv) with low picomolar

affinity," *The Journal of biological chemistry*, vol. 279, no. 18, pp. 18870–18877, Apr. 2004, doi: 10.1074/JBC.M309169200.

[61] J. A. Maynard, C. B. M. Maassen, S. H. Leppla, K. Brasky, B. L. Iverson, and G. Georgiou, "Protection against anthrax toxin by recombinant antibody fragments correlates with antigen affinity," *Nature biotechnology*, vol. 20, no. 6, pp. 597–601, 2002, doi: 10.1038/NBT0602-597.

[62] M. L. Chiu and G. L. Gilliland, "Engineering antibody therapeutics," *Current opinion in structural biology*, vol. 38, pp. 163–173, Jun. 2016, doi: 10.1016/J.SBI.2016.07.012.

[63] H. R. Hoogenboom and P. Chames, "Natural and designer binding sites made by phage display technology," *Immunology today*, vol. 21, no. 8, pp. 371–378, 2000, doi: 10.1016/S0167-5699(00)01667-4.

[64] E. T. Boder, K. S. Midelfort, and K. D. Wittrup, "Directed evolution of antibody fragments with monovalent femtomolar antigen-binding affinity," *Proceedings of the National Academy of Sciences*, vol. 97, no. 20, pp. 10701–10705, Sep. 2000, doi: 10.1073/PNAS.170297297.

[65] R. Rouet, D. Lowe, and D. Christ, "Stability engineering of the human antibody repertoire," *FEBS letters*, vol. 588, no. 2, pp. 269–277, Jan. 2014, doi: 10.1016/J.FEBSLET.2013.11.029.

[66] J. Davies and L. Riechmann, "'Camelising' human antibody fragments: NMR studies on VH domains," *FEBS letters*, vol. 339, no. 3, pp. 285–290, Feb. 1994, doi: 10.1016/0014-5793(94)80432-X.

[67] M. Arbabi Ghahroudi, A. Desmyter, L. Wyns, R. Hamers, and S. Muyldermans, "Selection and identification of single domain antibody fragments from camel heavy-chain antibodies," *FEBS letters*, vol. 414, no. 3, pp. 521–526, Sep. 1997, doi: 10.1016/S0014-5793(97)01062-4.

[68] R. H. J. van der Linden *et al.*, "Comparison of physical chemical properties of llama VHH antibody fragments and mouse monoclonal antibodies,"

Biochimica et biophysica acta, vol. 1431, no. 1, pp. 37–46, Apr. 1999, doi: 10.1016/S0167-4838(99)00030-8.

[69] P. A. Barthelemy *et al.*, "Comprehensive analysis of the factors contributing to the stability and solubility of autonomous human VH domains," *The Journal of biological chemistry*, vol. 283, no. 6, pp. 3639–3654, Feb. 2008, doi: 10.1074/JBC.M708536200.

[70] A. Knappik *et al.*, "Fully synthetic human combinatorial antibody libraries (HuCAL) based on modular consensus frameworks and CDRs randomized with trinucleotides," *Journal of molecular biology*, vol. 296, no. 1, pp. 57–86, Feb. 2000, doi: 10.1006/JMBI.1999.3444.

[71] A. Wörn and A. Plückthun, "Stability engineering of antibody single-chain Fv fragments," *Journal of molecular biology*, vol. 305, no. 5, pp. 989–1010, Feb. 2001, doi: 10.1006/JMBI.2000.4265.

[72] W. L. Martin, A. P. West, L. Gan, and P. J. Bjorkman, "Crystal structure at 2.8 A of an FcRn/heterodimeric Fc complex: mechanism of pH-dependent binding," *Molecular cell*, vol. 7, no. 4, pp. 867–877, 2001, doi: 10.1016/S1097-2765(01)00230-1.

[73] B. J. Booth *et al.*, "Extending human IgG half-life using structure-guided design," *mAbs*, vol. 10, no. 7, p. 1098, Oct. 2018, doi: 10.1080/19420862.2018.1490119.

[74] P. R. Hinton, J. M. Xiong, M. G. Johlfs, M. T. Tang, S. Keller, and N. Tsurushita, "An engineered human IgG1 antibody with longer serum half-life," *Journal of immunology (Baltimore, Md. : 1950)*, vol. 176, no. 1, pp. 346–356, Jan. 2006, doi: 10.4049/JIMMUNOL.176.1.346.

[75] W. F. Dall'Acqua, P. A. Kiener, and H. Wu, "Properties of human IgG1s engineered for enhanced binding to the neonatal Fc receptor (FcRn)," *The Journal of biological chemistry*, vol. 281, no. 33, pp. 23514–23524, Aug. 2006, doi: 10.1074/JBC.M604292200.

[76] R. Niwa and M. Satoh, “The current status and prospects of antibody engineering for therapeutic use: focus on glycoengineering technology,” *Journal of pharmaceutical sciences*, vol. 104, no. 3, pp. 930–941, 2015, doi: 10.1002/JPS.24316.

[77] S. Derer, C. Kellner, S. Berger, T. Valerius, and M. Peipp, “Fc engineering: design, expression, and functional characterization of antibody variants with improved effector function,” *Methods in molecular biology (Clifton, N.J.)*, vol. 907, pp. 519–536, 2012, doi: 10.1007/978-1-61779-974-7_30.

[78] A. K. Kakkar and S. Balakrishnan, “Obinutuzumab for chronic lymphocytic leukemia: promise of the first treatment approved with breakthrough therapy designation,” *Journal of oncology pharmacy practice : official publication of the International Society of Oncology Pharmacy Practitioners*, vol. 21, no. 5, pp. 358–363, Oct. 2015, doi: 10.1177/1078155214534868.

[79] M. Sachdeva and S. Dhingra, “Obinutuzumab: A FDA approved monoclonal antibody in the treatment of untreated chronic lymphocytic leukemia,” *International Journal of Applied and Basic Medical Research*, vol. 5, no. 1, p. 54, 2015, doi: 10.4103/2229-516X.149245.

[80] R. Liu, R. J. Oldham, E. Teal, S. A. Beers, and M. S. Cragg, “Fc-Engineering for Modulated Effector Functions—Improving Antibodies for Cancer Treatment,” *Antibodies*, vol. 9, no. 4, p. 64, Nov. 2020, doi: 10.3390/ANTIB9040064.

[81] E. A. van Erp, W. Luytjes, G. Ferwerda, and P. B. van Kasteren, “Fc-mediated antibody effector functions during respiratory syncytial virus infection and disease,” *Frontiers in Immunology*, vol. 10, no. MAR, p. 548, 2019, doi: 10.3389/FIMMU.2019.00548/BIBTEX.

[82] S. Bournazos, A. Gupta, and J. v. Ravetch, “The role of IgG Fc receptors in antibody-dependent enhancement,” *Nature Reviews Immunology 2020*

20:10, vol. 20, no. 10, pp. 633–643, Aug. 2020, doi: 10.1038/s41577-020-00410-0.

[83] S. Pecetta *et al.*, "Antibodies, epicenter of SARS-CoV-2 immunology," *Cell Death and Differentiation*, vol. 28, no. 2, p. 821, Feb. 2021, doi: 10.1038/S41418-020-00711-W.

[84] W. S. Lee, A. K. Wheatley, S. J. Kent, and B. J. DeKosky, "Antibody-dependent enhancement and SARS-CoV-2 vaccines and therapies," *Nature Microbiology 2020 5:10*, vol. 5, no. 10, pp. 1185–1191, Sep. 2020, doi: 10.1038/s41564-020-00789-5.

[85] E. Andreano *et al.*, "Extremely potent human monoclonal antibodies from COVID-19 convalescent patients," *Cell*, vol. 184, no. 7, pp. 1821-1835.e16, Apr. 2021, doi: 10.1016/J.CELL.2021.02.035.

[86] E. M. Cook *et al.*, "Antibodies That Efficiently Form Hexamers upon Antigen Binding Can Induce Complement-Dependent Cytotoxicity under Complement-Limiting Conditions," *Journal of immunology (Baltimore, Md.: 1950)*, vol. 197, no. 5, pp. 1762–1775, Sep. 2016, doi: 10.4049/JIMMUNOL.1600648.

[87] R. N. de Jong *et al.*, "A Novel Platform for the Potentiation of Therapeutic Antibodies Based on Antigen-Dependent Formation of IgG Hexamers at the Cell Surface," *PLoS biology*, vol. 14, no. 1, Jan. 2016, doi: 10.1371/JOURNAL.PBIO.1002344.

[88] J. Sevigny *et al.*, "Addendum: The antibody aducanumab reduces Aβ plaques in Alzheimer's disease," *Nature*, vol. 546, no. 7659, p. 564, Jun. 2017, doi: 10.1038/NATURE22809.

[89] A. C. Chan and P. J. Carter, "Therapeutic antibodies for autoimmunity and inflammation," *Nature reviews. Immunology*, vol. 10, no. 5, pp. 301–316, May 2010, doi: 10.1038/NRI2761.

[90] K. A. Robinson, O. A. Odelola, and I. J. Saldanha, “Palivizumab for prophylaxis against respiratory syncytial virus infection in children with cystic fibrosis,” *The Cochrane database of systematic reviews*, vol. 7, no. 7, Jul. 2016, doi: 10.1002/14651858.CD007743.PUB6.

[91] K. Kupferschmidt, “Successful Ebola treatments promise to tame outbreak,” *Science*, vol. 365, no. 6454, pp. 628–629, Aug. 2019, doi: 10.1126/SCIENCE.365.6454.628/ASSET/38FAB96C-11E2-4BA4-B3D7-16B3013DB27B/ASSETS/SCIENCE.365.6454.628.FP.PNG.

[92] T. E. Sizikova, G. v. Borisevlch, D. v. Shcheblyakov, D. A. Burmistrova, and V. N. Lebedev, “[The use of monoclonal antibodies for the treatment of Ebola virus disease],” *Voprosy virusologii*, vol. 63, no. 6, pp. 245–249, 2018, doi: 10.18821/0507-4088-2018-63-6-245-249.

[93] D. v. Zurawski and M. K. McLendon, “Monoclonal Antibodies as an Antibacterial Approach Against Bacterial Pathogens,” *Antibiotics (Basel, Switzerland)*, vol. 9, no. 4, Apr. 2020, doi: 10.3390/ANTIBIOTICS9040155.

[94] M. Unemo and W. M. Shafer, “Antimicrobial Resistance in Neisseria gonorrhoeae in the 21st Century: Past, Evolution, and Future,” *Clinical Microbiology Reviews*, vol. 27, no. 3, p. 587, 2014, doi: 10.1128/CMR.00010-14.

[95] M. P. Motley and B. C. Fries, “A New Take on an Old Remedy: Generating Antibodies against Multidrug-Resistant Gram-Negative Bacteria in a Postantibiotic World,” *mSphere*, vol. 2, no. 5, Oct. 2017, doi: 10.1128/MSPHERE.00397-17.

[96] A. Sörman, L. Zhang, Z. Ding, and B. Heyman, “How antibodies use complement to regulate antibody responses,” *Molecular immunology*, vol. 61, no. 2, pp. 79–88, 2014, doi: 10.1016/J.MOLIMM.2014.06.010.

[97] M. Noris and G. Remuzzi, “Overview of complement activation and regulation,” *Seminars in nephrology*, vol. 33, no. 6, pp. 479–492, Nov. 2013, doi: 10.1016/J.SEMNEPHROL.2013.08.001.

[98] N. S. Merle, S. E. Church, V. Fremeaux-Bacchi, and L. T. Roumenina, “Complement System Part I - Molecular Mechanisms of Activation and Regulation,” *Frontiers in immunology*, vol. 6, no. JUN, 2015, doi: 10.3389/FIMMU.2015.00262.

[99] N. S. Merle, R. Noe, L. Halbwachs-Mecarelli, V. Fremeaux-Bacchi, and L. T. Roumenina, “Complement System Part II: Role in Immunity,” *Frontiers in Immunology*, vol. 6, no. MAY, 2015, doi: 10.3389/FIMMU.2015.00257.

[100] A. H. Stephan, B. A. Barres, and B. Stevens, “The complement system: an unexpected role in synaptic pruning during development and disease,” *Annual review of neuroscience*, vol. 35, pp. 369–389, Jul. 2012, doi: 10.1146/ANNUREV-NEURO-061010-113810.

[101] H. F. Langer *et al.*, “Complement-mediated inhibition of neovascularization reveals a point of convergence between innate immunity and angiogenesis,” *Blood*, vol. 116, no. 22, pp. 4395–4403, Nov. 2010, doi: 10.1182/BLOOD-2010-01-261503.

[102] A. Janowska-Wieczorek, L. A. Marquez-Curtis, N. Shirvaikar, and M. Z. Ratajczak, “The Role of Complement in the Trafficking of Hematopoietic Stem/Progenitor Cells,” *Transfusion*, vol. 52, no. 12, p. 2706, Dec. 2012, doi: 10.1111/J.1537-2995.2012.03636.X.

[103] D. Gauvreau *et al.*, “A new effector of lipid metabolism: complement factor properdin,” *Molecular immunology*, vol. 51, no. 1, pp. 73–81, May 2012, doi: 10.1016/J.MOLIMM.2012.02.110.

[104] E. M. Conway, “Reincarnation of ancient links between coagulation and complement,” *Journal of thrombosis and haemostasis : JTH*, vol. 13 Suppl 1, no. S1, pp. S121–S132, Jun. 2015, doi: 10.1111/JTH.12950.

[105] U. Amara *et al.*, “Molecular intercommunication between the complement and coagulation systems,” *Journal of immunology (Baltimore, Md. : 1950)*, vol. 185, no. 9, pp. 5628–5636, Nov. 2010, doi: 10.4049/JIMMUNOL.0903678.

[106] A. Sahu, T. R. Kozel, and M. K. Pangburn, “Specificity of the thioester-containing reactive site of human C3 and its significance to complement activation.,” *Biochemical Journal*, vol. 302, no. Pt 2, p. 429, 1994, doi: 10.1042/BJ3020429.

[107] S. R. Barnum, “Complement: A primer for the coming therapeutic revolution,” *Pharmacology & therapeutics*, vol. 172, pp. 63–72, Apr. 2017, doi: 10.1016/J.PHARMTHERA.2016.11.014.

[108] S. A. Zwarthoff *et al.*, “Functional characterization of alternative and classical pathway C3/C5 convertase activity and inhibition using purified models,” *Frontiers in Immunology*, vol. 9, no. JUL, p. 1691, Jul. 2018, doi: 10.3389/FIMMU.2018.01691/BIBTEX.

[109] F. D. G. McGrath, M. C. Brouwer, G. J. Arlaud, M. R. Daha, C. E. Hack, and A. Roos, “Evidence that complement protein C1q interacts with C-reactive protein through its globular head region,” *Journal of immunology (Baltimore, Md. : 1950)*, vol. 176, no. 5, pp. 2950–2957, Mar. 2006, doi: 10.4049/JIMMUNOL.176.5.2950.

[110] U. Kishore *et al.*, “Structural and functional anatomy of the globular domain of complement protein C1q,” *Immunology letters*, vol. 95, no. 2, pp. 113–128, 2004, doi: 10.1016/J.IMLET.2004.06.015.

[111] M. W. Turner, “The role of mannose-binding lectin in health and disease,” *Molecular Immunology*, vol. 40, no. 7, pp. 423–429, Nov. 2003, doi: 10.1016/S0161-5890(03)00155-X.

[112] “Clonal variations in complement activation and deposition of C3b and C4b on model immune complexes - PubMed.” https://pubmed.ncbi.nlm.nih.gov/8262546/ (accessed Dec. 14, 2021).

[113] V. Krishnan, Y. Xu, K. Macon, J. E. Volanakis, and S. V. L. Narayana, “The structure of C2b, a fragment of complement component C2 produced during C3 convertase formation,” *Acta Crystallographica Section D: Biological Crystallography*, vol. 65, no. Pt 3, p. 266, 2009, doi: 10.1107/S0907444909000389.

[114] M. K. Pangburn, R. D. Schreiber, and H. J. Muller-Eberhard, “Formation of the initial C3 convertase of the alternative complement pathway. Acquisition of C3b-like activities by spontaneous hydrolysis of the putative thioester in native C3,” *The Journal of experimental medicine*, vol. 154, no. 3, pp. 856–867, Sep. 1981, doi: 10.1084/JEM.154.3.856.

[115] A. A. Korotaevskiy, L. G. Hanin, and M. A. Khanin, “Non-linear dynamics of the complement system activation,” *Mathematical biosciences*, vol. 222, no. 2, pp. 127–143, Dec. 2009, doi: 10.1016/J.MBS.2009.10.003.

[116] “Characterization of the initial C3 convertase of the alternative pathway of human complement - PubMed.” https://pubmed.ncbi.nlm.nih.gov/6559201/ (accessed Dec. 14, 2021).

[117] H. O. J. Morad, S. C. Belete, T. Read, and A. M. Shaw, “Time-course analysis of C3a and C5a quantifies the coupling between the upper and terminal Complement pathways in vitro,” *Journal of immunological methods*, vol. 427, pp. 13–18, Dec. 2015, doi: 10.1016/J.JIM.2015.09.001.

[118] D. Bubeck, “The making of a macromolecular machine: assembly of the membrane attack complex,” *Biochemistry*, vol. 53, no. 12, pp. 1908–1915, Apr. 2014, doi: 10.1021/BI500157Z.

[119] K. Jurianz *et al.*, “Complement resistance of tumor cells: basal and induced mechanisms,” *Molecular immunology*, vol. 36, no. 13–14, pp. 929–939, Sep. 1999, doi: 10.1016/S0161-5890(99)00115-7.

[120] E. Ballanti *et al.*, “Complement and autoimmunity.,” *Immunologic Research*, vol. 56, no. 2–3, pp. 477–491, Jul. 2013, doi: 10.1007/S12026-013-8422-Y.

[121] D. C. Mastellos *et al.*, “Compstatin: a C3-targeted complement inhibitor reaching its prime for bedside intervention,” *European journal of clinical investigation*, vol. 45, no. 4, pp. 423–440, Apr. 2015, doi: 10.1111/ECI.12419.

[122] J. Ren *et al.*, “Complement Depletion Deteriorates Clinical Outcomes of Severe Abdominal Sepsis: A Conspirator of Infection and Coagulopathy in Crime?,” *PLoS ONE*, vol. 7, no. 10, Oct. 2012, doi: 10.1371/JOURNAL.PONE.0047095.

[123] J. L. Edwards and M. A. Apicella, “The Molecular Mechanisms Used by Neisseria gonorrhoeae To Initiate Infection Differ between Men and Women,” *Clinical Microbiology Reviews*, vol. 17, no. 4, p. 965, Oct. 2004, doi: 10.1128/CMR.17.4.965-981.2004.

[124] B. L. Ligon, “Albert Ludwig Sigesmund Neisser: discoverer of the cause of gonorrhea,” *Seminars in pediatric infectious diseases*, vol. 16, no. 4, pp. 336–341, 2005, doi: 10.1053/J.SPID.2005.07.001.

[125] A. J. Cokkinis, “Sulphanilamide in Gonorrhoea,” *British medical journal*, vol. 2, no. 4009, pp. 905–909, Nov. 1937, doi: 10.1136/BMJ.2.4009.905.

[126] E. C. Haese, V. C. Thai, and C. M. Kahler, “Vaccine Candidates for the Control and Prevention of the Sexually Transmitted Disease Gonorrhea,” *Vaccines 2021, Vol. 9, Page 804*, vol. 9, no. 7, p. 804, Jul. 2021, doi: 10.3390/VACCINES9070804.

[127] “WHO publishes list of bacteria for which new antibiotics are urgently needed.” https://www.who.int/news/item/27-02-2017-who-publishes-list-of-bacteria-for-which-new-antibiotics-are-urgently-needed (accessed Dec. 14, 2021).

[128] M. Unemo and W. M. Shafer, “Antimicrobial Resistance in Neisseria gonorrhoeae in the 21st Century: Past, Evolution, and Future,” *Clinical Microbiology Reviews*, vol. 27, no. 3, p. 587, 2014, doi: 10.1128/CMR.00010-14.

[129] J. M. Spence, L. Wright, and V. L. Clark, “Laboratory Maintenance of Neisseria gonorrhoeae,” *Current Protocols in Microbiology*, vol. 8, no. 1, pp. 4A.1.1-4A.1.26, Feb. 2008, doi: 10.1002/9780471729259.MC04A01S8.

[130] B. Wesley Catlin, “Nutritional profiles of Neisseria gonorrhoeae, Neisseria meningitidis, and Neisseria lactamica in chemically defined media and the use of growth requirements for gonococcal typing,” *The Journal of infectious diseases*, vol. 128, no. 2, pp. 178–194, 1973, doi: 10.1093/INFDIS/128.2.178.

[131] S. J. Quillin and H. S. Seifert, “Neisseria gonorrhoeae host adaptation and pathogenesis,” *Nature reviews. Microbiology*, vol. 16, no. 4, pp. 226–240, Apr. 2018, doi: 10.1038/NRMICRO.2017.169.

[132] J. B. Patrone and D. C. Stein, “Effect of gonococcal lipooligosaccharide variation on human monocytic cytokine profile,” *BMC Microbiology*, vol. 7, p. 7, 2007, doi: 10.1186/1471-2180-7-7.

[133] “Lipooligosaccharides: The Principal Glycolipids of the Neisserial Outer Membrane on JSTOR.” https://www.jstor.org/stable/4454586 (accessed Dec. 14, 2021).

[134] Q. L. Yang and E. C. Gotschlich, “Variation of gonococcal lipooligosaccharide structure is due to alterations in poly-G tracts in lgt

genes encoding glycosyl transferases," *The Journal of experimental medicine*, vol. 183, no. 1, pp. 323–327, Jan. 1996, doi: 10.1084/JEM.183.1.323.

[135] M. A. Zelewska *et al.*, "Phase variable DNA repeats in Neisseria gonorrhoeae influence transcription, translation, and protein sequence variation," *Microbial Genomics*, vol. 2, no. 8, p. e000078, Aug. 2016, doi: 10.1099/MGEN.0.000078.

[136] E. C. Gotschlich, "Genetic locus for the biosynthesis of the variable portion of Neisseria gonorrhoeae lipooligosaccharide.," *Journal of Experimental Medicine*, vol. 180, no. 6, pp. 2181–2190, Dec. 1994, doi: 10.1084/JEM.180.6.2181.

[137] D. C. Braun and D. C. Stein, "The lgtABCDE gene cluster, involved in lipooligosaccharide biosynthesis in Neisseria gonorrhoeae, contains multiple promoter sequences," *Journal of bacteriology*, vol. 186, no. 4, pp. 1038–1049, Feb. 2004, doi: 10.1128/JB.186.4.1038-1049.2004.

[138] Y. Tong, D. Arking, S. Ye, B. Reinhold, V. Reinhold, and D. C. Stein, "Neisseria gonorrhoeae strain PID2 simultaneously expresses six chemically related lipooligosaccharide structures," *Glycobiology*, vol. 12, no. 9, pp. 523–533, Sep. 2002, doi: 10.1093/GLYCOB/CWF047.

[139] "Sialylation Lessens the Infectivity of Neisseria gonorrhoeae MS11mkC on JSTOR." https://www.jstor.org/stable/30128153 (accessed Dec. 14, 2021).

[140] J. G. Cole, N. B. Fulcher, and A. E. Jerse, "Opacity proteins increase Neisseria gonorrhoeae fitness in the female genital tract due to a factor under ovarian control," *Infection and Immunity*, vol. 78, no. 4, pp. 1629–1641, Apr. 2010, doi: 10.1128/IAI.00996-09/ASSET/51B19531-2D43-4C81-8C4C-194A575DD318/ASSETS/GRAPHIC/ZII9990985190007.JPEG.

[141] W. J. Black, R. S. Schwalbe, I. Nachamkin, and J. G. Cannon, “Characterization of Neisseria gonorrhoeae protein II phase variation by use of monoclonal antibodies,” *Infection and immunity*, vol. 45, no. 2, pp. 453–457, 1984, doi: 10.1128/IAI.45.2.453-457.1984.

[142] M. B. Johnson, L. M. Ball, K. P. Daily, J. N. Martin, L. Columbus, and A. K. Criss, “Opa+ Neisseria gonorrhoeae Exhibits Reduced Survival in Human Neutrophils Via Src Family Kinase-Mediated Bacterial Trafficking Into Mature Phagolysosomes,” *Cellular microbiology*, vol. 17, no. 5, p. 648, May 2015, doi: 10.1111/CMI.12389.

[143] E. R. Watkins, Y. H. Grad, S. Gupta, and C. O. Buckee, “Contrasting within- and between-host immune selection shapes Neisseria Opa repertoires,” *Scientific Reports 2014 4:1*, vol. 4, no. 1, pp. 1–8, Oct. 2014, doi: 10.1038/srep06554.

[144] M. Sadarangani, A. J. Pollard, and S. D. Gray-Owen, “Opa proteins and CEACAMs: pathways of immune engagement for pathogenic Neisseria,” *FEMS Microbiology Reviews*, vol. 35, no. 3, pp. 498–514, May 2011, doi: 10.1111/J.1574-6976.2010.00260.X.

[145] D. A. Fox, P. Larsson, R. H. Lo, B. M. Kroncke, P. M. Kasson, and L. Columbus, “Structure of the neisserial outer membrane protein Opa60: Loop flexibility essential to receptor recognition and bacterial engulfment,” *Journal of the American Chemical Society*, vol. 136, no. 28, pp. 9938–9946, Jul. 2014, doi: 10.1021/JA503093Y/SUPPL_FILE/JA503093Y_SI_001.PDF.

[146] A. R. Youssef, M. van der Flier, S. Estevão, N. G. Hartwig, P. van der Ley, and M. Virji, “Opa+ and Opa− Isolates of Neisseria meningitidis and Neisseria gonorrhoeae Induce Sustained Proliferative Responses in Human CD4+ T Cells,” *Infection and Immunity*, vol. 77, no. 11, p. 5170, Nov. 2009, doi: 10.1128/IAI.00355-09.

[147] H. C. Winther-Larsen, F. T. Hegge, M. Wolfgang, S. F. Hayes, J. P. M. van Putten, and M. Koomey, "Neisseria gonorrhoeae PilV, a type IV pilus-associated protein essential to human epithelial cell adherence," *Proceedings of the National Academy of Sciences of the United States of America*, vol. 98, no. 26, p. 15276, Dec. 2001, doi: 10.1073/PNAS.261574998.

[148] C. L. Giltner, Y. Nguyen, and L. L. Burrows, "Type IV Pilin Proteins: Versatile Molecular Modules," *Microbiology and Molecular Biology Reviews : MMBR*, vol. 76, no. 4, p. 740, Dec. 2012, doi: 10.1128/MMBR.00035-12.

[149] P. Hagblom, E. Segal, E. Billyard, and M. So, "Intragenic recombination leads to pilus antigenic variation in Neisseria gonorrhoeae," *Nature*, vol. 315, no. 6015, pp. 156–158, 1985, doi: 10.1038/315156A0.

[150] B. Maier, M. Koomey, and M. P. Sheetz, "A force-dependent switch reverses type IV pilus retraction," *Proceedings of the National Academy of Sciences*, vol. 101, no. 30, pp. 10961–10966, Jul. 2004, doi: 10.1073/PNAS.0402305101.

[151] C. L. Giltner, Y. Nguyen, and L. L. Burrows, "Type IV Pilin Proteins: Versatile Molecular Modules," *Microbiology and Molecular Biology Reviews : MMBR*, vol. 76, no. 4, p. 740, Dec. 2012, doi: 10.1128/MMBR.00035-12.

[152] J. L. Chlebek *et al.*, "PilT and PilU are homohexameric ATPases that coordinate to retract type IVa pili," *PLoS Genetics*, vol. 15, no. 10, 2019, doi: 10.1371/JOURNAL.PGEN.1008448.

[153] H. C. Winther-Larsen, F. T. Hegge, M. Wolfgang, S. F. Hayes, J. P. M. van Putten, and M. Koomey, "Neisseria gonorrhoeae PilV, a type IV pilus-associated protein essential to human epithelial cell adherence," *Proceedings of the National Academy of Sciences of the United States of*

America, vol. 98, no. 26, pp. 15276–15281, Dec. 2001, doi: 10.1073/PNAS.261574998.

[154] R. Allen Helm and H. Steven Seifert, "Pilin Antigenic Variation Occurs Independently of the RecBCD Pathway in Neisseria gonorrhoeae," *Journal of Bacteriology*, vol. 191, no. 18, p. 5613, Sep. 2009, doi: 10.1128/JB.00535-09.

[155] E. Rotman, D. M. Webber, and H. Steven Seifert, "Analyzing Neisseria gonorrhoeae Pilin Antigenic Variation Using 454 Sequencing Technology," *Journal of Bacteriology*, vol. 198, no. 18, p. 2470, 2016, doi: 10.1128/JB.00330-16.

[156] S. A. Hill and J. K. Davies, "Pilin gene variation in Neisseria gonorrhoeae: reassessing the old paradigms," *FEMS microbiology reviews*, vol. 33, no. 3, p. 521, May 2009, doi: 10.1111/J.1574-6976.2009.00171.X.

[157] A. Chen and H. S. Seifert, "Structure-Function Studies of the Neisseria gonorrhoeae Major Outer Membrane Porin," *Infection and Immunity*, vol. 81, no. 12, p. 4383, Dec. 2013, doi: 10.1128/IAI.00367-13.

[158] W. Achouak, T. Heulin, and J.-M. PagÃ¨s, "Multiple facets of bacterial porins," *FEMS Microbiology Letters*, vol. 199, no. 1, pp. 1–7, May 2001, doi: 10.1111/J.1574-6968.2001.TB10642.X.

[159] A. Sun *et al.*, "Predominant porB1A and porB1B genotypes and correlation of gene mutations with drug resistance in Neisseria gonorrhoeae isolates in Eastern China," *BMC Infectious Diseases*, vol. 10, p. 323, Nov. 2010, doi: 10.1186/1471-2334-10-323.

[160] R. C. Judd, "Protein I: structure, function, and genetics," *Clinical microbiology reviews*, vol. 2 Suppl, no. Suppl, Apr. 1989, doi: 10.1128/CMR.2.SUPPL.S41.

[161] J. L. Edwards and M. A. Apicella, "The Molecular Mechanisms Used by Neisseria gonorrhoeae To Initiate Infection Differ between Men and

Women," *Clinical Microbiology Reviews*, vol. 17, no. 4, p. 965, Oct. 2004, doi: 10.1128/CMR.17.4.965-981.2004.

[162] A. Sun *et al.*, "Predominant porB1A and porB1B genotypes and correlation of gene mutations with drug resistance in Neisseria gonorrhoeae isolates in Eastern China," *BMC Infectious Diseases*, vol. 10, no. 1, pp. 1–9, Nov. 2010, doi: 10.1186/1471-2334-10-323/TABLES/3.

[163] S. Ram, D. P. McQuillen, S. Gulati, C. Elkins, M. K. Pangburn, and P. A. Rice, "Binding of Complement Factor H to Loop 5 of Porin Protein 1A: A Molecular Mechanism of Serum Resistance of Nonsialylated Neisseria gonorrhoeae," *The Journal of Experimental Medicine*, vol. 188, no. 4, p. 671, Aug. 1998, doi: 10.1084/JEM.188.4.671.

[164] J. D. Lenz and J. P. Dillard, "Pathogenesis of Neisseria gonorrhoeae and the Host Defense in Ascending Infections of Human Fallopian Tube," *Frontiers in Immunology*, vol. 9, no. NOV, p. 2710, Nov. 2018, doi: 10.3389/FIMMU.2018.02710.

[165] A. Lovett and J. A. Duncan, "Human immune response and the natural history of neisseria gonorrhoeae infection," *Frontiers in Immunology*, vol. 10, no. FEB, p. 3187, 2019, doi: 10.3389/FIMMU.2018.03187/BIBTEX.

[166] Y. Liu *et al.*, "Experimental vaccine induces Th1-driven immune responses and resistance to Neisseria gonorrhoeae infection in a murine model," *Mucosal Immunology 2017 10:6*, vol. 10, no. 6, pp. 1594–1608, Mar. 2017, doi: 10.1038/mi.2017.11.

[167] S. Gulati *et al.*, "Complement alone drives efficacy of a chimeric antigonococcal monoclonal antibody," *PLOS Biology*, vol. 17, no. 6, p. e3000323, Jun. 2019, doi: 10.1371/JOURNAL.PBIO.3000323.

[168] T. Dutta Ray, L. A. Lewis, S. Gulati, P. A. Rice, and S. Ram, "Novel blocking human IgG directed against the pentapeptide repeat motifs of Neisseria meningitidis Lip/H.8 and Laz lipoproteins," *Journal of*

immunology (Baltimore, Md. : 1950), vol. 186, no. 8, pp. 4881–4894, Apr. 2011, doi: 10.4049/JIMMUNOL.1003623.

[169] L. A. Lewis *et al.*, "Phosphoethanolamine substitution of lipid A and resistance of Neisseria gonorrhoeae to cationic antimicrobial peptides and complement-mediated killing by normal human serum," *Infection and immunity*, vol. 77, no. 3, pp. 1112–1120, 2009, doi: 10.1128/IAI.01280-08.

[170] L. A. Lewis and S. Ram, "Complement interactions with the pathogenic Neisseriae: clinical features, deficiency states, and evasion mechanisms," *FEBS letters*, vol. 594, no. 16, pp. 2670–2694, Aug. 2020, doi: 10.1002/1873-3468.13760.

[171] C. A. Nairn, J. A. Cole, P. v. Patel, N. J. Parsons, J. E. Fox, and H. Smith, "Cytidine 5'-monophospho-N-acetylneuraminic acid or a related compound is the low Mr factor from human red blood cells which induces gonococcal resistance to killing by human serum," *Journal of general microbiology*, vol. 134, no. 12, pp. 3295–3306, 1988, doi: 10.1099/00221287-134-12-3295.

[172] S. Gulati *et al.*, "Utilizing CMP-Sialic Acid Analogs to Unravel Neisseria gonorrhoeae Lipooligosaccharide-Mediated Complement Resistance and Design Novel Therapeutics," *PLoS pathogens*, vol. 11, no. 12, 2015, doi: 10.1371/JOURNAL.PPAT.1005290.

[173] L. K. McNeil *et al.*, "Role of Factor H Binding Protein in Neisseria meningitidis Virulence and Its Potential as a Vaccine Candidate To Broadly Protect against Meningococcal Disease," *Microbiology and Molecular Biology Reviews : MMBR*, vol. 77, no. 2, p. 234, Jun. 2013, doi: 10.1128/MMBR.00056-12.

[174] M. Unemo and W. M. Shafer, "Antibiotic resistance in Neisseria gonorrhoeae: origin, evolution, and lessons learned for the future," *Annals of the New York Academy of Sciences*, vol. 1230, pp. E19–E28, Aug. 2011, doi: 10.1111/j.1749-6632.2011.06215.x.

[175] M. Unemo and R. A. Nicholas, “Emergence of multidrug-resistant, extensively drug-resistant and untreatable gonorrhea,” *Future microbiology*, vol. 7, no. 12, pp. 1401–1422, Dec. 2012, doi: 10.2217/FMB.12.117.

[176] C. L. Satterwhite *et al.*, “Sexually transmitted infections among US women and men: prevalence and incidence estimates, 2008,” *Sexually transmitted diseases*, vol. 40, no. 3, pp. 187–193, Mar. 2013, doi: 10.1097/OLQ.0B013E318286BB53.

[177] D. L. Gullette, J. L. Rooker, and R. L. Kennedy, “Factors Associated With Sexually Transmitted Infections in Men and Women,” *Journal of community health nursing*, vol. 26, no. 3, p. 121, Jul. 2009, doi: 10.1080/07370010903034425.

[178] D. A. Leight, J. le Franc, and A. R. Turnbull, “SENSITIVITY TO PENICILLIN OF Neisseria gonorrhoeae* RELATIONSHIP TO THE RESULTS OF TREATMENT,” *Brit. J. vener. Dis*, p. 151, 1969, doi: 10.1136/sti.45.2.151.

[179] M. Ohnishi *et al.*, “Ceftriaxone-Resistant Neisseria gonorrhoeae, Japan,” *Emerging Infectious Diseases*, vol. 17, no. 1, p. 148, Jan. 2011, doi: 10.3201/EID1701.100397.

[180] D. of STD Prevention, “Sexually Transmitted Disease Surveillance 2011,” 2012, Accessed: Dec. 15, 2021. [Online]. Available: http://www.cdc.gov/std/program/pupestd.htm

[181] B. S. Graham and D. M. Ambrosino, “History of Passive Antibody Administration for Prevention and Treatment of Infectious Diseases,” *Current opinion in HIV and AIDS*, vol. 10, no. 3, p. 129, May 2015, doi: 10.1097/COH.0000000000000154.

[182] P. Domingo, V. Pomar, A. Mauri, and N. Barquet, “Standing on the shoulders of giants: two centuries of struggle against meningococcal

disease," *The Lancet. Infectious Diseases*, vol. 19, no. 8, p. e284, Aug. 2019, doi: 10.1016/S1473-3099(19)30040-4.

[183] R. Dixit, J. Herz, R. Dalton, and R. Booy, "Benefits of using heterologous polyclonal antibodies and potential applications to new and undertreated infectious pathogens," *Vaccine*, vol. 34, no. 9, p. 1152, Feb. 2016, doi: 10.1016/J.VACCINE.2016.01.016.

[184] V. G. Hemming, "Use of Intravenous Immunoglobulins for Prophylaxis or Treatment of Infectious Diseases," *Clinical and Diagnostic Laboratory Immunology*, vol. 8, no. 5, p. 859, 2001, doi: 10.1128/CDLI.8.5.859-863.2001.

[185] S. Welkos, S. Little, A. Friedlander, D. Fritz, and P. Fellows, "The role of antibodies to Bacillus anthracis and anthrax toxin components in inhibiting the early stages of infection by anthrax spores," *Microbiology (Reading, England)*, vol. 147, no. Pt 6, pp. 1677–1685, 2001, doi: 10.1099/00221287-147-6-1677.

[186] D. P. Humphreys and M. H. Wilcox, "Antibodies for Treatment of Clostridium difficile Infection," *Clinical and Vaccine Immunology : CVI*, vol. 21, no. 7, p. 913, 2014, doi: 10.1128/CVI.00116-14.

[187] D. v. Zurawski and M. K. McLendon, "Monoclonal Antibodies as an Antibacterial Approach Against Bacterial Pathogens," *Antibiotics*, vol. 9, no. 4, Apr. 2020, doi: 10.3390/ANTIBIOTICS9040155.

[188] S. Gulati, D. P. McQuillen, R. E. Mandrell, D. B. Jani, and P. A. Rice, "Immunogenicity of Neisseria gonorrhoeae Lipooligosaccharide Epitope 2C7, Widely Expressed In Vivo with No Immunochemical Similarity to Human Glycosphingolipids," *The Journal of Infectious Diseases*, vol. 174, no. 6, pp. 1223–1237, Dec. 1996, doi: 10.1093/INFDIS/174.6.1223.

[189] S. Gulati, J. Shaughnessy, S. Ram, and P. A. Rice, “Targeting Lipooligosaccharide (LOS) for a Gonococcal Vaccine,” *Frontiers in immunology*, vol. 10, no. FEB, 2019, doi: 10.3389/FIMMU.2019.00321.

[190] M. W. Russell, A. E. Jerse, and S. D. Gray-Owen, “Progress Toward a Gonococcal Vaccine: The Way Forward ,” *Frontiers in Immunology* , vol. 10. p. 2417, 2019. [Online]. Available: https://www.frontiersin.org/article/10.3389/fimmu.2019.02417

[191] J. L. Edwards, M. P. Jennings, M. A. Apicella, and K. L. Seib, “Is gonococcal disease preventable? The importance of understanding immunity and pathogenesis in vaccine development,” *Critical Reviews in Microbiology*, vol. 42, no. 6, p. 928, Nov. 2016, doi: 10.3109/1040841X.2015.1105782.

[192] H. Petousis-Harris *et al.*, “Effectiveness of a group B outer membrane vesicle meningococcal vaccine against gonorrhoea in New Zealand: a retrospective case-control study,” *The Lancet*, vol. 390, no. 10102, pp. 1603–1610, Sep. 2017, doi: 10.1016/S0140-6736(17)31449-6.

[193] C. Schwechheimer and M. J. Kuehn, “Outer-membrane vesicles from Gram-negative bacteria: biogenesis and functions,” *Nature reviews. Microbiology*, vol. 13, no. 10, p. 605, Sep. 2015, doi: 10.1038/NRMICRO3525.

[194] A. T. Jan, “Outer Membrane Vesicles (OMVs) of gram-negative bacteria: A perspective update,” *Frontiers in Microbiology*, vol. 8, no. JUN, p. 1053, Jun. 2017, doi: 10.3389/FMICB.2017.01053/BIBTEX.

[195] M. O’Ryan, J. Stoddard, D. Toneatto, J. Wassil, and P. M. Dull, “A Multi-Component Meningococcal Serogroup B Vaccine (4CMenB): The Clinical Development Program,” *Drugs*, vol. 74, no. 1, p. 15, 2014, doi: 10.1007/S40265-013-0155-7.

[196] I. Vacca *et al.*, “Neisserial Heparin Binding Antigen (NHBA) Contributes to the Adhesion of Neisseria meningitidis to Human Epithelial Cells,” *PLoS ONE*, vol. 11, no. 10, Oct. 2016, doi: 10.1371/JOURNAL.PONE.0162878.

[197] M. Biagini *et al.*, “Expression of factor H binding protein in meningococcal strains can vary at least 15-fold and is genetically determined,” *Proceedings of the National Academy of Sciences of the United States of America*, vol. 113, no. 10, pp. 2714–2719, Mar. 2016, doi: 10.1073/PNAS.1521142113/-/DCSUPPLEMENTAL.

[198] M. Comanducci *et al.*, “NadA, a Novel Vaccine Candidate of Neisseria meningitidis,” *The Journal of Experimental Medicine*, vol. 195, no. 11, p. 1445, Jun. 2002, doi: 10.1084/JEM.20020407.

[199] R. Rappuoli, “Reverse vaccinology,” *Current opinion in microbiology*, vol. 3, no. 5, pp. 445–450, 2000, doi: 10.1016/S1369-5274(00)00119-3.

[200] “Pneumonia of unknown cause – China.” https://www.who.int/emergencies/disease-outbreak-news/item/2020-DON229 (accessed Dec. 16, 2021).

[201] P. S, B. M, F. U, N. M, B. C, and Z. M, “Impact of vaccination on the spread of SARS-CoV-2 infection in north-east Italy nursing homes. A propensity score and risk analysis,” *Age and ageing*, Dec. 2021, doi: 10.1093/AGEING/AFAB224.

[202] “FDA Approves First COVID-19 Vaccine | FDA.” https://www.fda.gov/news-events/press-announcements/fda-approves-first-covid-19-vaccine (accessed Dec. 16, 2021).

[203] Y. C. Wu, C. S. Chen, and Y. J. Chan, “The outbreak of COVID-19: An overview,” *Journal of the Chinese Medical Association*, vol. 83, no. 3, pp. 217–220, 2020, doi: 10.1097/JCMA.0000000000000270.

[204] M. Pal, G. Berhanu, C. Desalegn, and V. Kandi, “Severe Acute Respiratory Syndrome Coronavirus-2 (SARS-CoV-2): An Update,” *Cureus*, vol. 12, no. 3, Mar. 2020, doi: 10.7759/CUREUS.7423.

[205] A. A. T. Naqvi *et al.*, “Insights into SARS-CoV-2 genome, structure, evolution, pathogenesis and therapies: Structural genomics approach,” *Biochimica et Biophysica Acta. Molecular Basis of Disease*, vol. 1866, no. 10, p. 165878, Oct. 2020, doi: 10.1016/J.BBADIS.2020.165878.

[206] C. B. Jackson, M. Farzan, B. Chen, and H. Choe, “Mechanisms of SARS-CoV-2 entry into cells,” *Nature Reviews Molecular Cell Biology 2021 23:1*, vol. 23, no. 1, pp. 3–20, Oct. 2021, doi: 10.1038/s41580-021-00418-x.

[207] S. S. Hwang *et al.*, “Cryo-EM structure of the 2019-nCoV spike in the prefusion conformation,” *Science (New York, N.Y.)*, vol. 367, no. 6483, pp. 1255–1260, Mar. 2020, doi: 10.1126/SCIENCE.ABB2507.

[208] A. G. Harrison, T. Lin, and P. Wang, “Mechanisms of SARS-CoV-2 Transmission and Pathogenesis,” *Trends in Immunology*, vol. 41, no. 12, p. 1100, Dec. 2020, doi: 10.1016/J.IT.2020.10.004.

[209] H. Yang and Z. Rao, “Structural biology of SARS-CoV-2 and implications for therapeutic development,” *Nature Reviews Microbiology 2021 19:11*, vol. 19, no. 11, pp. 685–700, Sep. 2021, doi: 10.1038/s41579-021-00630-8.

[210] M. Bakhiet and S. Taurin, “SARS-CoV-2: Targeted managements and vaccine development,” *Cytokine & growth factor reviews*, vol. 58, pp. 16–29, Apr. 2021, doi: 10.1016/J.CYTOGFR.2020.11.001.

[211] T. Tiller, C. E. Busse, and H. Wardemann, “Cloning and expression of murine Ig genes from single B cells,” *Journal of immunological methods*, vol. 350, no. 1–2, pp. 183–193, Oct. 2009, doi: 10.1016/J.JIM.2009.08.009.

[212] F. Mancini, F. Micoli, F. Necchi, M. Pizza, F. Berlanda Scorza, and O. Rossi, “GMMA-Based Vaccines: The Known and The Unknown,”

Frontiers in Immunology, vol. 12, p. 3122, Aug. 2021, doi: 10.3389/FIMMU.2021.715393/BIBTEX.

[213] T. J. O. Wyckoff and C. R. H. Raetz, "The active site of Escherichia coli UDP-N-acetylglucosamine acyltransferase. Chemical modification and site-directed mutagenesis," *Journal of Biological Chemistry*, vol. 274, no. 38, pp. 27047–27055, Sep. 1999, doi: 10.1074/jbc.274.38.27047.

[214] G. Blanchard-Rohner, A. S. Pulickal, C. M. Jol-van Der Zijde, M. D. Snape, and A. J. Pollard, "Appearance of peripheral blood plasma cells and memory B cells in a primary and secondary immune response in humans," *Blood*, vol. 114, no. 24, pp. 4998–5002, Dec. 2009, doi: 10.1182/BLOOD-2009-03-211052.

[215] S. M. Lightman, A. Utley, and K. P. Lee, "Survival of long-lived plasma cells (LLPC): Piecing together the puzzle," *Frontiers in Immunology*, vol. 10, no. MAY, p. 965, 2019, doi: 10.3389/FIMMU.2019.00965/BIBTEX.

[216] J. Huang *et al.*, "Isolation of human monoclonal antibodies from peripheral blood B cells," *Nature protocols*, vol. 8, no. 10, pp. 1907–1915, Oct. 2013, doi: 10.1038/NPROT.2013.117.

[217] A. M. Awanye *et al.*, "Immunogenicity profiling of protein antigens from capsular group B Neisseria meningitidis," *Scientific Reports 2019 9:1*, vol. 9, no. 1, pp. 1–14, May 2019, doi: 10.1038/s41598-019-43139-0.

[218] J. H. Zhang, T. D. Y. Chung, and K. R. Oldenburg, "A Simple Statistical Parameter for Use in Evaluation and Validation of High Throughput Screening Assays," *Journal of biomolecular screening*, vol. 4, no. 2, pp. 67–73, 1999, doi: 10.1177/108705719900400206.

[219] O. Rossi, E. Molesti, A. Saul, C. Giannelli, F. Micoli, and F. Necchi, "Intra-Laboratory Evaluation of Luminescence Based High-Throughput Serum Bactericidal Assay (L-SBA) to Determine Bactericidal Activity of

Human Sera against Shigella," *High-throughput*, vol. 9, no. 2, pp. 1–12, Jun. 2020, doi: 10.3390/HT9020014.

[220] E. A. Semchenko, C. J. Day, and K. L. Seib, "The Neisseria gonorrhoeae Vaccine Candidate NHBA Elicits Antibodies That Are Bactericidal, Opsonophagocytic and That Reduce Gonococcal Adherence to Epithelial Cells," *Vaccines*, vol. 8, no. 2, Jun. 2020, doi: 10.3390/VACCINES8020219.